(12) INTERNATIONAL APPLICATION PUBLISHED UNDER THE PATENT COOPERATION TREATY (PCT)

(19) World Intellectual Property Organization
International Bureau

(43) International Publication Date
17 June 2021 (17.06.2021)

WIPO | PCT

(10) International Publication Number
WO 2021/118934 A1

(51) International Patent Classification:
C12M 3/00 (2006.01) *C12M 1/12* (2006.01)
C12N 5/00 (2006.01) *C12M 1/34* (2006.01)
C12M 3/06 (2006.01) *B01L 3/00* (2006.01)

(21) International Application Number:
PCT/US2020/063636

(22) International Filing Date:
07 December 2020 (07.12.2020)

(25) Filing Language: English

(26) Publication Language: English

(30) Priority Data:
62/945,501 09 December 2019 (09.12.2019) US

(71) Applicant: **GEORGIA TECH RESEARCH CORPORATION** [US/US]; 926 Dalney Street NW, Atlanta, GA 30318 (US).

(72) Inventors: **KIM, YongTae**; 926 Dalney Street NW, Atlanta, GA 30318 (US). **AHN, Song, Ih**; 926 Dalney Street NW, Atlanta, GA 30318 (US). **KIM, Taeyoung**; 926 Dalney Street NW, Atlanta, GA 30318 (US). **YOON, Jeongkee**; 926 Dalney Street NW, Atlanta, GA 30318 (US).

(74) Agent: **HALSTEAD, David, P.** et al.; Foley Hoag LLP, 155 Seaport Boulevard, Boston, MA 02210-2600 (US).

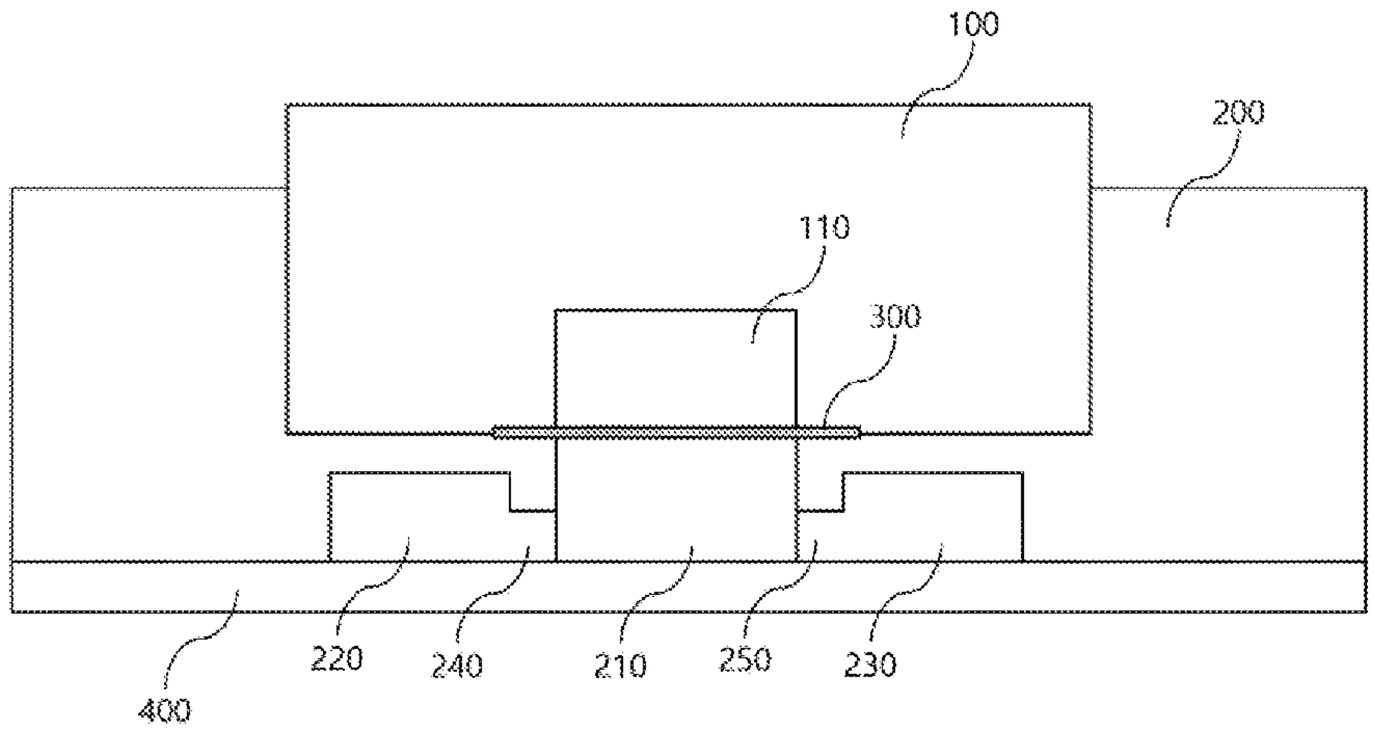
(81) Designated States *(unless otherwise indicated, for every kind of national protection available)*: AE, AG, AL, AM, AO, AT, AU, AZ, BA, BB, BG, BH, BN, BR, BW, BY, BZ, CA, CH, CL, CN, CO, CR, CU, CZ, DE, DJ, DK, DM, DO, DZ, EC, EE, EG, ES, FI, GB, GD, GE, GH, GM, GT, HN, HR, HU, ID, IL, IN, IR, IS, IT, JO, JP, KE, KG, KH, KN, KP, KR, KW, KZ, LA, LC, LK, LR, LS, LU, LY, MA, MD, ME, MG, MK, MN, MW, MX, MY, MZ, NA, NG, NI, NO, NZ, OM, PA, PE, PG, PH, PL, PT, QA, RO, RS, RU, RW, SA, SC, SD, SE, SG, SK, SL, ST, SV, SY, TH, TJ, TM, TN, TR, TT, TZ, UA, UG, US, UZ, VC, VN, WS, ZA, ZM, ZW.

(84) Designated States *(unless otherwise indicated, for every kind of regional protection available)*: ARIPO (BW, GH, GM, KE, LR, LS, MW, MZ, NA, RW, SD, SL, ST, SZ, TZ, UG, ZM, ZW), Eurasian (AM, AZ, BY, KG, KZ, RU, TJ, TM), European (AL, AT, BE, BG, CH, CY, CZ, DE, DK, EE, ES, FI, FR, GB, GR, HR, HU, IE, IS, IT, LT, LU, LV, MC, MK, MT, NL, NO, PL, PT, RO, RS, SE, SI, SK, SM, TR), OAPI (BF, BJ, CF, CG, CI, CM, GA, GN, GQ, GW, KM, ML, MR, NE, SN, TD, TG).

Published:
— *with international search report (Art. 21(3))*
— *before the expiration of the time limit for amending the claims and to be republished in the event of receipt of amendments (Rule 48.2(h))*

(54) Title: MICROENGINEERED TISSUE BARRIER SYSTEM

Fig. 1



(57) **Abstract:** The present disclosure relates to a microfluidic device for simulating the structure and function of an *in vivo* tissue barrier. Specifically, the present disclosure relates to a microfluidic device that can be used as a model for new drug development and toxicity assessment and the like by simulating the structure and function of a two-dimensional-three-dimensional connective tissue barrier or a three-dimensional tissue barrier and thus replacing animal models, a method of culturing cells in the microfluidic device, and a method of simulating an organ or a body part using the microfluidic device.

WO 2021/118934 A1

MICROENGINEERED TISSUE BARRIER SYSTEM

CROSS-REFERENCE TO RELATED APPLICATION

This application claims the benefit of the following U.S. Provisional Application No.: 62/945,501, filed December 9, 2019, the entire contents of which are incorporated herein by reference.

BACKGROUND

Organ-on-a-chip was developed in which an organ tissue is integrated in a chip form in order to solve ethical problems and problems due to differences between different species in the use of experimental animal models for examining efficacy and side effects of a drug. Organ-on-a-chip is a technology that implements a desired function by culturing cells constituting a specific organ in a small chip, and thus simulating the morphology and physiological property of that organ. Organ-on-a-chip can be used to study in detail the cell behavior of a specific organ and the mechanism of physicochemical reactions in microenvironment, and can be used as a model for new drug development and toxicity assessment.

In the development of organ-on-a-chip, a cell culture model using a conventional two-dimensional (2D) cell culture has a problem in not being able to explain tissue-specific differentiated functions of many cell types or not being able to accurately predict tissue function and drug activity *in vivo* since it uses a petri dish to culture cells on the bottom of the dish in two dimensions.

In particular, in the case of brain tissue cells having neurons, astrocytes and the like having three-dimensional contact *in vivo*, due to the limitation of the above two-dimensional cell culture model, there is an increasing need for a three-dimensional cell culture model that well simulates the spatial structure and biochemical complexity of a living tissue.

Since the three-dimensional cell culture model well mimics the *in vivo* situation, it can implement the complexity of directional growth and intercellular connectivity in *in vitro* experiments, and it is useful for capturing the signaling pathway and drug responsiveness of various disease states well compared to the two-dimensional cell culture model in studying tissue functions on a molecular basis.

On the other hand, the microfluidic engineering technology developed along with the semiconductor process technology enabled mass production of a structure having a micro-level size with high accuracy. In particular, photolithography and soft lithography technologies have made it possible to easily produce microchannel structures through stamping using semi-permanent molds, and through this, there have been attempts to simulate microstructures such as blood vessels of the

human body and cell layers of organs *in vitro*.

Existing research has been carried out in the form of preparing a chip consisting of a polydimethylsiloxane (PDMS) microchannel and a porous membrane using photolithography or soft lithography technology, and implementing the cell layer structure of an organ through cell culture inside the chip. However, in an organ-on-a-chip using a microfluidic device made of PDMS material, there are many cases in which drugs or proteins were adsorbed on the surface of PDMS and disappeared, constituting a limitation that is difficult to overcome when attempting to simulate an *in vivo* environment that will have greater applicability in the actual pharmaceutical industry.

Thus, a need exists for an organ-on-a-chip that more closely simulates the structure and function of an *in vivo* two-dimensional-three-dimensional connective tissue barrier or a three-dimensional tissue barrier.

SUMMARY

The present disclosure relates to a microfluidic device for simulating the structure and function of an *in vivo* tissue barrier. Specifically, the present disclosure relates to a microfluidic device that can be used as a model for new drug development and toxicity assessment and the like by simulating the structure and function of a two-dimensional-three-dimensional connective tissue barrier or a three-dimensional tissue barrier and thus replacing animal models, a method of culturing cells in the microfluidic device, and a method of simulating an organ or a body part using the microfluidic device. Therefore, the present disclosure provides an improvement to the organ-on-a-chip that uses a conventional microfluidic device. The microfluidic device described herein more closely simulates the structure and function of an *in vivo* two-dimensional-three-dimensional connective tissue barrier or a three-dimensional tissue barrier.

An object of the present disclosure is to provide a microfluidic device that exhibits more similar structure and function to the *in vivo* tissue barrier compared to the conventional organ-on-a-chip by solving ethical problems and problems due to differences between different species in the use of experimental animal models and forming the structure of a two-dimensional-three-dimensional connective tissue barrier or a three-dimensional tissue barrier.

The present disclosure provides a microfluidic device comprising an insert comprising a first central channel; a base comprising a second central channel, a third side channel, a fourth side channel, a fifth passage channel connecting the second central channel and the third side channel, and a sixth passage channel connecting the second central channel and the fourth side channel; and a porous membrane positioned between the insert and the base.

The present disclosure provides a method of culturing cells in a microfluidic device, the

method comprising a step of assembling the microfluidic device; a step of injecting second cells into the second central channel and then inverting the microfluidic device and culturing them; a step of injecting hydrogel comprising third cells into the second central channel and then culturing them; and a step of inverting the microfluidic device and then injecting first cells into the first central channel and culturing them.

In addition, the present disclosure provides a method of simulating the structure and function of an organ or a body part using the microfluidic device, wherein the method of simulating an organ or a body part comprises a step of perfusing a first fluid through the first central channel; and a step of perfusing a second fluid into a third side channel, a second central channel, and a fourth side channel.

The microfluidic device of the present disclosure can be used for the evaluation of drug efficacy by simulating the main structures of various *in vivo* tissue barriers including the blood–brain barrier and material transport phenomenon.

The microfluidic device of the present disclosure enables precise quantification of the distribution of nanoparticles around the tissue barrier, and since the insert is detachable from the base, cells contained in the microfluidic device can be selectively separated without damage and used for analysis. In addition, the insert is capable of being separated from the base, subjected to a necessary treatment such as drug application, and then reassembled to observe a cellular reaction.

The microfluidic device of the present disclosure is capable of three-dimensional culture of cells, thereby implementing the spatial structure and biochemical complexity of cells *in vivo* and thus better simulating the structure and function of the tissue barrier.

BRIEF DESCRIPTION OF DRAWINGS

Throughout the figures, the following labels are used to identify specific features.

100: insert

101: first fastening head

110: first central channel

111: first cell

112: inlet of the first central channel

113: outlet of the first central channel

200: base

201: insert insertion groove

202: second fastening head

210: second central channel

211: second cell

212: third cell

213: hydrogel

214: inlet of the second central channel

215: outlet of the second central channel

220: third side channel

221: inlet of the third side channel

222: outlet of the third side channel

230: fourth side channel

231: inlet of the fourth side channel

232: outlet of the fourth side channel

240: fifth passage channel

250: sixth passage channel

260: seventh passage channel

270: eighth passage channel

280: first fluid reservoir

290: second fluid reservoir

300: porous membrane

400: bottom part

500: cover

501: inlet of the first central channel in the cover

502: outlet of the first central channel in the cover

Fig. 1 is a cross-sectional view of a microfluidic device.

Fig. 2 is a cross-sectional view of a microfluidic device.

Fig. 3 is a perspective view of a microfluidic device.

Fig. 4 is an exploded view of a microfluidic device

Fig. 5 is a combined view of a microfluidic device.

Fig. 6 is a cross-sectional view of a microfluidic device comprising cells and hydrogel

Fig. 7 is a cross-sectional view of a microfluidic device comprising cells and hydrogel.

Fig. 8 is a cross-section view showing a configuration for attaching and detaching an insert and a base.

Fig. 9 is a cross-sectional view showing a configuration for attaching and detaching an

insert and a base and an attachment and detachment method.

Fig. 10 is a cross-sectional view showing a configuration for attaching and detaching an insert and a base and an attachment and detachment method.

Fig. 11 is a cross-sectional view showing the fluid flow in a base of a microfluidic device.

Fig. 12 is a perspective view of an insert.

Fig. 13 is a perspective view of an insert.

Fig. 14 is a perspective view of a base.

Fig. 15 is a plan view of a base.

Fig. 16 is a bottom view and an enlarged bottom view of a base.

Fig. 17 is a perspective view of a cover.

Fig. 18 is a perspective view and a cross-sectional view showing a configuration for attaching and detaching an insert and a base and an attachment and detachment method.

Fig. 19 is a plan view of a microfluidic device in the form in which an insert and a base are attached.

Fig. 20 is an A-A' cross-sectional view and an enlarged cross-sectional view of the microfluidic device of Fig. 19 in the form in which an insert and a base are attached.

Fig. 21 is a front view of a microfluidic device in the form in which an insert and a base are attached.

Fig. 22 is a bottom view and an enlarged bottom view of a microfluidic device in the form in which an insert and a base are attached.

Fig. 23 is a perspective view of a microfluidic device comprising a cover.

Fig. 24 is a perspective view showing a fluid flow in a microchannel included in an insert.

Fig. 25 is a cross-sectional view showing a fluid flow in a microchannel included in a base.

Fig. 26 shows the cell morphology of human brain microvascular endothelial cells (HBMEC), human brain vascular pericytes (HBVP), or human astrocytes (HA) when cultured in endothelial medium (E), pericyte medium (P), or astrocyte medium (A), which is its respective culture medium, and when cultured in E+G (E+A+M) medium, which a mixed medium.

Fig. 27 is a graph showing the cell activity of human brain microvascular endothelial cells (HBMEC), human brain vascular pericytes (HBVP), or human astrocytes (HA) when cultured in endothelial medium (E), astrocyte medium (A), pericyte medium (P), microglia medium (M), E+G+P (E+A+M+P) medium, or E+G (E+A+M) medium, respectively.

Fig. 28 is a graph showing the cell activity of human brain microvascular endothelial cells (HBMEC), human brain vascular pericytes (HBVP), or human astrocytes (HA) when cultured in E+G (E+A+M) medium or E+G+P (E+A+M+P) medium, which is a mixed medium, respectively.

Fig. 29 is a schematic diagram showing a method of culturing cells in a microfluidic device.

Fig. 30 is a heat map showing the results of RT-qPCR showing the expression level of blood–brain barrier specific proteins in a single culture of human brain microvascular endothelial cells (HBMEC) and in a microfluidic device simulating blood–brain barrier (BBB) (n=3).

Fig. 31 is a graph showing the gene expression level of blood–brain barrier specific junctional proteins in a single culture of human brain microvascular endothelial cells (HBMEC) and in a microfluidic device simulating blood–brain barrier (BBB) (n=3, *$p < 0.05$ by student t-test).

Fig. 32 is a graph showing the gene expression level of blood–brain barrier specific receptor proteins in a single culture of human brain microvascular endothelial cells (HBMEC) and in a microfluidic device simulating blood–brain barrier (BBB) (n=3, *$p < 0.05$ by student t-test).

Fig. 33 is a graph showing the TEER value measured in a single culture of human brain microvascular endothelial cells (HBMEC) and in a microfluidic device simulating blood–brain barrier (BBB) (n =11 (EC), n = 12 (BBB), **$p < 0.01$ by student t-test).

Fig. 34 is a graph showing the TEER value according to the difference in shear stress of the blood simulation flow measured in a microfluidic device simulating blood–brain barrier (BBB) (n = 5 (No shear), n= 4 (0.4 dyne cm^{-2}), n = 12 (4 dyne cm^{-2}), *$p < 0.05$ by student t-test).

Fig. 35 is a graph showing the permeability coefficient (P) measured in a cell-free culture, in a single culture of human brain microvascular endothelial cells (HBMEC), and in a microfluidic device simulating blood–brain barrier (BBB) (n = 4, *$p < 0.05$, ****$p < 0.001$ vs. No cell, #$p < 0.05$, ##$p < 0.01$ vs. EC, student t-test).

Fig. 36 shows the morphology of human astrocytes (HA) cultured on the 2D Matrigel-coated surface and the morphology of human astrocytes (HA) cultured inside the 3D Matrigel.

Fig. 37 is a graph comparing the cell body size of human astrocytes (HA) cultured on the 2D Matrigel-coated surface and inside the 3D Matrigel.

Fig. 38 is a graph comparing the process length of human astrocytes (HA) cultured on the 2D Matrigel-coated surface and inside the 3D Matrigel.

Fig. 39 is a graph comparing the expression level of GFAP, VIM, and LCN2 in human astrocytes (HA) cultured on the 2D Matrigel-coated surface and inside the 3D Matrigel (n = 4, ***$p < 0.005$, ****$p < 0.001$ by student t-test).

Fig. 40 is a graph comparing the expression level of LCN2 according to the concentration of IL-1β treated on human astrocytes (HA) cultured on the 2D Matrigel-coated surface.

Fig. 41 is a graph comparing the expression level of LCN2 according to the concentration

of IL-1β treated on human astrocytes (HA) cultured inside the 3D Matrigel.

Fig. 42 shows the expression of AQP-4 and α-syn when astrocytes are cultured on the 2D Matrigel-coated surface (Scale bars = 50 μm).

Fig. 43 shows the expression of AQP-4 and α-syn when astrocytes are cultured inside the 3D Matrigel (Scale bars = 20 μm).

Fig. 44 is a graph showing the polarization level of AQP-4 when only human astrocytes (HA) are cultured (A), when human astrocytes (HA) and human brain microvascular endothelial cells (HBMEC) are cultured (E+A), and when human brain microvascular endothelial cells (HBMEC), human brain vascular pericytes (HBVP) and human astrocytes (HA) are cultured togethter (E+P+A) (n =4, *p < 0.05 by student t-test).

Fig. 45 is a graph showing the size distribution of synthesized eHNP-A1.

Fig. 46 is a graph showing the quantification of the relative distribution of eHNP-A1 in each organ *in vivo* (mean ± s.e.m, n = 4).

Fig. 47 shows the distribution of eHNP-A1 in the brain.

Fig. 48 is a graph showing the relative fluorescence intensity of the culture medium comprising eHNP-A1 sampled from a first central channel (vascular channel) (n = 12; **p < 0.01 by student t-test, mean ± s.e.m.).

Fig. 49 is a graph showing the relative fluorescence intensity of the culture medium comprising eHNP-A1 sampled from a central channel (perivascular channel) (n =5,).

Fig. 50 is a graph showing the distribution of eHNP-A1 in a first central channel (vascular), human brain microvascular endothelial cells (HBMEC), and a second central channel (perivascular).

Fig. 51 is a FACS (fluorescence-activated cell sorting) plot for the number of human brain microvascular endothelial cells (HBMEC), human astrocytes (HA), and human brain vascular pericytes (HBVP), which are eHNP-A1 positive.

Fig. 52 is a graph quantifying the cell portions observed in FIG. 51.

DETAILED DESCRIPTION

Hereinafter, the embodiments and examples of the present application will be described in detail with reference to the accompanying drawings so that those of ordinary skill in the art to which the present disclosure belongs can easily practice the present disclosure. However, the present application can be implemented in various forms and is not limited to the embodiments and examples described herein.

Throughout the specification of the present application, unless otherwise stated, when a

certain part "comprises" a certain constituent element, it means that the certain part may further comprise other constituent elements rather than exclude other constituent elements.

The present disclosure provides a microfluidic device comprising an insert comprising a first central channel; a base comprising a second central channel, a third side channel, a fourth side channel, a fifth passage channel connecting the second central channel and the third side channel, and a sixth passage channel connecting the second central channel and the fourth side channel; and a porous membrane positioned between the insert and the base.

As used herein, the term "microfluidic device" refers to a device comprising microchannels and the like provided to allow fluid to flow on a substrate made of various materials including plastic, glass, metal, or silicon including organic polymer materials.

As used herein, the term "microchannel" refers to a channel of microscopic size having a dimension of millimeter, micrometer, or nanometer through which fluid can flow.

As used herein, the term "insert" may refer to an object in a shape that is capable of being inserted into a groove formed in another object, but is not limited thereto.

In some embodiments, the insert is detachable from the base, and the base may comprise a groove into which the insert is capable of being inserted. Preferably, the insert comprises a first fastening head, the base comprises a second fastening head, wherein the first fastening head and the second fastening head are hooked to each other so that the insert and the base can be attached and detached by a snap fit. In this case, in order to prevent leakage between the first central channel and the second central channel, the porous membrane may serve as a gasket by receiving a strong pressure between the insert and the base.

As used herein, the term "fastening head" may be made of a material having elasticity such as plastic, rubber, silicon and the like, and each may be elastically deformed to achieve the attachment and detachment by a snap fit, but is not limited thereto.

As used herein, the term "snap fit" refers to a fastening manner in which a fastening force is formed by the interaction of grooves that are hooked to each other without additional parts or fastening instruments.

In some embodiments, the third side channel and the fourth side channel do not contact the porous membrane. Preferably, the third side channel and the fourth side channel may have a lower height than that of the second central channel, and more preferably, the ratio of the height of the second central channel to the height of the third side channel and the fourth side channel may be between 1:0.1 and 1:0.9.

In some embodiments, the first central channel, the second central channel, the third side channel, and the fourth side channel comprise an inlet and an outlet capable of inducing and

controlling the perfusion of the liquid agent. The method capable of inducing and controlling the perfusion may include a method of using a hydrostatic pressure difference between the inlet and the outlet, and a method of connecting an external pump to the inlet and the outlet, but is not limited thereto.

In some embodiments, the fifth passage channel and the sixth passage channel have a lower channel height than those of the second central channel, the third side channel, and the fourth side channel. Preferably, the ratio of the height of the second central channel and the height of the fifth passage channel and the sixth passage channel may be between 1:0.03 and 1:0.2, and the ratio of the height of the third side channel and the fourth side channel and the height of the fifth passage channel and the sixth passage channel may be between 1:0.03 and 1:0.7.

In some embodiments, the base comprises a first fluid reservoir and a second fluid reservoir. In addition, the base may comprise a seventh passage channel connecting the third side channel and the first fluid reservoir, and an eighth passage channel connecting the fourth side channel and the second fluid reservoir. Preferably, the seventh passage channel and the eighth passage channel may have a lower channel height than those of the second central channel, the third side channel, and the fourth side channel. Preferably, the ratio of the height of the second central channel and the height of the seventh passage channel and the eighth passage channel may be between 1:0.02 and 1:0.05, and the ratio of the height of the third side channel and the fourth side channel and the height of the seventh passage channel and the eighth passage channel may be between 1:0.02 and 1:0.5. More preferably, the height of the seventh passage channel and the eighth passage channel may be 50 μm or less.

In some embodiments, the seventh passage channel and the eighth passage channel are perpendicular to the direction of the second central channel.

In some embodiments, the microfluidic device is made of plastic, glass, metal, or silicon, but is not limited thereto. Preferably, it may be made of plastic using injection molding technology.

In some embodiments, the first central channel comprises tissue barrier cells. The tissue barrier cells may include vascular endothelial cells; skin cells; cancer cells; secretory gland cells; muscle cells; and epithelial cells of bronchi, large intestine, small intestine, pancreas, and kidney. Preferably, it may be a vascular endothelial cell. More preferably, it may be a human brain microvascular endothelial cell (HBMEC).

As used herein, the term "cell" refers to a biological cell, including a plant cell, an animal cell (such as, a mammalian cell), a bacterial cell and a fungal cell and the like.

As used herein, the term "tissue barrier cell" refers to a cell that plays a role in maintaining a specific structure of a tissue, and plays a role in protecting the tissue from external stimuli. In

addition, it refers to a cell that plays a role in selectively permeating a substance using a strong binding force between tissue barrier cells or an extracellular matrix, and maintaining homeostasis in the concentration of the substance in the tissue. The tissue barrier cells include epithelial tissue cells and vascular endothelial cells.

In some embodiments, the second central channel comprises internal tissue cells and hydrogel.

The internal tissue cells may include astrocytes, pericytes, nerve cells, neural stem cells, glial cells, cardiac myocytes, smooth muscle cells, intestinal epithelial cells, keratinocytes, skin fibroblasts, podocytes, and glomerular endothelial cells. Preferably, it may be an astrocyte and a pericyte. More preferably, it may be a human astrocyte (HA) and a human brain vascular pericyte (HBVP).

As used herein, the term "internal tissue cell" refers to a cell that makes up the organs and tissues of the human body, and includes all cells that make up the human body tissue including, but not limited to, epithelial tissue, muscle tissue, nervous tissue, or connective tissue.

The hydrogel may be one or more selected from the group consisting of collagen, laminin, hyaluronic acid, mineral, fibrin, fibronectin, elastin, peptide, polyethylene glycol, and alginate. Preferably, the hydrogel may be collagen gel, fibrin gel, laminin gel, Matrigel, animal derived tumor basement membrane extract gel, tissue decellularized extracellular matrix gel, peptide gel, polyethylene glycol gel, or alginate gel, but is not limited thereto. More preferably, it is laminin gel or Matrigel.

The hydrogel may be spatially confined in the second central channel by surface tension due to a height difference between the second central channel and the fifth passage channel and a height difference between the second central channel and the sixth passage channel.

As used herein, the term "hydrogel" is a hydrophilic polymer crosslinked by cohesive force such as covalent bonds, hydrogen bonds, van der waals bonds, or physical bonds, and refers to a material having a three-dimensional polymer network structure that is capable of swelling since it contains a large amount of water in an aqueous solution therein.

In some embodiments, each of one or more cells selected from the group consisting of cells included in the first central channel, cells included in the second central channel, and cells attached to the porous membrane are separated by separating the insert from the base, and cell analysis such as gene analysis may be performed using the separated cells.

In some embodiments, the insert is capable of being separated from the base, and being subjected to a necessary treatment such as drug application to the first central channel, and then being reassembled to the base to observe a cellular reaction.

The present disclosure provides a method of culturing cells in a microfluidic device, the method comprising a step of assembling a microfluidic device, wherein the microfluidic device is comprises an insert comprising a first central channel; a base comprising a second central channel, a third side channel, and a fourth side channel; and a porous membrane positioned between the insert and the base, wherein the insert is detachable from the base; a step of injecting second cells into the second central channel and then inverting the microfluidic device and culturing them; a step of injecting hydrogel comprising third cells into the second central channel and then culturing them; and a step of inverting the microfluidic device and then injecting first cells into the first central channel and culturing them.

In some embodiments, the first central channel, the second central channel, the third side channel, and the fourth side channel include an inlet and an outlet capable of inducing and controlling the perfusion of the liquid agent, and the second cells and the hydrogel comprising the third cells may be injected through the inlet of the second central channel, and the first cells may be injected through the inlet of the first central channel.

In some embodiments, the first cells are selected from the group consisting of vascular endothelial cells; skin cells; cancer cells; secretory gland cells; muscle cells; and epithelial cells of bronchi, large intestine, small intestine, pancreas, or kidney; the second cells may be selected from the group consisting of pericytes, glial cells, cardiac myocytes, smooth muscle cells, intestinal epithelial cells, keratinocytes, skin fibroblasts, podocytes, and glomerular endothelial cells; and the third cells may be selected from the group consisting of astrocytes, nerve cells, and neural stem cells. Preferably, the first cells may be vascular endothelial cells, the second cells may be pericytes, and the third cells may be astrocytes. More preferably, the first cells may be human brain microvascular endothelial cells (HBMEC), the second cells may be human brain vascular pericytes (HBVP), and the third cells may be human astrocytes (HA).

The present disclosure provides a method of culturing cells in a microfluidic device, the method comprising a step of assembling a microfluidic device, wherein the microfluidic device is comprises an insert comprising a first central channel; a base comprising a second central channel, a third side channel, and a fourth side channel; and a porous membrane positioned between the insert and the base, wherein the insert is detachable from the base; a step of injecting 1 to 50 μl of human brain vascular pericytes (HBVP) at a concentration of 10^4 cells/ml or more into the second central channel and then inverting the microfluidic device and culturing them; a step of injecting hydrogel comprising 1 to 50 μl of human astrocytes (HA) at a concentration of 10^3 cells/ml or more into the second central channel and then culturing them; and a step of inverting the microfluidic device and then injecting 1 to 50 μl of human brain microvascular endothelial cells (HBMEC) at a

concentration of 10^5 cells/ml or more into the first central channel and culturing them.

The present disclosure provides a method of simulating an organ or a body part in a microfluidic device, wherein the microfluidic device is comprises an insert comprising a first central channel; a base comprising a second central channel, a third side channel, a fourth side channel, a first fluid reservoir, and a second fluid reservoir; and a porous membrane positioned between the insert and the base, wherein the insert is detachable from the base, wherein the method comprises a step of perfusing a first fluid through the first central channel; and a step of injecting a second fluid into the first fluid reservoir to sequentially reach the third side channel, the second central channel, the fourth side channel, and the second fluid reservoir. The organ or body part may include blood–brain barrier, lung, liver, heart, retina, large intestine, small intestine, pancreas, and kidney, but is not limited thereto. Preferably, the organ or body part is blood–brain barrier (BBB).

In some embodiments, the base comprises a fifth passage channel connecting the second central channel and the third side channel, a sixth passage channel connecting the second central channel and the fourth side channel, a seventh passage channel connecting the third side channel and the first fluid reservoir, and an eighth passage channel connecting the fourth side channel and the second fluid reservoir.

In some embodiments, the first fluid is perfused with a shear stress of 1 to 10 dyne/cm^2, and preferably, it may be perfused with a shear stress of 4 to 6 dyne/cm^2. The flow of the first fluid may play a role in simulating the flow of blood *in vivo*.

In some embodiments, the flow rate of the second fluid is maintained at 1 to 100 μl/h for at least 12 hours by using the hydrostatic pressure difference between the first fluid reservoir and the second fluid reservoir, and preferably, it may be maintained at 10 to 15 μl/h. The flow of the second fluid may play a role in simulating the interstitial flow *in vivo*.

The present disclosure provides a method of analyzing physiological, pharmacological or toxicological effects of an agent, said method comprising: a) providing a microfluidic device according to Claim 1; b) introducing the agent into the microfluidic device; and c) evaluating physiological, pharmacological or toxicological effects of the agent. The above agent may include a drug, toxin or pathogen.

Hereinafter, the microfluidic device of the present disclosure will be described in detail with reference to the drawings. The present disclosure may include a microfluidic device embodied in the form of Figs. 1 to 25, but is not limited thereto. In particular, although specific examples of the microfluidic device of the present disclosure are illustrated in Figs. 12 to 25, the present disclosure is not limited to the specific examples, and includes various modifications capable of being made by those of ordinary skill in the art to which the present disclosure belongs.

The microfluidic device according to one example of the present disclosure comprises an insert (100), a base (200), and a porous membrane (300) positioned between the insert (100) and the base (200).

Referring to Fig. 1, the insert (100) comprises a first central channel (110), and the base (200) comprises a second central channel (210), a third side channel (220), a fourth side channel (230), a fifth passage channel (240) connecting the second central channel (210) and the third side channel (220), and a sixth passage channel (250) connecting the second central channel (210) and the fourth side channel (230). In some embodiments, a bottom part (400) is attached to the lower end of the base (200).

Referring to Figs. 2 and 3, the base (200) of the microfluidic device may comprise a first fluid reservoir (280) and a second fluid reservoir (290), and it may comprise a seventh passage channel (260) connecting the third side channel (220) and the first fluid reservoir (280), and an eighth passage channel (270) connecting the fourth side channel (230) and the second fluid reservoir (290).

Referring to Figs. 4 and 5, the porous membrane (300) of the microfluidic device exists between the first central channel (110) and the second central channel (210), and the seventh passage channel (260) and the eighth passage channel (270) may be formed perpendicular to the direction of the second central channel (210).

Referring to Figs. 6 and 7, the first central channel (110) of the microfluidic device may comprise first cells (111), and a second central channel (210) may comprise second cells (211), third cells (212), and/or hydrogel (213). In some embodiments, the first cells (111) are attached to the upper surface of the porous membrane (300) to be cultured, and the second cells (211) may be attached to the lower surface of the porous membrane (300) to be cultured, and the third cells (212) may be 3D cultured inside the hydrogel (213).

Referring to Figs. 8 to 10 and Fig. 18, the base (200) of the microfluidic device comprises an insert insertion groove (201) into which the insert (100) is capable of being inserted, so that the insert (100) can be detachable from the base (200). In addition, the insert (100) comprises a first fastening head (101), and the base (200) comprises a second fastening head (202), and the first fastening head (101) and the second fastening head (202) are hooked to each other so that the insert (100) and the base (200) can be attached and detached by a snap fit.

Referring to Figs. 12 and 13, the insert (100) of the microfluidic device may comprise an inlet (112) and an outlet (113) of the first central channel, an inlet (214) and an outlet (215) of the second central channel, an inlet (221) and an outlet (222) of the third side channel, and an inlet (231) and an outlet (232) of the fourth side channel. The inlet (112) and the outlet (113) of the first

central channel may be connected to the first central channel (110) in a tube shape, and the precise measurement of the TEER value may be possible by inserting the electrode at a certain position and depth through the tube.

Referring to Figs. 14 to 16 and Fig. 19, the base (200) of the microfluidic device may be a structure to which one or more inserts (100) are detachable. Preferably, it may be a structure to which the four inserts (100) are detachable.

Referring to Figs. 17 and 23, the microfluidic device may comprise a cover (500). The cover (500) may comprise an inlet (501) and an outlet (502) of the first central channel in the cover. The inlet (501) and the outlet (502) of the first central channel in the cover may be in an openable form in order to prevent leakage of fluid.

Referring to Fig. 24, a fluid is injected through the inlet (112) of the first central channel included in the insert (100) of the microfluidic device, and the fluid may be perfused in the direction of the outlet (113) of the first central channel through the first central channel (110).

Referring to Figs. 11 and 25, by injecting a fluid into the first fluid reservoir (280) included in the base (200) of the microfluidic device, the fluid may be sequentially perfused through the third side channel (220), the second central channel (210), the fourth side channel (230), and the second fluid reservoir (290). Preferably, by injecting a fluid into the first fluid reservoir (280) included in the base (200) of the microfluidic device, the fluid may be sequentially perfused through the seventh passage channel (260), the third side channel (220), the fifth passage channel (240), the second central channel (210), the sixth passage channel (250), the fourth side channel (230), the eighth passage channel (270), and the second fluid reservoir (290).

The present disclosure is to be described in more detail through the following examples, but the following examples are for illustrative purposes only and are not intended to limit the scope of the present disclosure.

Example 1: Culture and viability of endothelial cells, pericytes, and astrocytes

In order to optimize the culture conditions for co-culture of human brain microvascular endothelial cells (HBMEC), human brain vascular pericytes (HBVP), and human astrocytes (HA), the metabolic activity of each cell was compared using the MTS (3-(4,5-dimethylthiazol-2-yl)-5-(3-carboxymethoxyphenyl)-2-(4-sulfophenyl)-2H-tetrazolium) analysis method under six medium conditions. The six medium conditions are as follows, and the glial cell medium (G) refers to 1:1 mixture of astrocyte medium (A) and microglia medium (M).

(i) E : endothelial medium

(ii) A : astrocyte medium

(iii) P : pericyte medium

(iv) M : microglia medium

(v) E+G (E+A+M): 1:1:1 mixture of endothelial medium (E), astrocyte medium (A), and microglia medium (M)

(vi) E+G+P (E+A+M+P): 1:1:1:1 mixture of endothelial medium (E), astrocyte medium (A), microglia medium (M), and pericyte medium (P)

Human brain microvascular endothelial cells (HBMEC), human brain vascular pericytes (HBVP) and human astrocytes (HA) were cultured for 3 days under the six medium conditions, and then CellTiter 96 AQueous One Solution Cell Proliferation Assay (Promega, Madison, WI, USA) was added to each cell. After 4 h of incubation, the optical absorbance of each sample was measured at 490 nm using Cytation 5 plate reader (BioTek, Winooski, VT, USA). Data represent mean ± s.d. of n = 6 by student t-test (*$p < 0.05$, ****$p < 0.001$).

As shown in Fig. 26, it was confirmed that the cell culture of human brain microvascular endothelial cells (HBMEC), human brain vascular pericytes (HBVP), or human astrocytes (HA) was more excellent when cultured in E+G (E+A+M) medium, which a mixed medium, than when cultured in endothelial medium (E), pericyte medium (P), or astrocyte medium (A), which is its respective culture medium.

In addition, as shown in Figs. 27 and 28, it was confirmed that both human brain microvascular endothelial cells (HBMEC) and human brain vascular pericytes (HBVP) had excellent viability in E+G and E+G+P media, and human astrocytes (HA) had excellent viability in E+G medium.

According to the above experiment results, in the following examples, cell culture was carried out using E+G (E+A+M) medium, which is 1:1:1 mixture of endothelial medium (E), astrocyte medium (A), and microglia medium (M).

Example 2: Preparation of microfluidic device simulating blood–brain barrier (BBB)

Using the assembled microfluidic device, a microfluidic device simulating blood–brain barrier (BBB) was prepared in the following manner.

As shown in Fig. 29, 10 μl of human brain vascular pericytes (HBVP) at a concentration of 10^6 to 10^7 cells/ml was injected into the second central channel, and incubated for 1 h so that the pericytes could be evenly attached to the surface of the porous membrane by inverting the microfluidic device, and then the culture solution was replaced. After at least 6 h, 10 μl of human astrocytes (HA) at a concentration of 10^5 to 10^6 cells/ml embedded in Matrigel was injected into the second central channel. The culture was carried out for 1 h so that Matrigel was hardened, and the

culture solution was injected into the third side channel and the fourth side channel, and then the culture was carried out for at least 6 h. The microfluidic device was inverted again, and then 15 μl of human brain microvascular endothelial cells (HBMEC) at a concentration of 7×10^7 cells/ml was injected into the first central channel and cultured for 1 h, and then the culture solution was replaced.

Example 3: Confirmation of expression level of blood–brain barrier (BBB) specific protein

In order to test a three-dimensional tissue barrier function of the microfluidic device simulating blood–brain barrier (BBB) prepared in Example 2 comprising human brain microvascular endothelial cells (HBMEC), human brain vascular pericytes (HBVP) and human astrocytes (HA), the expression level of the blood–brain barrier specific protein was confirmed through qRT-PCR analysis. For comparison, the protein expression was confirmed together when only human brain microvascular endothelial cells (HBMEC) were single-cultured.

RNA from HBMECs and HAs were isolated and collected using the RNeasy Mini kit (Qiagen GmBH, Hilden, Germany), and the amount of collected RNA samples were measured by Cytation 5 plate reader. 800 ng of HBMEC RNA and 280 ng of HA RNA were reverse-transcribed into cDNA with T100 Thermal Cycler (Bio-Rad, Hercules, CA, USA) using High-capacity cDNA Reverse Transcription kit (Applied Biosystems, Foster City, CA, USA). To analyze endothelial specific gene expressions in HBMECs (n= 3), microfluidic qRT-PCR was performed with Flex Six IFC (Fluidigm, South San Francisco, CA, USA) using the Fluidigm Biomark system (Fluidigm). The target genes were assessed using commercially available primers, the primers used in the experiment are shown in Table 1 below.

Table 1

Experiment	Gene Symbol	Gene Name	TaqMan Assay ID #
Control	GAPDH	Glyceraldehyde-3-phosphate dehydrogenase	Hs02786624_g1
HBMEC Fluidigm	vWF	von Willebrand factor	Hs01109446_m1
	SELE	Selectin E	Hs00174057_m1
	PECAM1	Platelet and endothelial cell adhesion molecule 1	Hs01065279_m1
	VECAD	Cadherin 5 (CDH5)	Hs00901465_m1
	OCLN	Occludin	Hs00170162_m1
	ZO-1	Tight junction protein 1 (TJP1)	Hs01551861_m1
	CAT1	Solute carrier family 7 member 1 (SLC7A1)	Hs00931450_m1
	LAT1	Solute carrier family 7 member 5 (SLC7A5)	Hs00185826_m1
	OCT1	Solute carrier family 22 member 1 (SLC22A1)	Hs00427552_m1
	GLUT1	Solute carrier family 2 member 1 (SLC2A1)	Hs00892681_m1

	CERP	ATP binding cassette subfamily A member 1 (ABCA1)	Hs01059137_m1
	P-GP	ATP binding cassette subfamily B member 1 (ABCB1)	Hs00184500_m1
	MRP1	ATP binding cassette subfamily C member 1 (ABCC1)	Hs01561483_m1
	LRP1	LDL receptor related protein 1	Hs00233856_m1
	AGER	Advanced glycosylation end-product receptor	Hs00542584_g1
	ICAM1	Intercellular adhesion molecule 1	Hs00164932_m1
	VCAM1	Vascular cell adhesion molecule 1	Hs01003372_m1

As shown in Fig. 30, it was confirmed that the expression of all blood–brain barrier (BBB) specific proteins used in the evaluation, including proteins that control the regulation of junctional formation, carrier-mediated transport, active efflux or amyloid beta (Aβ) transport in the BBB, was increased in a microfluidic device simulating the BBB comprising human brain microvascular endothelial cells (HBMEC), human brain vascular pericytes (HBVP) and human astrocytes (HA) compared to when a single culture of only human brain microvascular endothelial cells (HBMEC) was carried out. In particular, as shown in Figs. 31 and 32, it was confirmed that the gene expression level of blood–brain barrier specific junctional proteins and receptor proteins was remarkably increased compared to when a single culture of endothelial cells was carried out.

Example 4: Comparison of TEER (Transendothelial electrical resistance) value

In order to test a three-dimensional tissue barrier function of the microfluidic device simulating blood–brain barrier (BBB) prepared in Example 2 comprising human brain microvascular endothelial cells (HBMEC), human brain vascular pericytes (HBVP) and human astrocytes (HA), the TEER (Transendothelial electrical resistance) value was measured. For comparison, the TEER value was confirmed together when a single culture of only human brain microvascular endothelial cells (HBMEC) was carried out. TEER (Transendothelial electrical resistance) is a method of measuring the electrical resistance of a cell layer using Ohm's law, and is one of the factors indicating how the cell barrier made of the cell layer functions well. The stronger the cell layers bind to each other, the stronger the expression of the junction protein, which forms the binding between cells, and the paracellular material transport is limited, and thus the electrical resistance value is increased. The human blood–brain barrier is a barrier in which the material transport is extremely limited, and its TEER value is estimated to be 5000 $\Omega.cm^2$ [Lauschke K, Frederiksen L, Hall VJ (2017) Paving the way toward complex blood-brain barrier models using pluripotent stem cells. Stem Cells Dev 26(12):857–874], and the rat blood–brain barrier was measured to be 5900 $\Omega.cm^2$. [Butt AM, Jones HC, Abbott NJ (1990) Electrical resistance across the

blood-brain barrier in anaesthetized rats: a developmental study. J Physiol 429:47–62]

The TEER value of a barrier layer of the microfluidic device simulating blood–brain barrier (BBB) and a single culture layer of human brain microvascular endothelial cells (HBMEC) was measured using a custom electrode adapter made with Rj11 plug and Ag, Ag/AgCl electrode wires (381 μm in diameter and 3 cm in length, A-M Systems, Sequim, WA, USA) connected to EVOM2 volt-ohmmeter (Word Precision Instruments, Sarasota, FL, USA) which generates a constant 10 μA of AC current at 12.5 Hz. To reduce background resistance and error, the electrode wires were placed in a tygon tubing (1/32“ID x 3/32“OD, Cole-Parmer, Vernon Hills, IL, USA) filled with culture medium and inserted into the channels. After 1 min of stabilization, 5 multiple readings were averaged for each device. To calculate TEER, the measurements in the absence of the cells were subtracted from the resistance of each device, and then the values were multiplied by the surface area of layer.

As shown in Fig. 33, the TEER value in the microfluidic device simulating blood–brain barrier (BBB) was higher compared to when a single culture of human brain microvascular endothelial cells (HBMEC) was carried out, and thus it was confirmed that the blood–brain barrier (BBB) could be better simulated when human brain microvascular endothelial cells (HBMEC), human brain vascular pericytes (HBVP) and human astrocytes (HA) were cultured together.

Example 5: Comparison of TEER value according to the difference in shear stress of blood simulation flow

In order to test the difference in a three-dimensional tissue barrier function according to the shear stress of blood simulation flow applied to the first central channel of the microfluidic device simulating blood–brain barrier (BBB) prepared in Example 2, each TEER (Transendothelial electrical resistance) value was measured by the same method as in Example 4 when no shear stress was applied to the first central channel, when a shear stress of 0.4 dyne cm^{-2} was applied, and when a shear stress of 4 dyne cm^{-2} was applied.

As a result, as shown in Fig. 34, it was confirmed that when a shear stress of 4 dyne cm^{-2} was applied, when a shear stress of 0.4 dyne cm^{-2} was applied, and when no shear stress was applied, the TEER values were sequentially high.

Example 6: Comparison of permeability coefficient

In order to test a three-dimensional tissue barrier function of the microfluidic device simulating blood–brain barrier (BBB) prepared in Example 2 comprising human brain microvascular endothelial cells (HBMEC), human brain vascular pericytes (HBVP) and human

astrocytes (HA), the permeability coefficient was measured from the diffusion of 4 kDa and 40 kDa FITC-dextran. For comparison, the permeability coefficient was confirmed together when cells were not cultured and when only human brain microvascular endothelial cells (HBMEC) were single-cultured.

The cells in the microfluidic device were cultured for 60 h, and then the culture medium containing FITC-dextran (Sigma-Aldrich) of 4 kDa or 40 kDa at a concentration of 500 μg/mL was injected into the first central channel of the microfluidic device at a flow rate of 16 μL/min using PhD Ultra syringe pump (Harvard Apparatus). Simultaneously, culture medium from one side channel was sampled at 4 μL/min with a syringe pump for 1 h. Fluorescence intensities of 500 μg/mL of FITC-dextran solution and the sampled solutions are measured using a Cytation 5 plate reader (n = 4). The dextran concentrations (C) in the solutions were calculated with the measured fluorescence intensity values using a standard calibration curve, permeability coefficients (P) were calculated using the following equation.

$$P = V\frac{\frac{dC}{dt}}{\Delta C}$$

(V : the volume of the sampled solution, $\frac{dC}{dt}$: the concentration difference in the channel in the base over time, ΔC : the concentration difference across the barrier)

As shown in Fig. 35, it was confirmed that the three-dimensional tissue barrier of the microfluidic device simulating blood–brain barrier (BBB) comprising human brain microvascular endothelial cells (HBMEC), human brain vascular pericytes (HBVP) and human astrocytes (HA) exhibited remarkably low permeability coefficient at both 4 kDa and 40 kDa compared to when the cells were not cultured, and when only human brain microvascular endothelial cells (HBMEC) were single-cultured. That is, it was confirmed that when all three cells were cultured, they performed the function most similar to the blood–brain barrier.

Example 7: Comparison of structure and function of astrocytes according to culture method

In the astrocyte culture in the second central channel of the microfluidic device simulating blood–brain barrier (BBB) prepared in Example 2 comprising human brain microvascular endothelial cells (HBMEC), human brain vascular pericytes (HBVP) and human astrocytes (HA), the difference between 2D culture and 3D culture was compared. Preserving the morphological and physiological properties of healthy astrocytes plays an important role in simulating the function of the blood–brain barrier.

In order to compare the structure and function of human astrocytes (HA) in 2D and 3D

cultures, HAs were seeded at a density of 1×10^6 cells/mL in Matrigel (Growth factor-reduced; Corning, NY, USA) coated 24-wells and in 3D Matrigel (5 mg/mL). After 1 day of culture, cells were stimulated with 1 ng/mL or 10 ng/mL of recombinant human interleukin-1-beta (IL-1β; Gibco, Grand Island, NY, USA) and incubated for another 20 h for analysis.

Comparison of structure of astrocytes according to culture method

As shown in Figs. 36 to 38, when human astrocytes (HA) were cultured on the 2D Matrigel-coated surface, a flat polygonal enlarged cell body shape having short processes was shown. On the other hand, when human astrocytes (HA) were cultured inside the 3D Matrigel, a small cell body shape having thin and long processes distributed radially was observed.

Comparison of function of astrocytes according to culture method

The gene expression level of the reactive gliosis marker in 2D or 3D cultured human astrocytes (HA) was confirmed through qRT-PCR analysis. To analyze glial reactivity of HA in 2D and 3D culture system (n= 4), standard qRT-PCR was performed with a StepOnePlus Real-Time PCR system (Applied Biosystems) using TaqMan Fast Universal PCR Master Mix (Applied Biosystems). The target genes were assessed using commercially available primers, and the primers used in the experiment are shown in Table 2 below.

Table 2

Experiment	Gene Symbol	Gene Name	TaqMan Assay ID #
Control	GAPDH	Glyceraldehyde-3-phosphate dehydrogenase	Hs02786624_g1
HA RT-qPCR	GFAP	Glial fibrillary acidic protein	Hs00909233_m1
	VIM	Vimentin	Hs00958111_m1
	LCN2	Lipocalin-2	Hs01008571_m1

As shown in Fig. 39, it was confirmed that the expression of vimentin (VIM) and lipocalin-2 (LCN2), which are reactive gliosis markers, was significantly reduced in 3D cultured human astrocytes (HA) compared to 2D cultured human astrocytes (HA). LCN2 is a gene that plays an important role in neuroinflammation by mediating the pro-inflammatory response, and is known to increase its expression in reactive astrocytes. On the other hand, there was no significant difference in the expression level of glial fibrillary acidic protein (GFAP), which is a representative astrocyte marker.

In addition, as shown in Figs. 40 and 41, it was confirmed that the expression level of LCN2 was dose-dependently controlled in both 2D and 3D cultures when treated with interleukin-1β (IL-1β), which is an inflammatory cytokine.

Therefore, it was confirmed that the 3D cultured human astrocytes (HA) exhibited similar morphology and gene expression to astrocytes *in vivo* compared to 2D culture, and thus were suitable for simulating the structure and function of the blood-brain barrier.

Example 8: Comparison of expression of AQP-4 and α-syn according to astrocyte culture method

In the astrocyte culture in the second central channel of the microfluidic device simulating blood–brain barrier (BBB) prepared in Example 2 comprising human brain microvascular endothelial cells (HBMEC), human brain vascular pericytes (HBVP) and human astrocytes (HA), the expression of Aquaporin-4 (AQP-4) and α-syn (α-syntrophin) according to 2D culture and 3D culture was compared. Astrocytes in the perivascular space control water homeostasis in the brain through AQP-4, which is a water channel protein of the terminal processes, and thus the polarization of AQP-4 in the astrocytic end-feet processes plays an important role in simulating the homeostasis control and physiological conditions of the blood-brain barrier. α-syn is known as an anchor that controls the polarization of AQP-4 to the astrocytic end-feet.

To visualize cell-specific marker expression, human astrocyte (HA) samples in 2D and 3D cultures cultured in Example 7 were fixed with 2% paraformaldehyde (PFA; Santa Cruz Biotechnology, San Diego, CA, USA) for 15 min at room temperature. After permeabilizing in 0.1% Triton X (Sigma-Aldrich) in PBS for 15 min, the samples were blocked with 2% bovine serum albumin (BSA; Sigma-Aldrich) in PBS for 1 h at room temperature. Subsequently, the samples were incubated with primary antibodies at 4 °C overnight, washed three times with 1% BSA. They were treated with GFAP, AQP4, and α-syn antibodies, respectively, at 4° C for 6 h. Nuclei were counterstained with 4,6-diamino-2-phenylindole (DAPI; Invitrogen) and stored in PBS before imaging. Fluorescently visualized samples were examined using a confocal microscope (LSM 700, Carl Zeiss, Oberkochen, Germany).

As shown in Figs. 42 and 43, it was confirmed that when astrocytes were cultured in 2D, AQP-4 and α-syn were expressed in a diffused form, whereas when cultured in 3D, they were polarized to the astrocytic end-feet.

Therefore, it was confirmed that the 3D cultured human astrocytes (HA) performed a function similar to that of the astrocytes *in vivo* compared to 2D culture, and thus was a suitable form in simulating the function of the blood-brain barrier.

Example 9: Comparison of AQP-4 expression according to cultured cells

The AQP-4 expression polarization level was confirmed in the microfluidic device

simulating blood–brain barrier (BBB) prepared in Example 2 comprising human brain microvascular endothelial cells (HBMEC), human brain vascular pericytes (HBVP) and human astrocytes (HA). For comparison, the AQP-4 expression was confirmed together when only human astrocytes (HA) were cultured, and when human astrocytes (HA) and human brain microvascular endothelial cells (HBMEC) were cultured.

After visualizing the AQP-4 expression in each sample in the same manner as in Example 8, distribution of AQP4 was quantified by measuring the fluorescence intensity profile along the z-axis in z-stack images of the perivascular channel using ImageJ (NIH, Bethesda, MD, USA). After calculating the average of the fluorescence intensity in each of the channel included in the insert (vascular) and the channel included in the base (parenchymal), the average of the fluorescence intensity in the channel included in the insert (vascular) was divided by the average of the fluorescence intensity in the channel included in the base (parenchymal) to calculate the AQP-4 polarization index.

As shown in Fig. 44, it was confirmed that the polarization level of AQP-4 was increased when human brain microvascular endothelial cells (HBMEC), human brain vascular pericytes (HBVP) and human astrocytes (HA) were cultured together (E+P+A) compared to when only human astrocytes (HA) were cultured (A) or when human astrocytes (HA) and human brain microvascular endothelial cells (HBMEC) were cultured (E+A).

Therefore, it was confirmed that the polarization of AQP-4 was significantly induced in the presence of pericytes, and it was confirmed that the water transport system of the blood–brain barrier (BBB) can be simulated when human brain microvascular endothelial cells (HBMEC), human brain vascular pericytes (HBVP) and human astrocytes (HA) are cultured together.

Example 10: Analysis of nanoparticle transport through blood–brain barrier (BBB)

The transport of nanoparticles through a structure simulating blood–brain barrier was monitored and quantified in the microfluidic device simulating blood–brain barrier (BBB) prepared in Example 2 comprising human brain microvascular endothelial cells (HBMEC), human brain vascular pericytes (HBVP) and human astrocytes (HA). In the study of drug delivery in the central nervous system, quantifying the transport of drug-containing compounds to the brain at the cellular and molecular level is an important task.

Synthesis of HDL mimicking nanoparticle eHNP-A1

HDL mimicking disc-shaped nanoparticle eHNP-A1 composed of lipid (DMPC), apolipoprotein A1, and a fluorescence marker was synthesized in a physiologically appropriate size

and configuration using microfluidic technology. The size distribution of the synthesized eHNP-A1 was measured and shown in Fig. 45.

Confirmation of biodistribution of systemically administered eHNP-A1

1 mg/kg of eHNP-A1 was systemically administered to the mouse via tail vein injection. Injection of 200 μL saline was served as control. 24 h after administration, mice were sacrificed and perfused with saline and 4% PFA for 15 min. Then organs (brain, heart, lung, liver, kidneys, and spleen) were harvested to visualize their DiR content using an *in vivo* imaging system (IVIS; Perkin Elmer, Waltham, MA, USA). To visualize the eHNP-A1 internalization inside the brain tissue, the harvested brain tissues were cryosectioned into 10 μm slices and stained with DAPI using the DAPI-containing antifade mounting medium (H-1200; Vector Laboratories, Burlingame, CA, USA). The slides were then imaged under a confocal microscope (Zeiss LSM 780).

As a result, as shown in Fig. 46, it was confirmed that the amount of eHNP-A1 accumulated in the brain was at most 3% of the systemic accumulation amount. In addition, as shown in Fig. 47, it was confirmed that the systemically administered eHNP-A1 was locally distributed around the cell nucleus of the brain.

Distribution of eHNP-A1 in microfluidic device simulating blood–brain barrier

In order to quantify the distribution of eHNP-A1 in the microfluidic device simulating blood–brain barrier (BBB) prepared in Example 2 and confirm material transport mechanism, eHNP-A1 in the first central channel (vascular) was incubated for 2 h. In addition, in order to test whether eHNP-A1 passes through the blood–brain barrier through transcytosis, one of the major transport mechanism of HDL, using scavenger receptor class B type 1 (SR-B1), an HDL receptor of brain endothelial cells, SR-B1 was blocked by treatment with BLT-1 (block lipid transporter-1). Thereafter, the relative fluorescence intensity of the culture medium comprising eHNP-A1 sampled from each of the first central channel (vascular) and the second central channel (perivascular) was measured. In addition, a FACS (fluorescence-activated cell sorting) analysis was performed on the distribution of human brain microvascular endothelial cells (HBMEC), human astrocytes (HA), and human brain vascular pericytes (HBVP), which are eHNP-A1 positive.

As shown in Figs. 48 and 49, after SR-B1 was blocked, the amount of eHNP-A1 remaining in the first central channel was significantly increased, whereas the amount of eHNP-A1 transported to the second central channel did not change significantly. In addition, as shown in Fig. 50, it was confirmed that the amount of eHNP-A1 absorbed by human brain microvascular endothelial cells (HBMEC) or transported to the second central channel upon treatment with BLT-1

was reduced by about 3 times, and as shown in Figs. 51 and 52, it was confirmed that the total eHNP-A1 positive cells were reduced upon treatment with BLT-1.

Therefore, it was confirmed that the interaction between cells and nanoparticles can be monitored and the distribution of nanoparticles can be quantified using the microfluidic device simulating blood–brain barrier (BBB) prepared in Example 2.

CLAIMS

1. A microfluidic device comprising:

an insert comprising a first central channel;

a base comprising a second central channel, a third side channel, a fourth side channel, a fifth passage channel connecting the second central channel and the third side channel, and a sixth passage channel connecting the second central channel and the fourth side channel; and

a porous membrane positioned between the insert and the base.

2. The microfluidic device according to claim 1, wherein the insert is detachable from the base.

3. The microfluidic device according to claim 1 or 2, wherein the base comprises a groove into which the insert is capable of being inserted.

4. The microfluidic device according to any one of claims 1-3, wherein the insert comprises a first fastening head,

the base comprises a second fastening head, and

the first fastening head and the second fastening head are hooked to each other so that the insert and the base are attached and detached by a snap fit.

5. The microfluidic device according to any one of claims 1-4, wherein the third side channel and the fourth side channel do not contact the porous membrane.

6. The microfluidic device according to any one of claims 1-5, wherein the first central channel, the second central channel, the third side channel, and the fourth side channel comprise an inlet and an outlet capable of inducing and controlling the perfusion of the liquid agent.

7. The microfluidic device according to any one of claims 1-6, wherein the fifth passage channel and the sixth passage channel have a lower channel height than the second central channel, the third side channel, and the fourth side channel.

8. The microfluidic device according to any one of claims 1-7, wherein the base further comprises a first fluid reservoir and a second fluid reservoir.

9. The microfluidic device according to claim 8, wherein the base comprises a seventh passage channel connecting the third side channel and the first fluid reservoir, and an eighth passage channel connecting the fourth side channel and the second fluid reservoir.

10. The microfluidic device according to claim 9, wherein the seventh passage channel and the eighth passage channel have a lower channel height than the second central channel, the third side channel, and the fourth side channel.

11. The microfluidic device according to claim 9 or 10, wherein the seventh passage channel and the eighth passage channel are formed perpendicular to the direction of the second central channel.

12. The microfluidic device according to any one of claims 1-11, wherein the microfluidic device is made of plastic, glass, metal, or silicon.

13. The microfluidic device according to any one of claims 1-12, wherein the first central channel comprises tissue barrier cells.

14. The microfluidic device according to claim 13, wherein the tissue barrier cells are one or more selected from the group consisting of vascular endothelial cells; skin cells; cancer cells; secretory gland cells; muscle cells; and epithelial cells of bronchi, large intestine, small intestine, pancreas, or kidney.

15. The microfluidic device according to any one of claims 1-14, wherein the second central channel comprises internal tissue cells and hydrogel.

16. The microfluidic device according to claim 15, wherein the internal tissue cells are one or more selected from the group consisting of astrocytes, pericytes, nerve cells, neural stem cells, glial cells, cardiac myocytes, smooth muscle cells, intestinal epithelial cells, keratinocytes, skin fibroblasts, podocytes, and glomerular endothelial cells.

17. The microfluidic device according to claim 15 or 16, wherein the hydrogel is one or more selected from the group consisting of collagen, laminin, hyaluronic acid, mineral, fibrin,

fibronectin, elastin, peptide, polyethylene glycol, and alginate.

18. The microfluidic device according to wherein 1-17, wherein each of one or more cells selected from the group consisting of cells included in the first central channel, cells included in the second central channel, and cells attached to the porous membrane is capable of being separated by separating the insert from the base.

19. A method of culturing cells in a microfluidic device, the method comprising:

a step of assembling a microfluidic device, wherein the microfluidic device is comprises an insert comprising a first central channel; a base comprising a second central channel, a third side channel, and a fourth side channel; and a porous membrane positioned between the insert and the base, wherein the insert is detachable from the base;

a step of injecting second cells into the second central channel and then inverting the microfluidic device and culturing them;

a step of injecting hydrogel comprising third cells into the second central channel and then culturing them; and

a step of inverting the microfluidic device and then injecting first cells into the first central channel and culturing them.

20. The method of culturing cells in a microfluidic device according to claim 19, wherein the first central channel, the second central channel, the third side channel, and the fourth side channel comprise an inlet and an outlet capable of inducing and controlling the perfusion of the liquid agent,

the second cells and the hydrogel comprising the third cells are injected through the inlet of the second central channel, and

the first cells are injected through the inlet of the first central channel.

21. The method of culturing cells in a microfluidic device according to claim 19 or 20, wherein the first cells are selected from the group consisting of vascular endothelial cells; skin cells; cancer cells; secretory gland cells; muscle cells; and epithelial cells of bronchi, large intestine, small intestine, pancreas, or kidney;

the second cells are selected from the group consisting of pericytes, glial cells, cardiac myocytes, smooth muscle cells, intestinal epithelial cells, keratinocytes, skin fibroblasts, podocytes, and glomerular endothelial cells; and

the third cells are selected from the group consisting of astrocytes, nerve cells, and neural stem cells.

22. A method of simulating an organ or a body part in a microfluidic device, wherein the microfluidic device is comprising an insert comprising a first central channel; a base comprising a second central channel, a third side channel, a fourth side channel, a first fluid reservoir, and a second fluid reservoir; and a porous membrane positioned between the insert and the base, wherein the insert is detachable from the base, wherein the method comprises

a step of perfusing a first fluid through the first central channel; and

a step of injecting a second fluid into the first fluid reservoir to sequentially reach the third side channel, the second central channel, the fourth side channel, and the second fluid reservoir.

23. The method of simulating an organ or a body part according to claim 22, wherein the base further comprises a fifth passage channel connecting the second central channel and the third side channel, a sixth passage channel connecting the second central channel and the fourth side channel, a seventh passage channel connecting the third side channel and the first fluid reservoir, and an eighth passage channel connecting the fourth side channel and the second fluid reservoir.

24. The method of simulating an organ or a body part according to claim 22 or 23, wherein the first fluid is perfused with a shear stress of 1 to 10 dyne/cm^2.

25. The method of simulating an organ or a body part according to any one of claims 22-24, wherein the flow rate of the second fluid is maintained at 1 to 100 μl/h for at least 12 hours by using the hydrostatic pressure difference between the first fluid reservoir and the second fluid reservoir.

26. A method of analyzing physiological, pharmacological or toxicological effects of an agent, said method comprising:

a) providing a microfluidic device according to Claim 1;

b) introducing the agent into the microfluidic device; and

c) evaluating physiological, pharmacological or toxicological effects of the agent.

27. The method of analyzing physiological, pharmacological or toxicological effects of an

agent according to claim 26, wherein the agent is a drug, toxin or pathogen.

Fig. 1

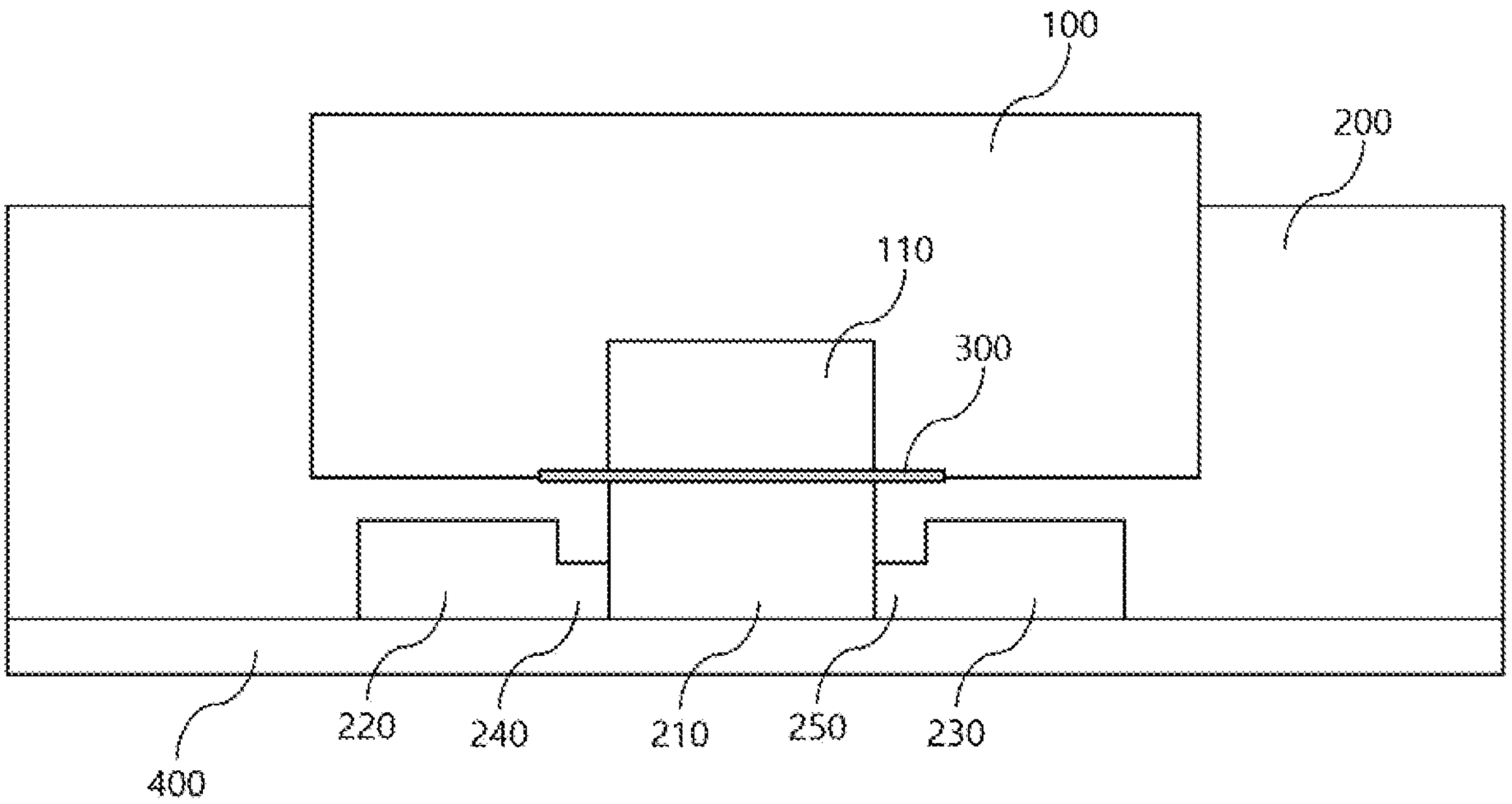

100
200
110
300
400
220
240
210
250
230

Fig. 2

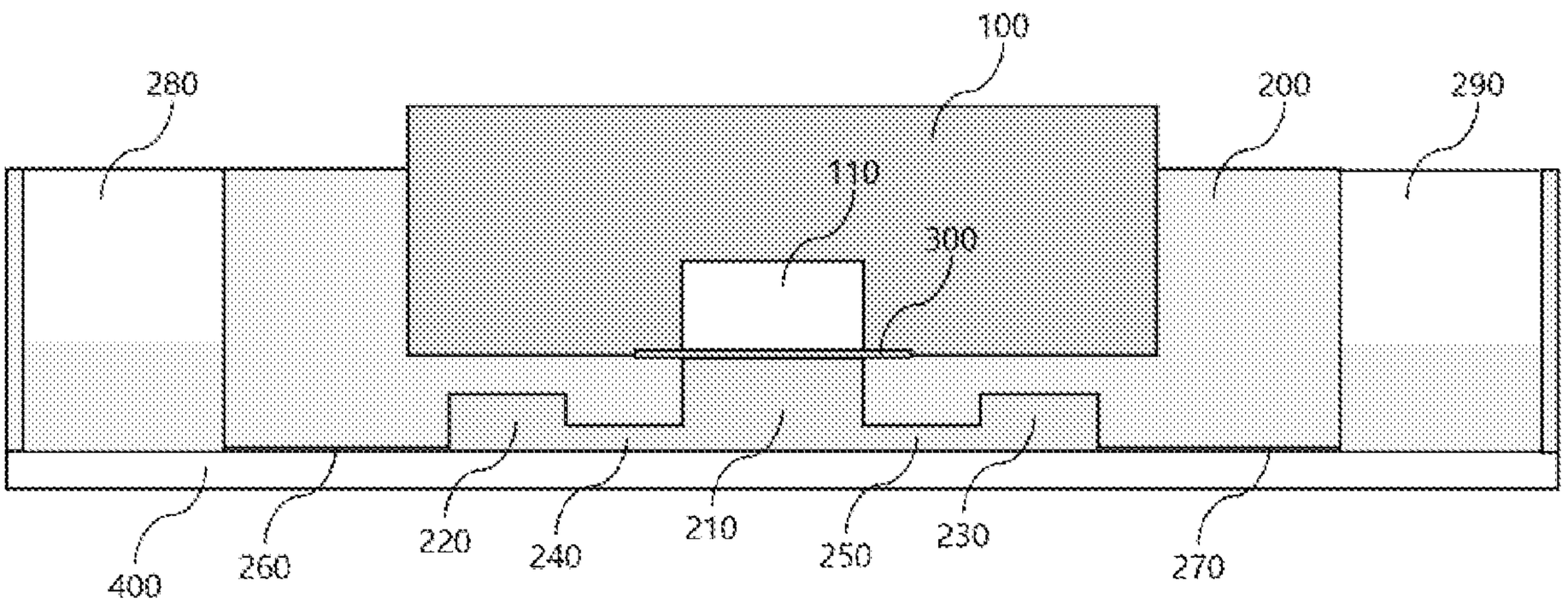

100
280
200
290
110
300
400
260
220
240
210
250
230
270

Fig. 3

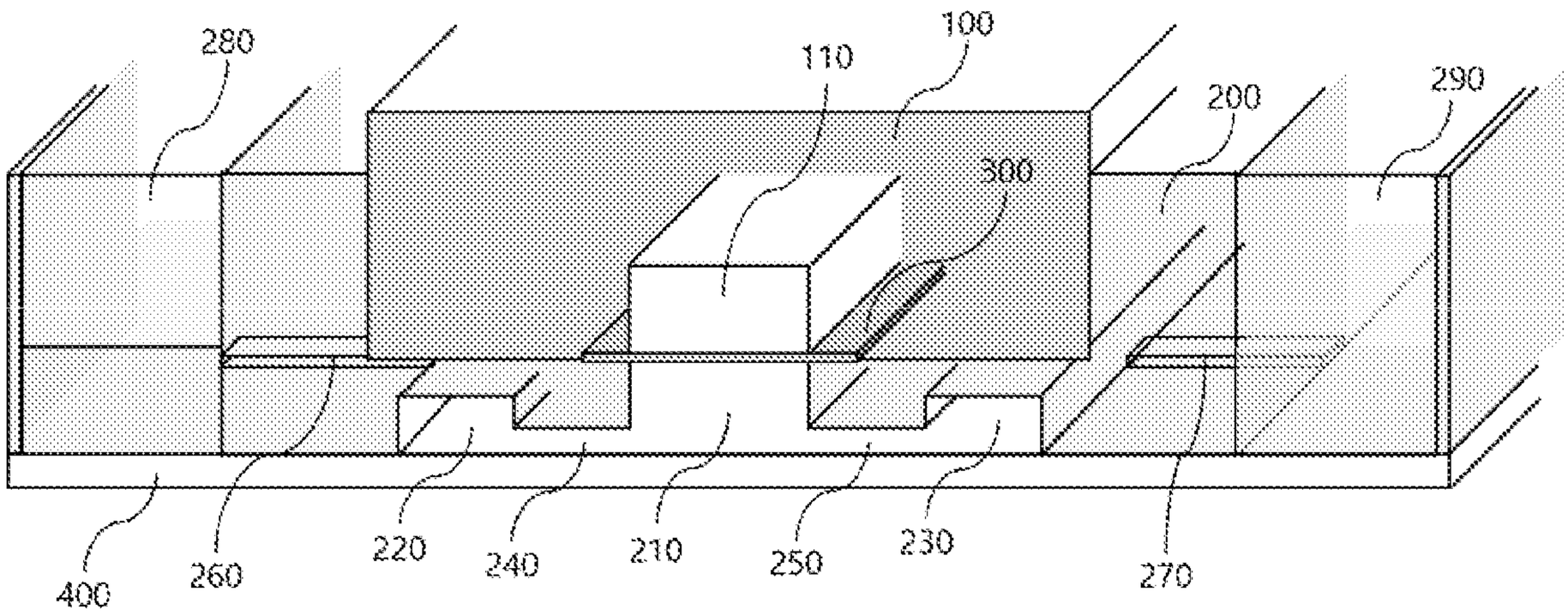

280
110
100
200
290
300
400
260
220
240
210
250
230
270

Fig. 4

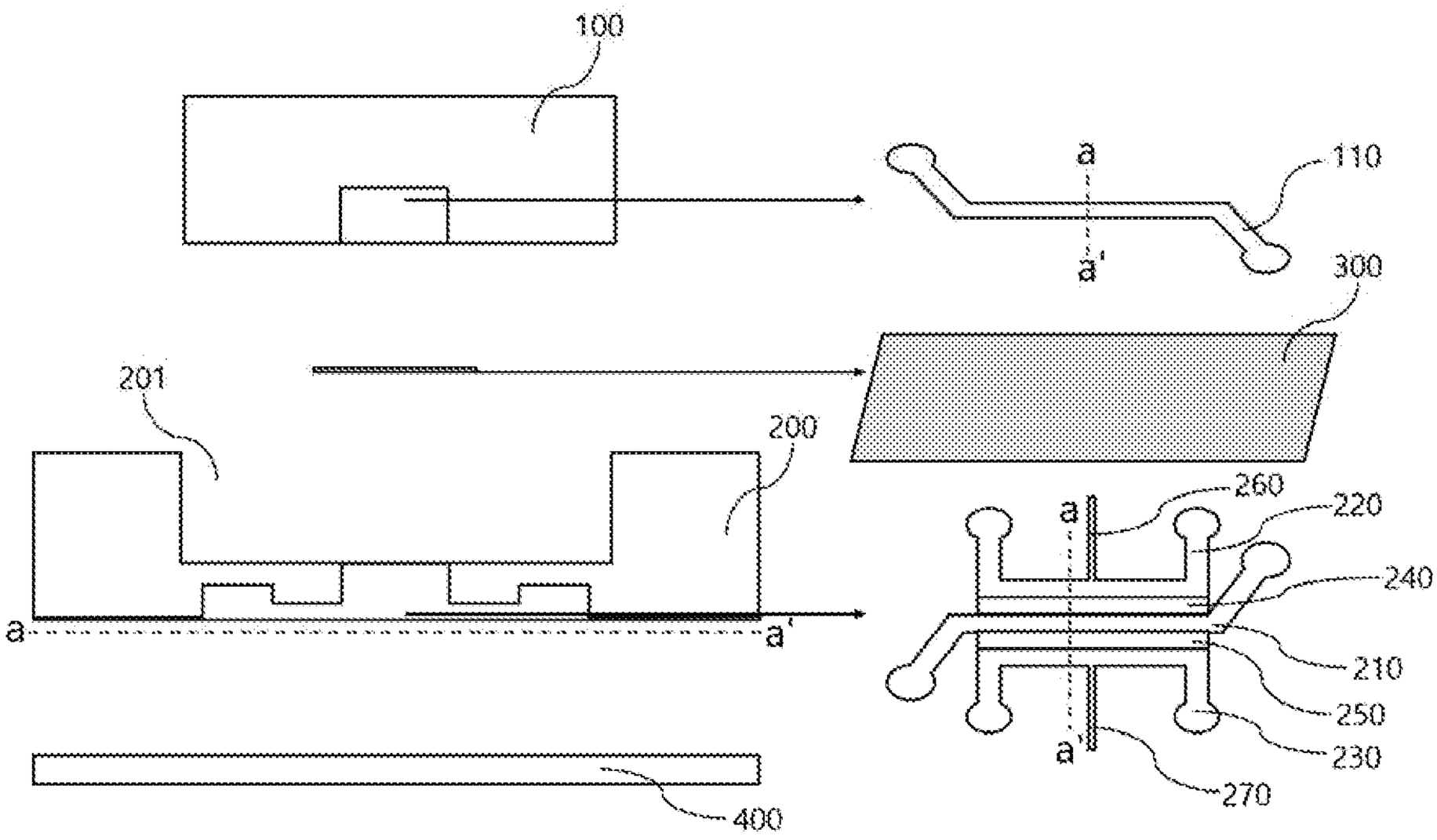

100
a
110
a'
300
201
200
260
220
240
210
250
230
270
400

Fig. 5

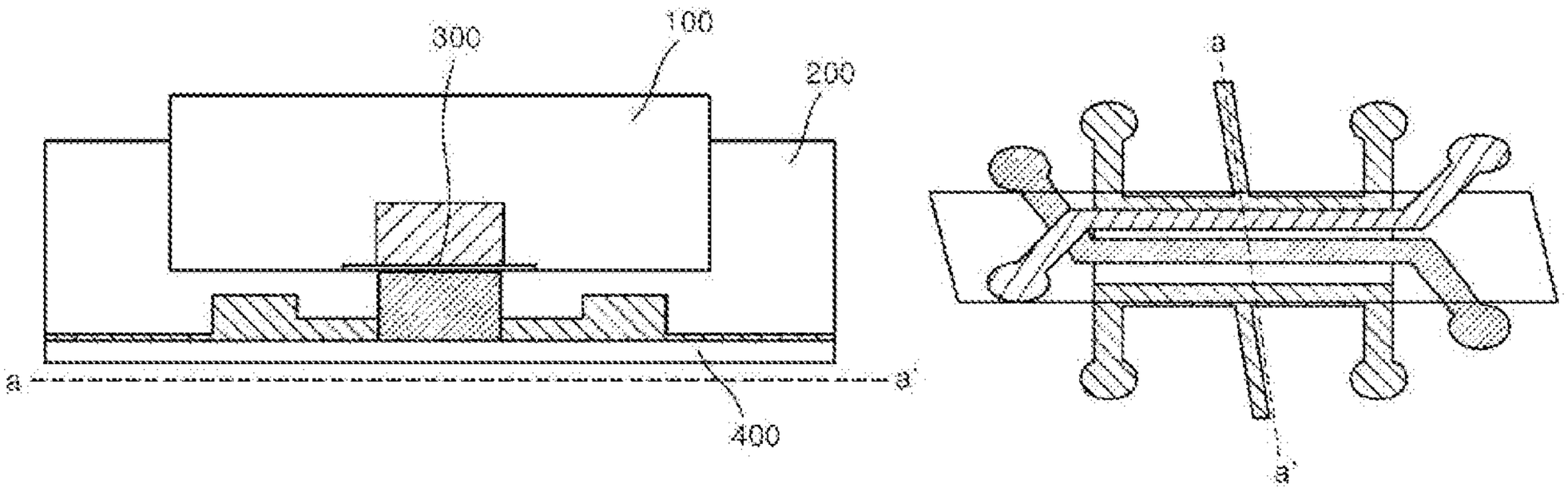


Fig. 6

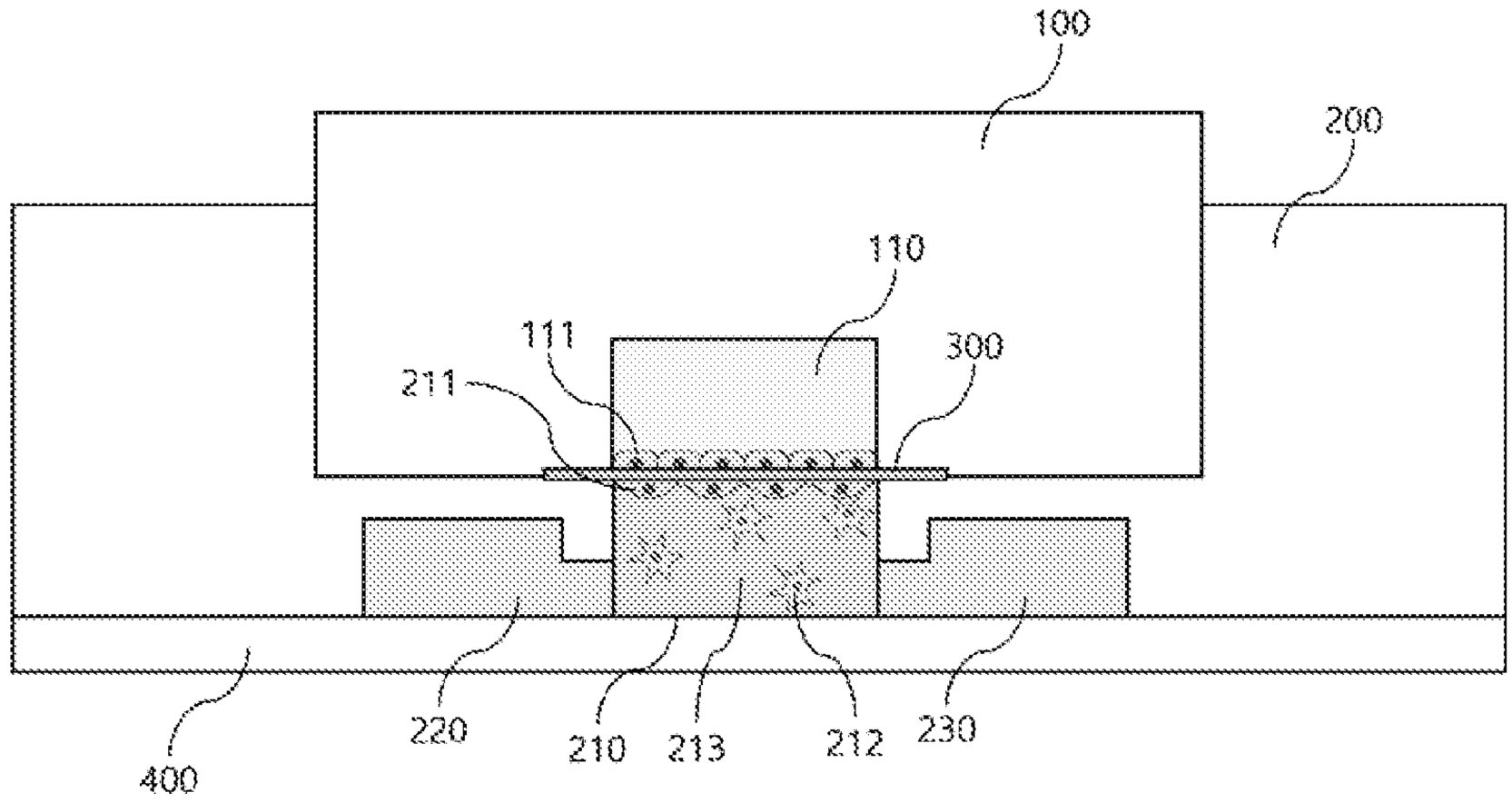


Fig. 7

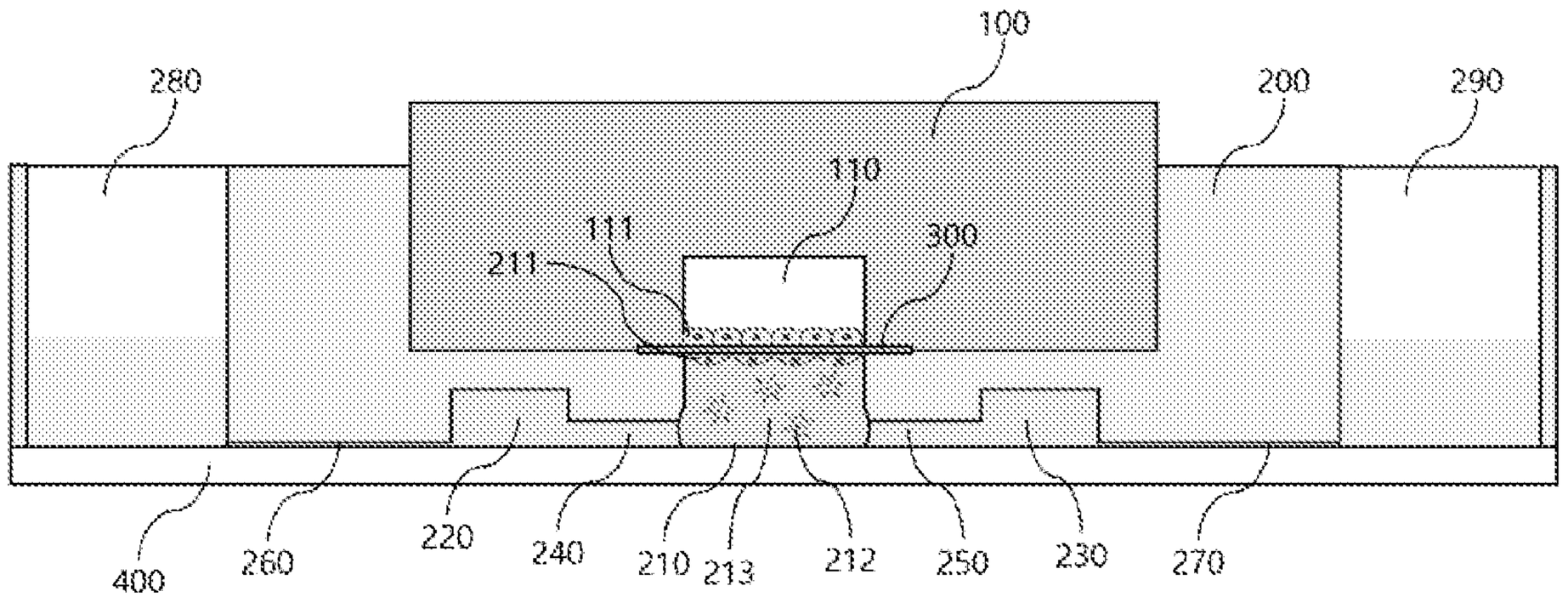


Fig. 8

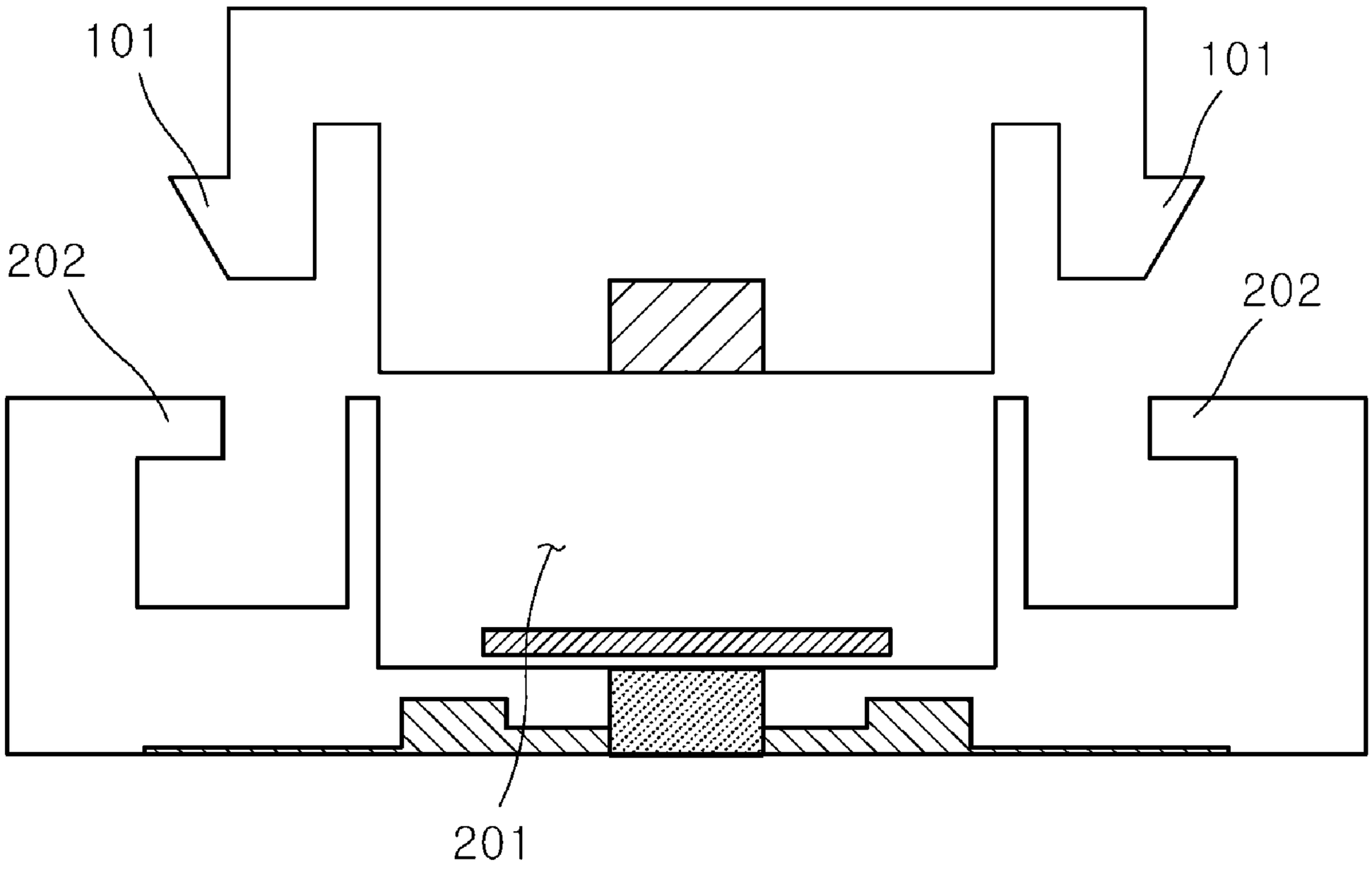


Fig. 9

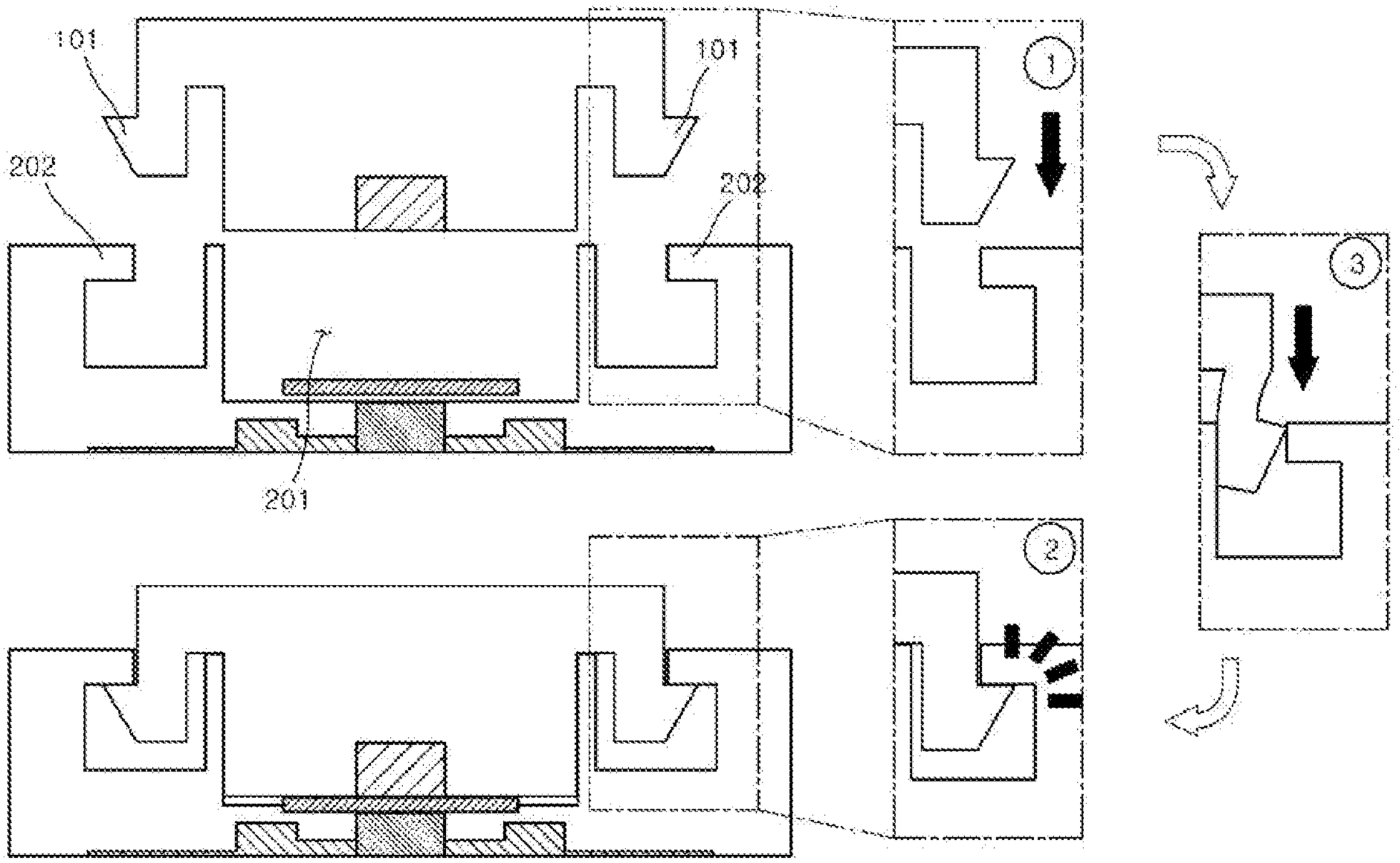


Fig. 10

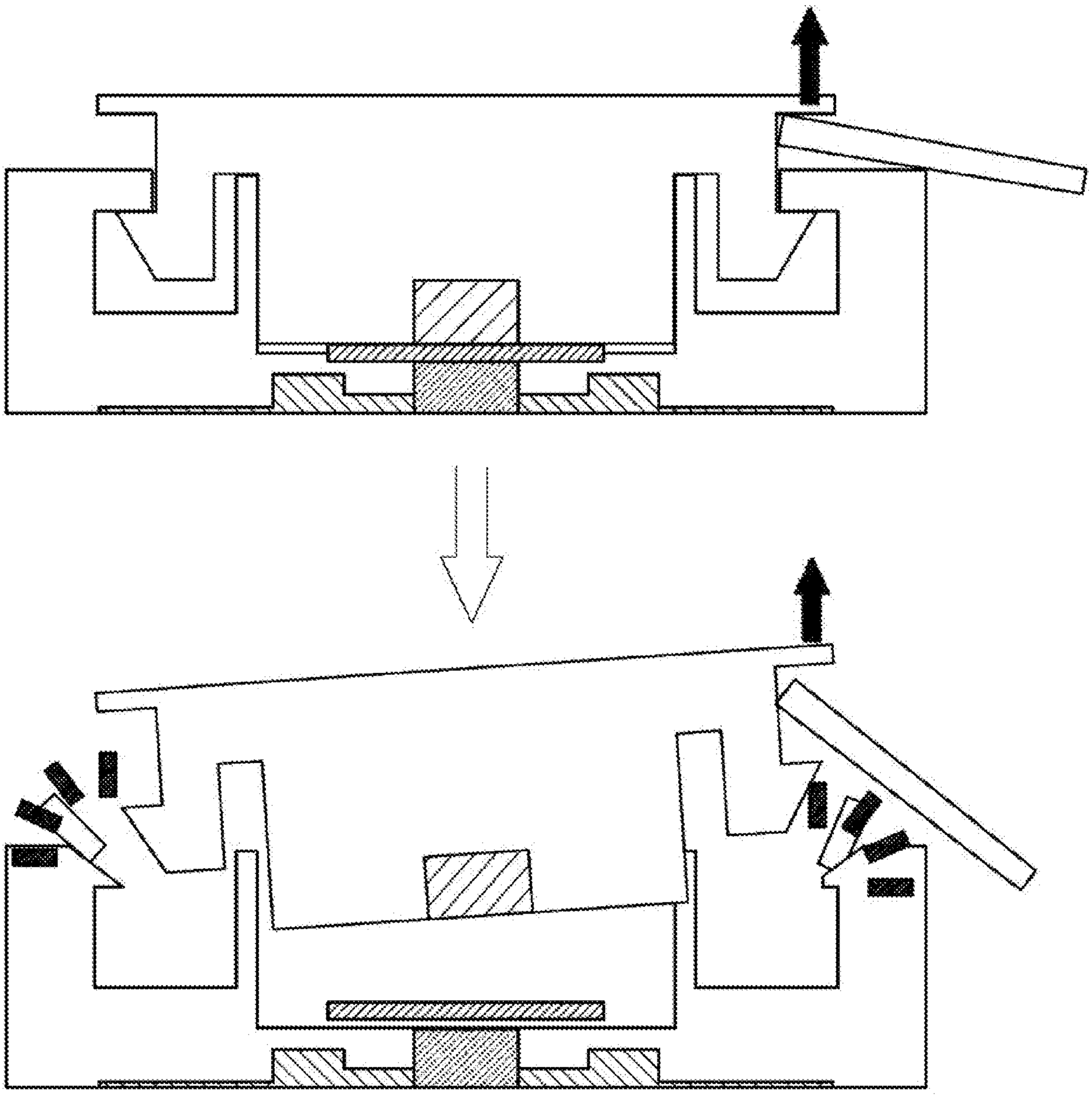


Fig. 11

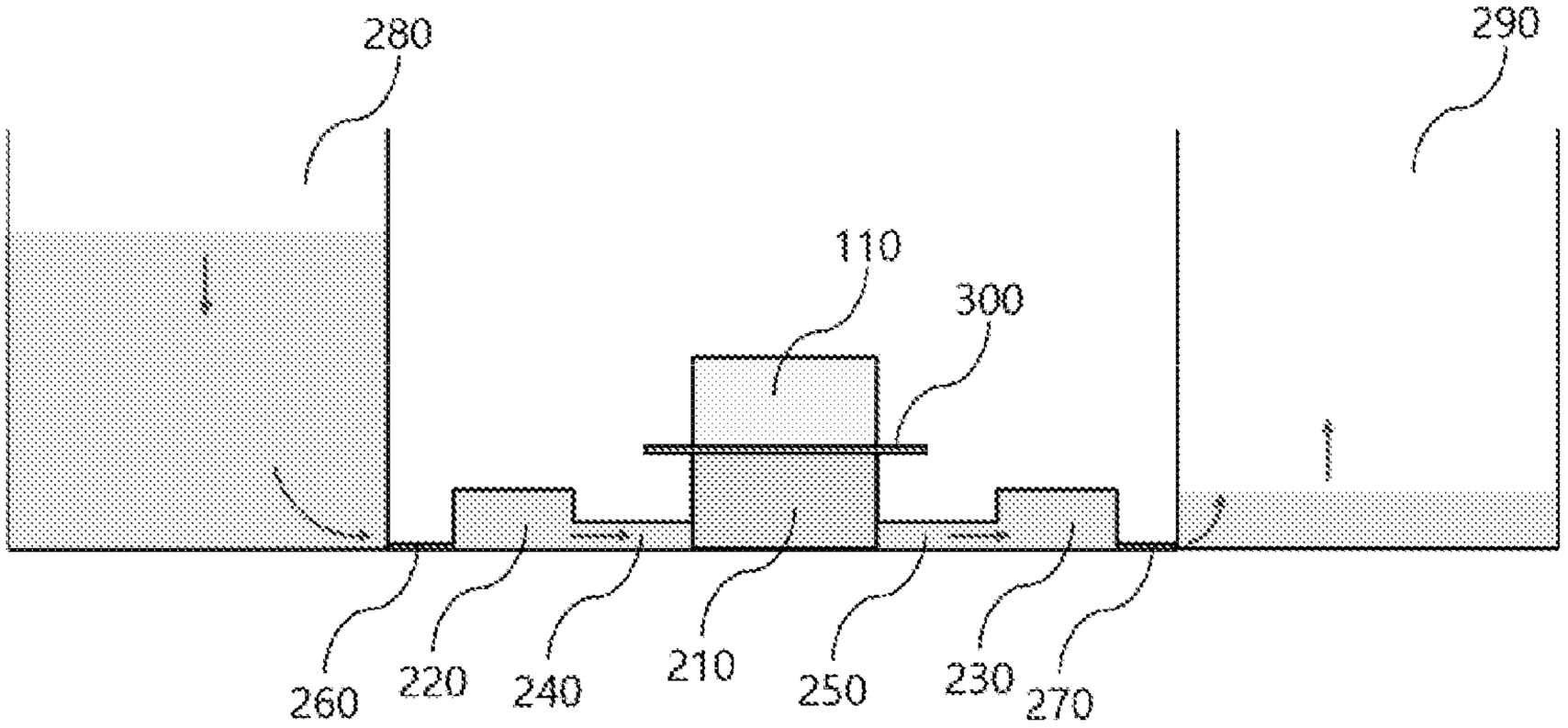

280
290
110
300
260
220
240
210
250
230
270

Fig. 12

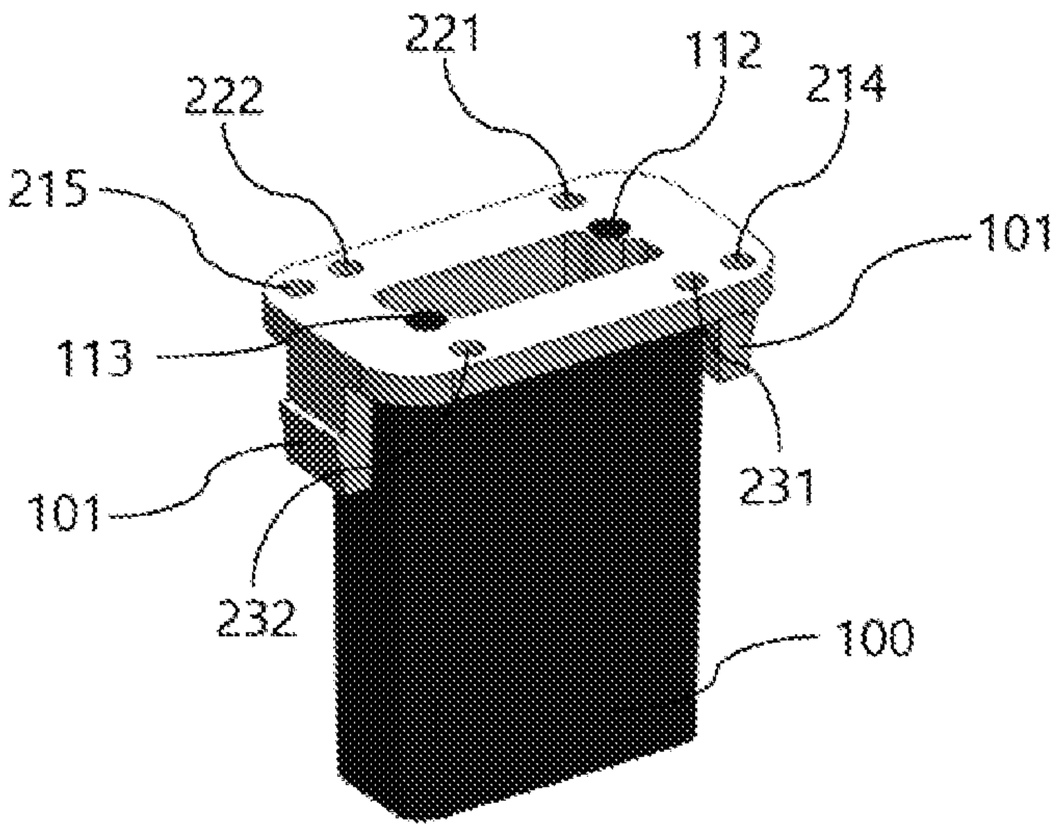

221
112
214
222
215
101
113
101
231
232
100

Fig. 13

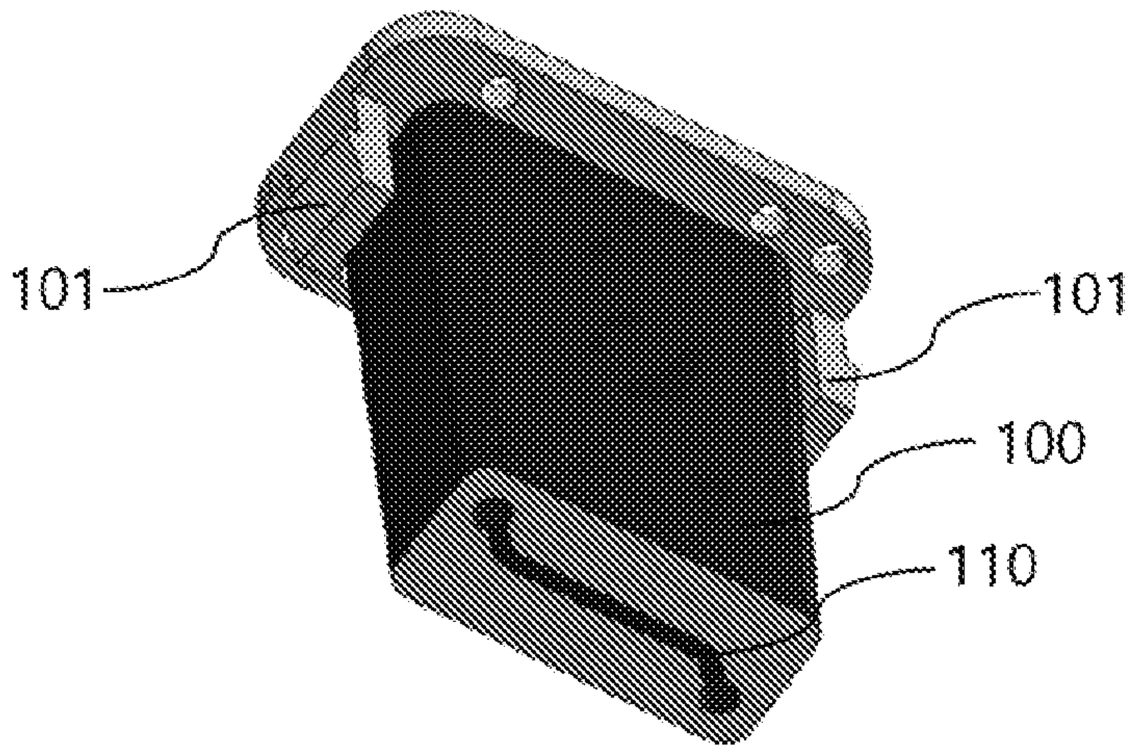


Fig. 14

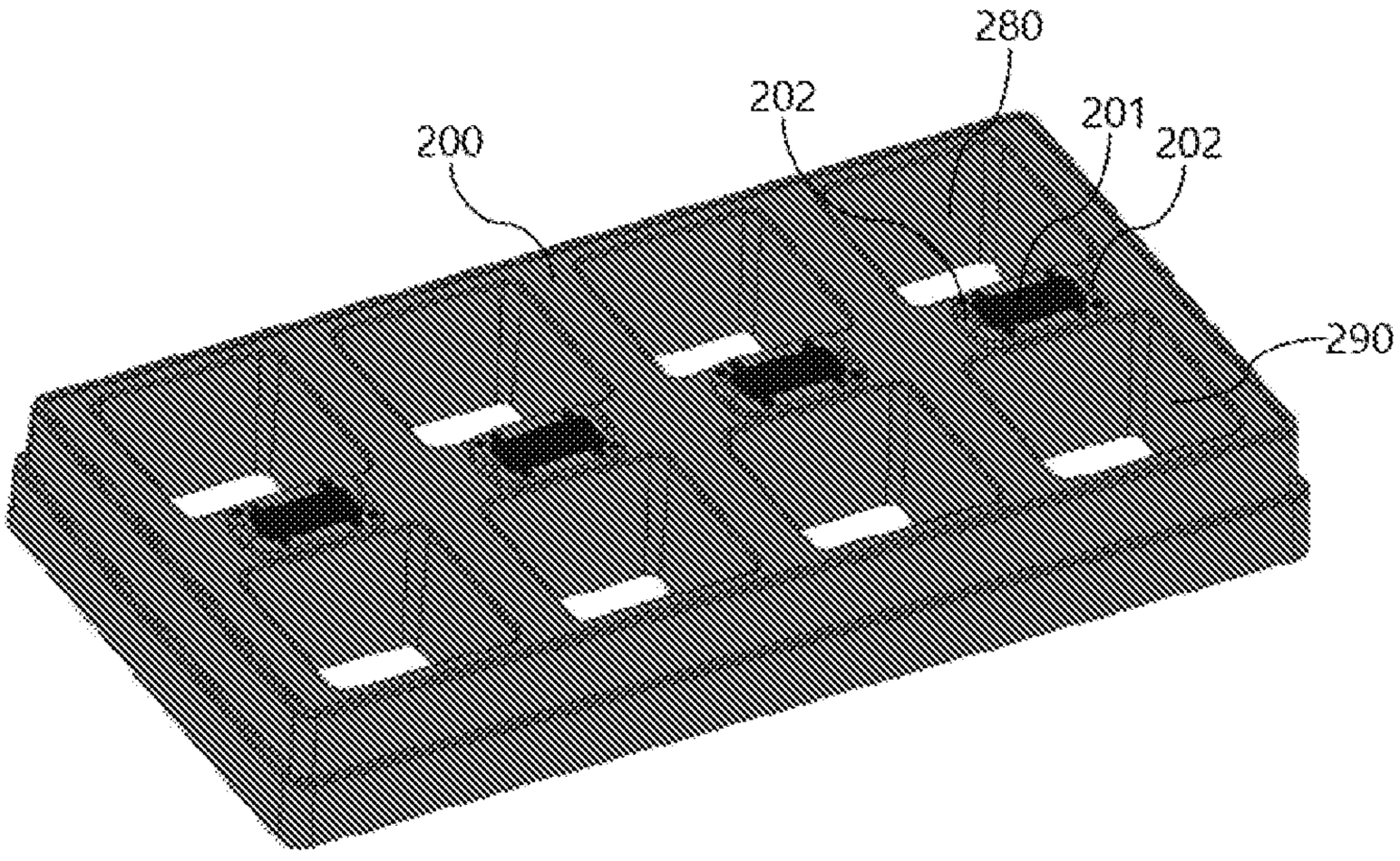


Fig. 15

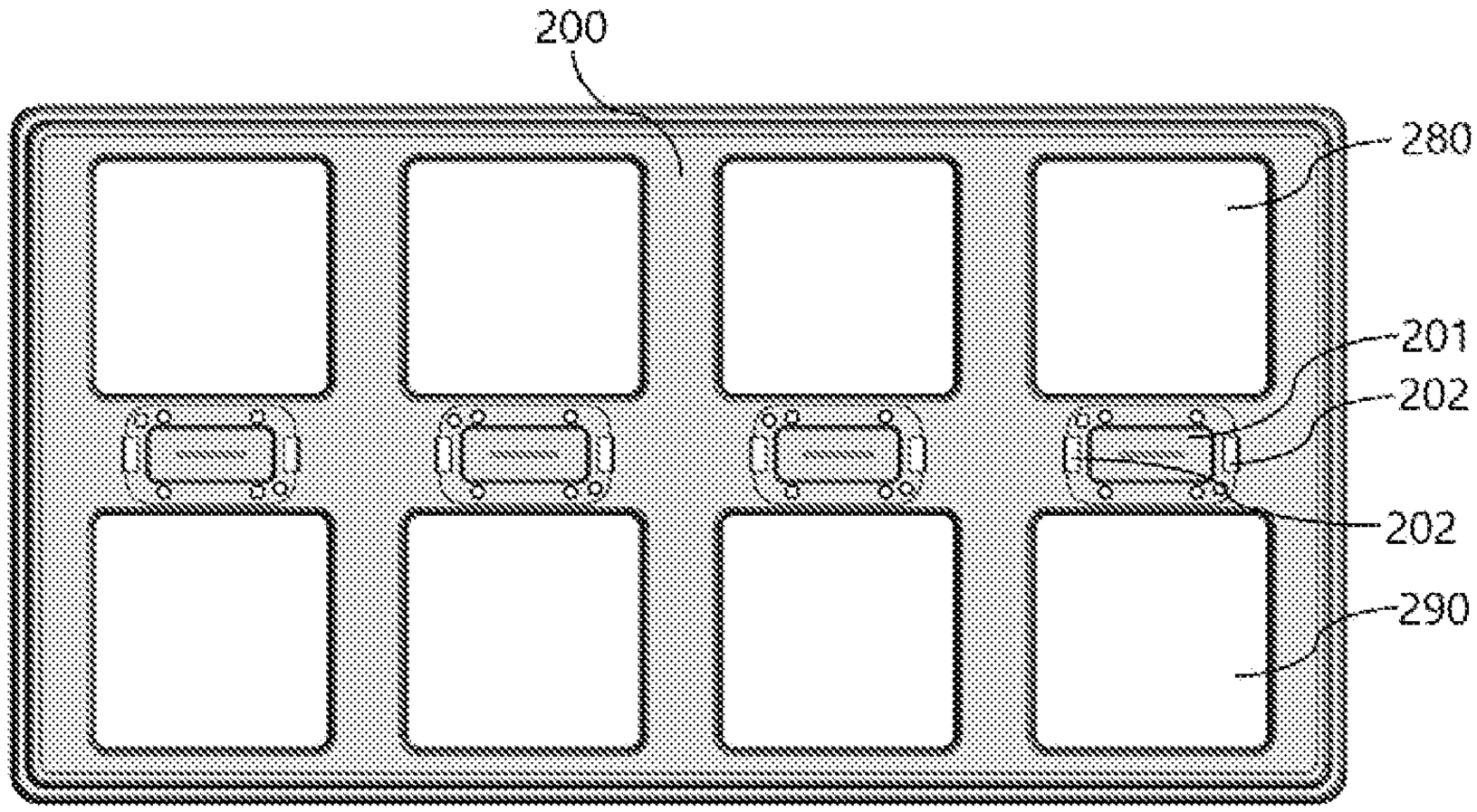


Fig. 16

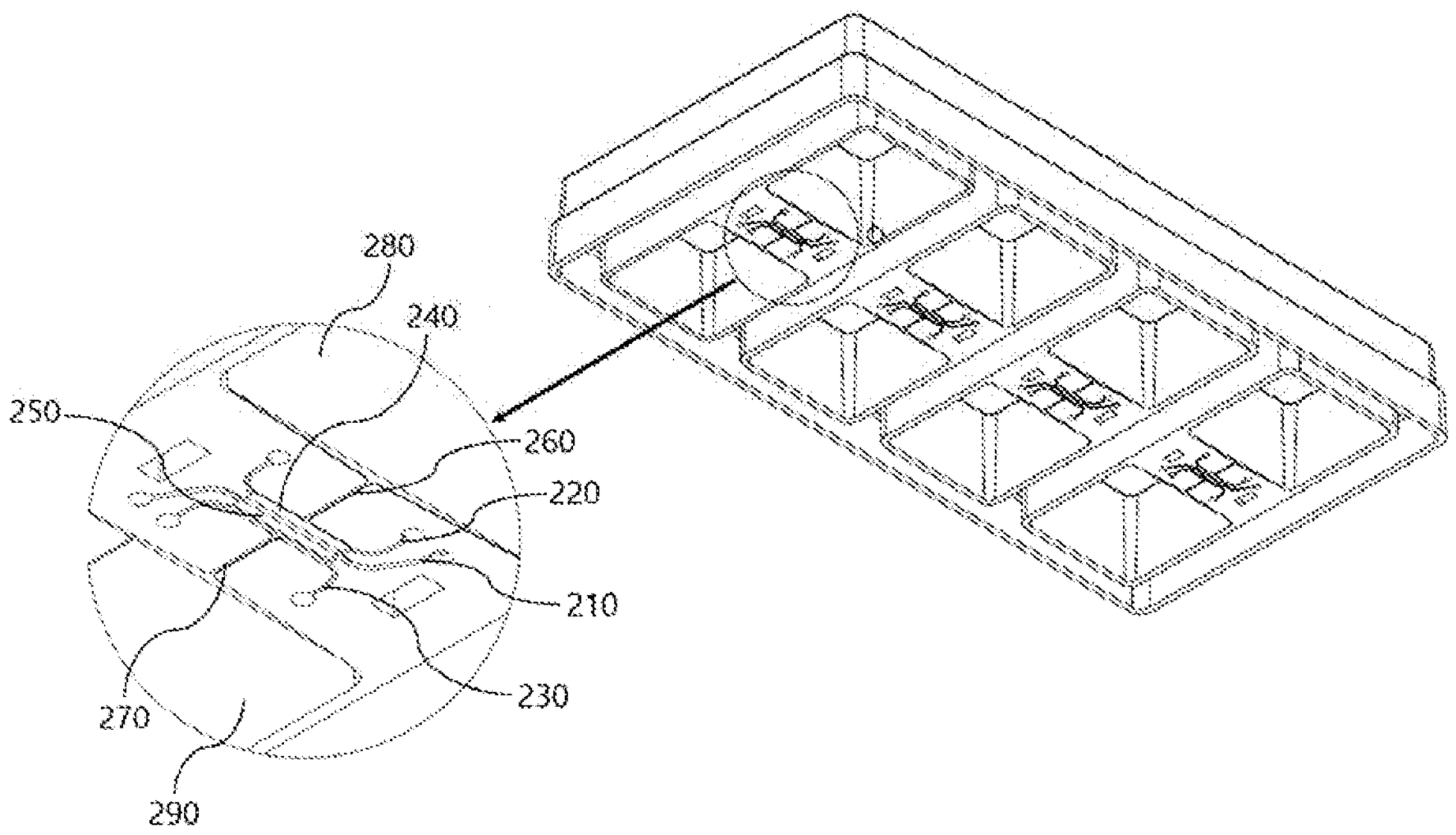


Fig. 17

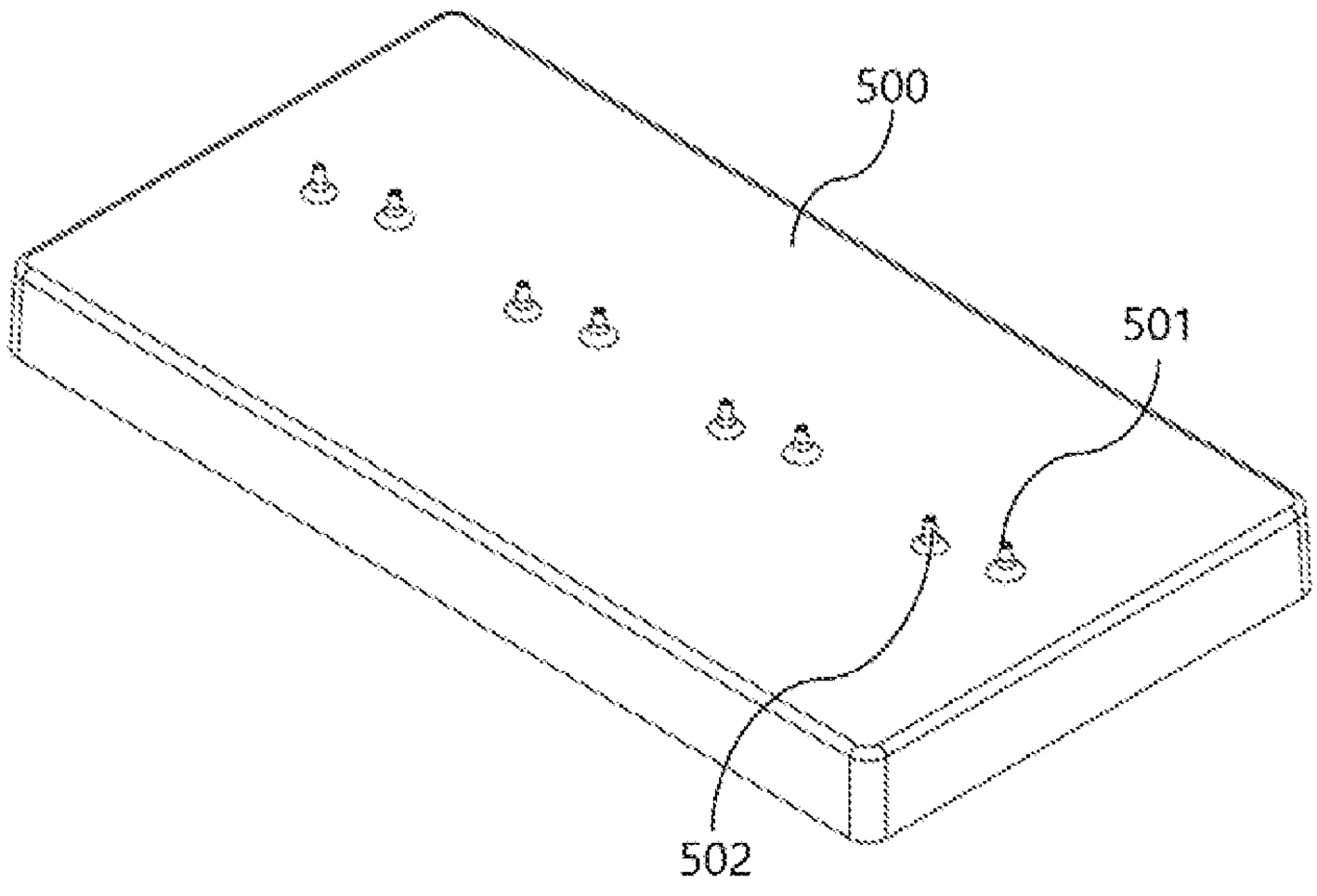


Fig. 18

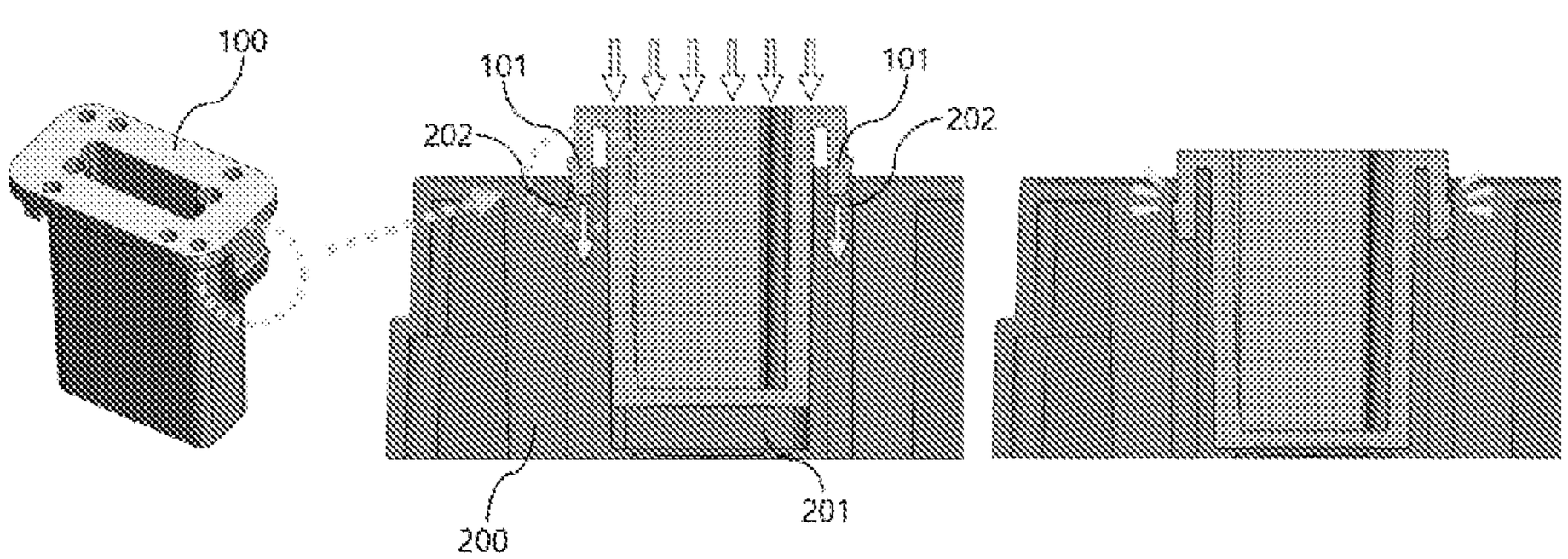


Fig. 19

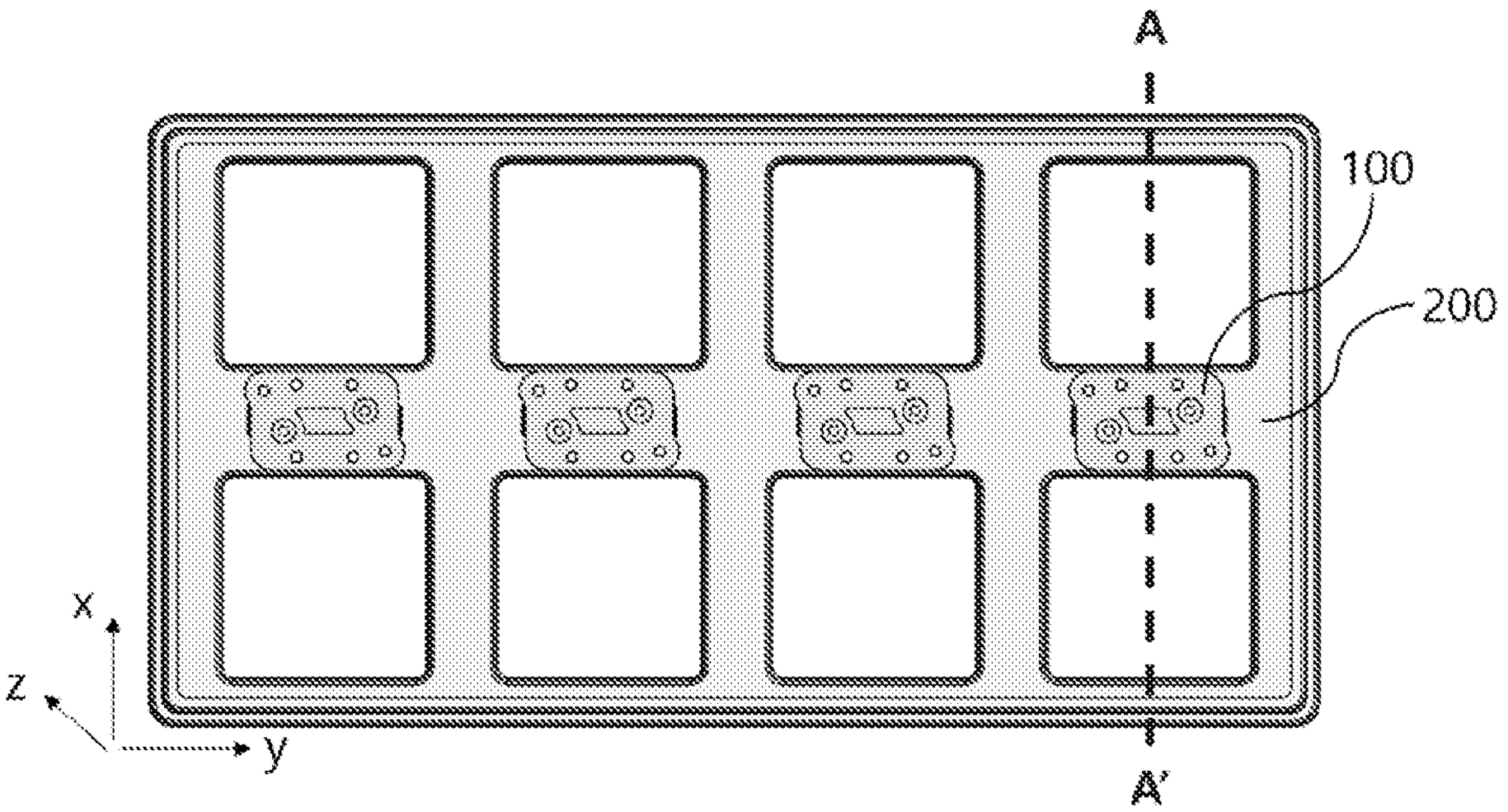

A
100
200
x
z
y
A'

Fig. 20

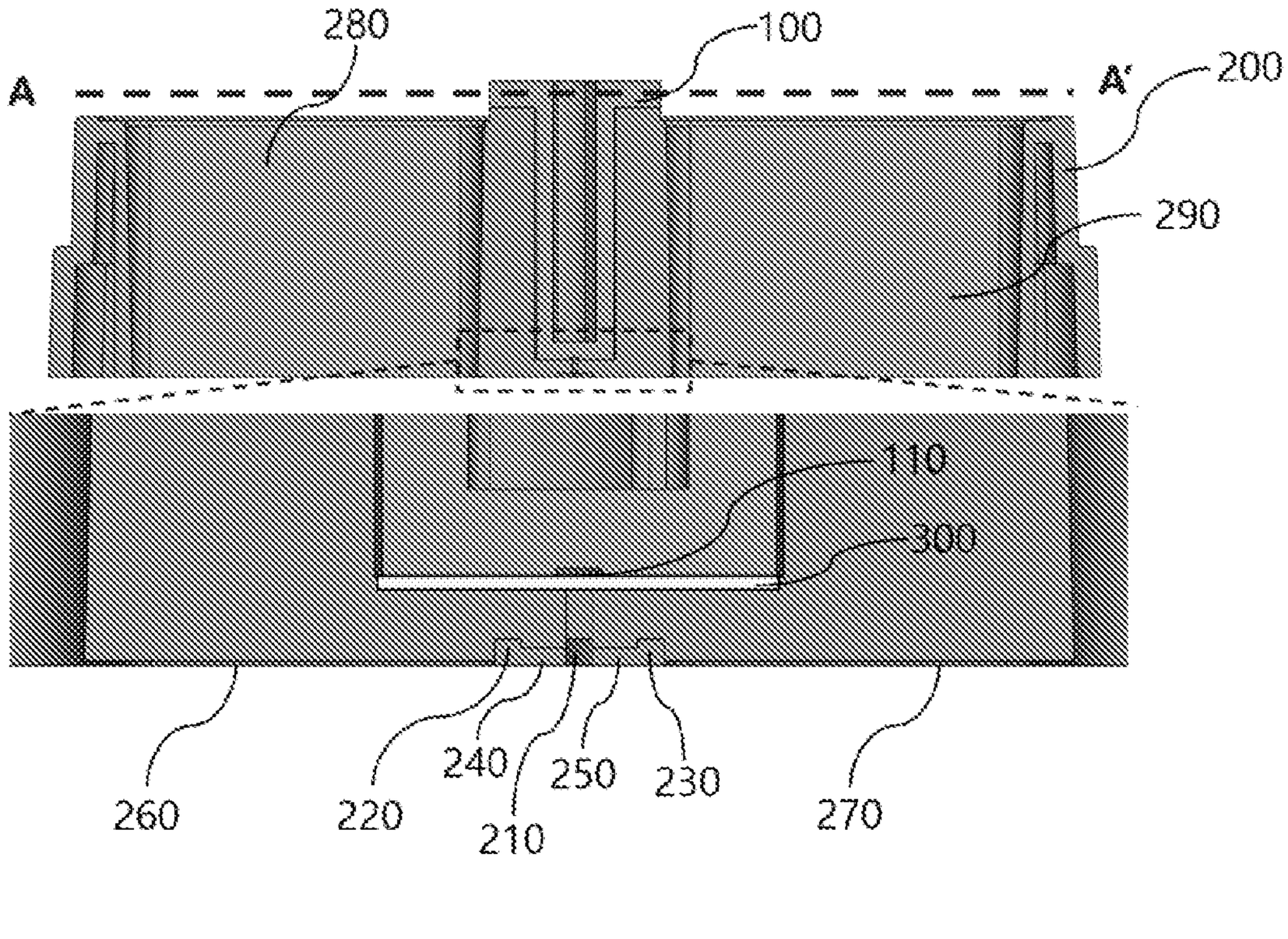

280
100
A
A'
200
290
110
300
260
220
240
210
250
230
270

Fig. 21

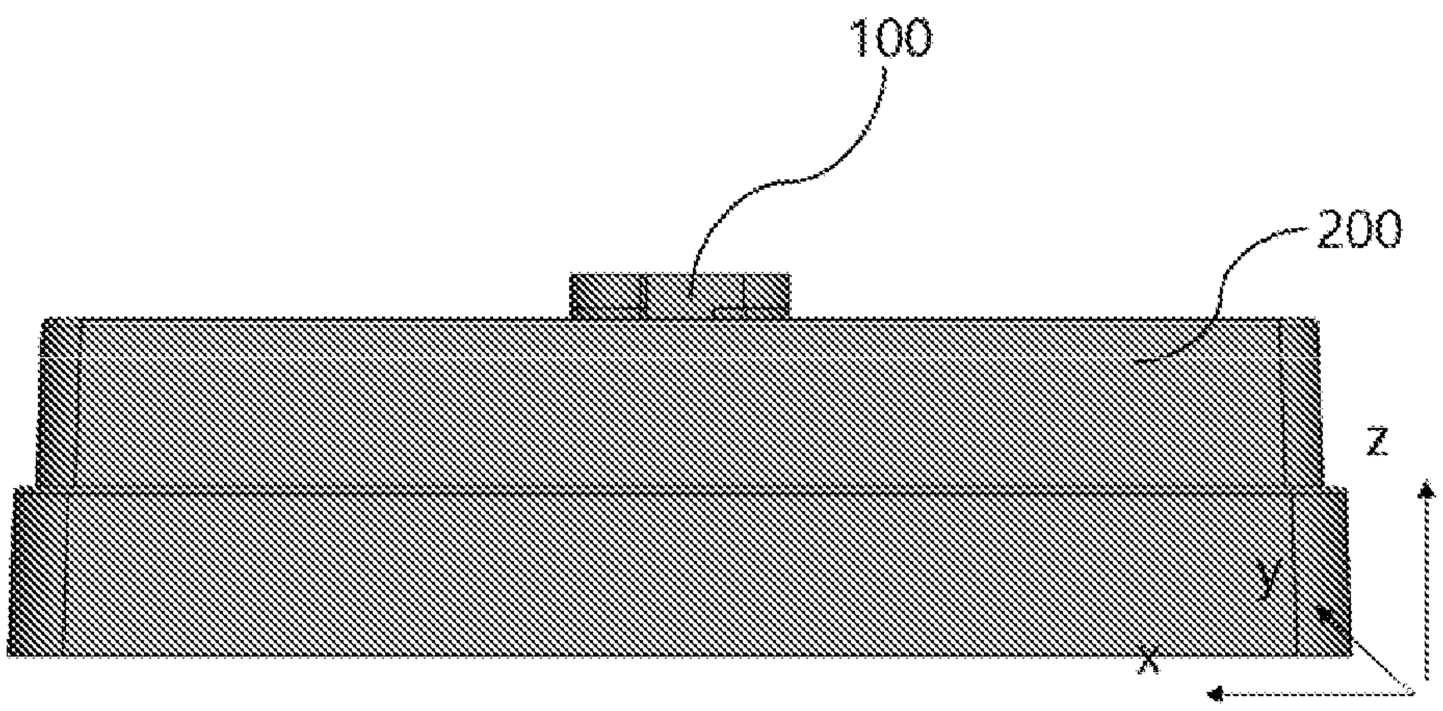


Fig. 22

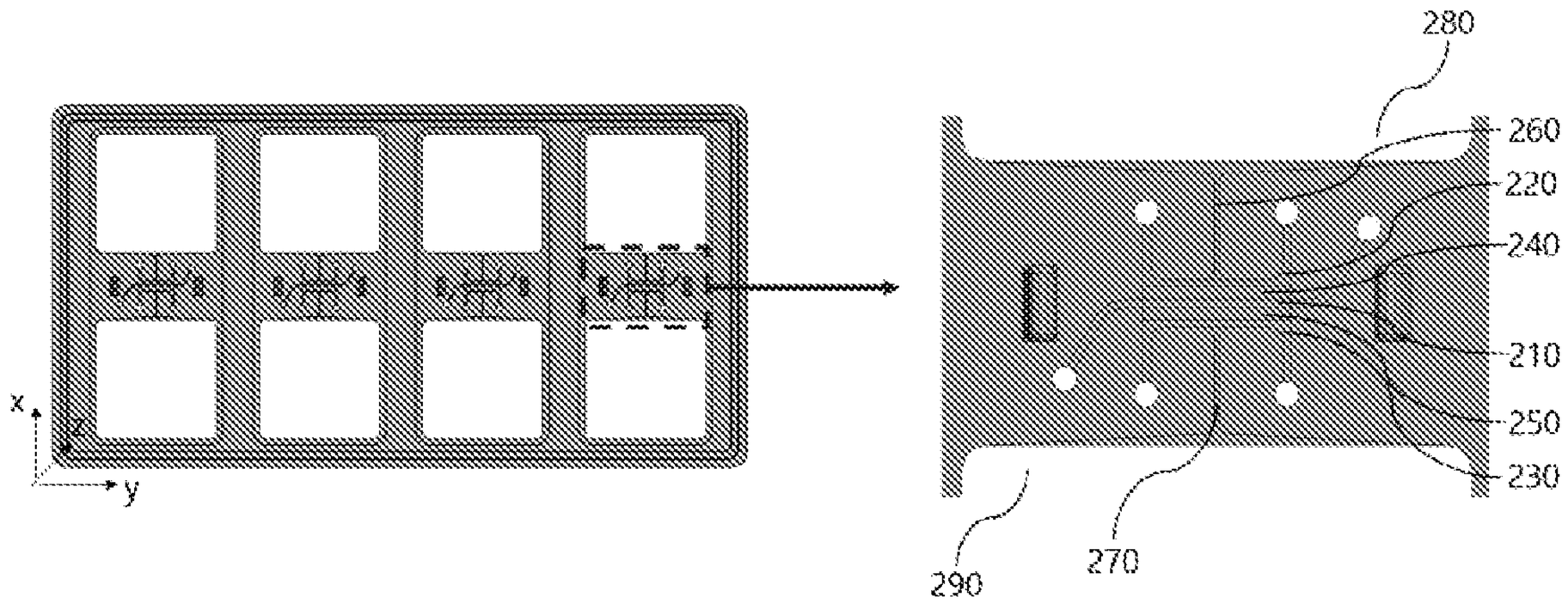


Fig. 23

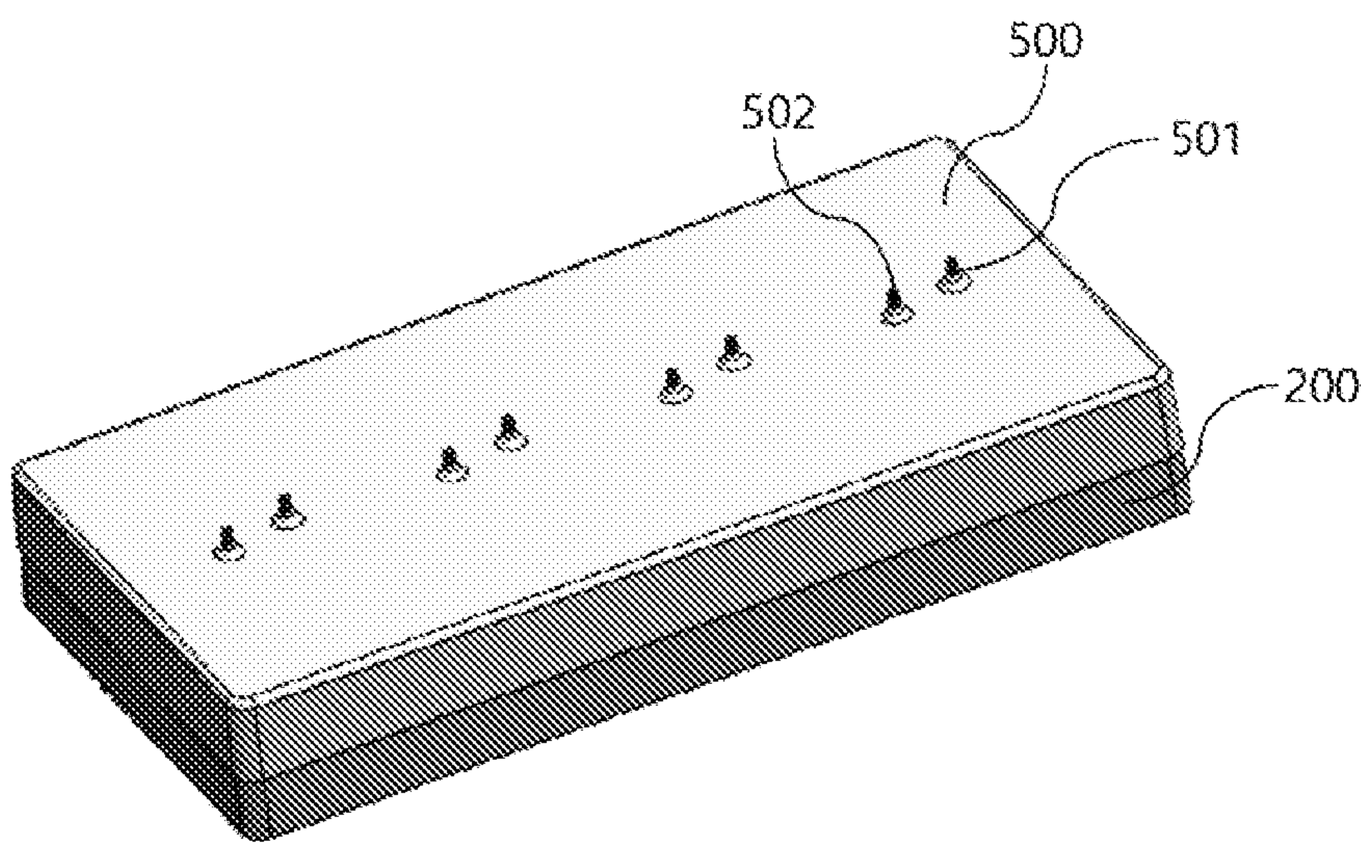


Fig. 24

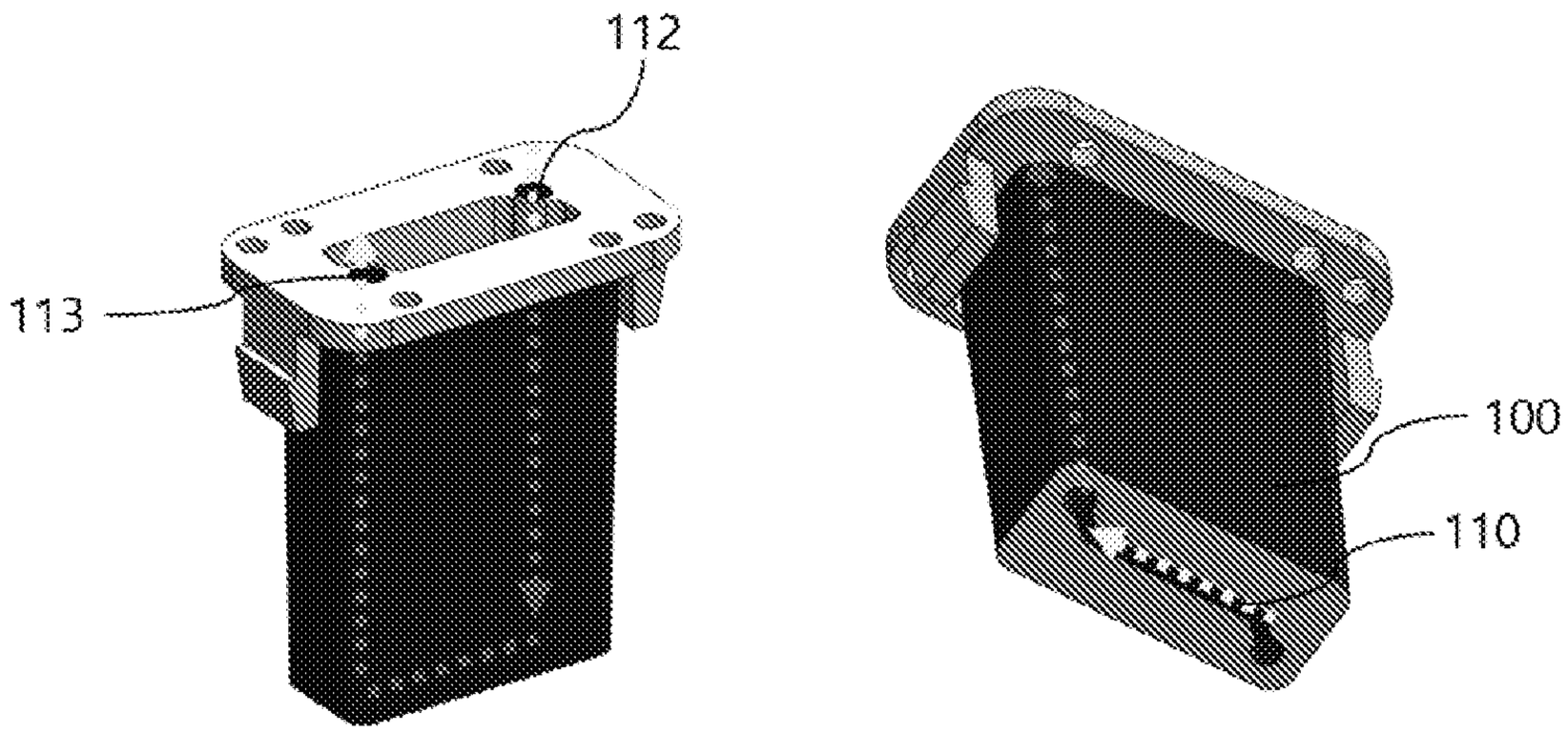


Fig. 25

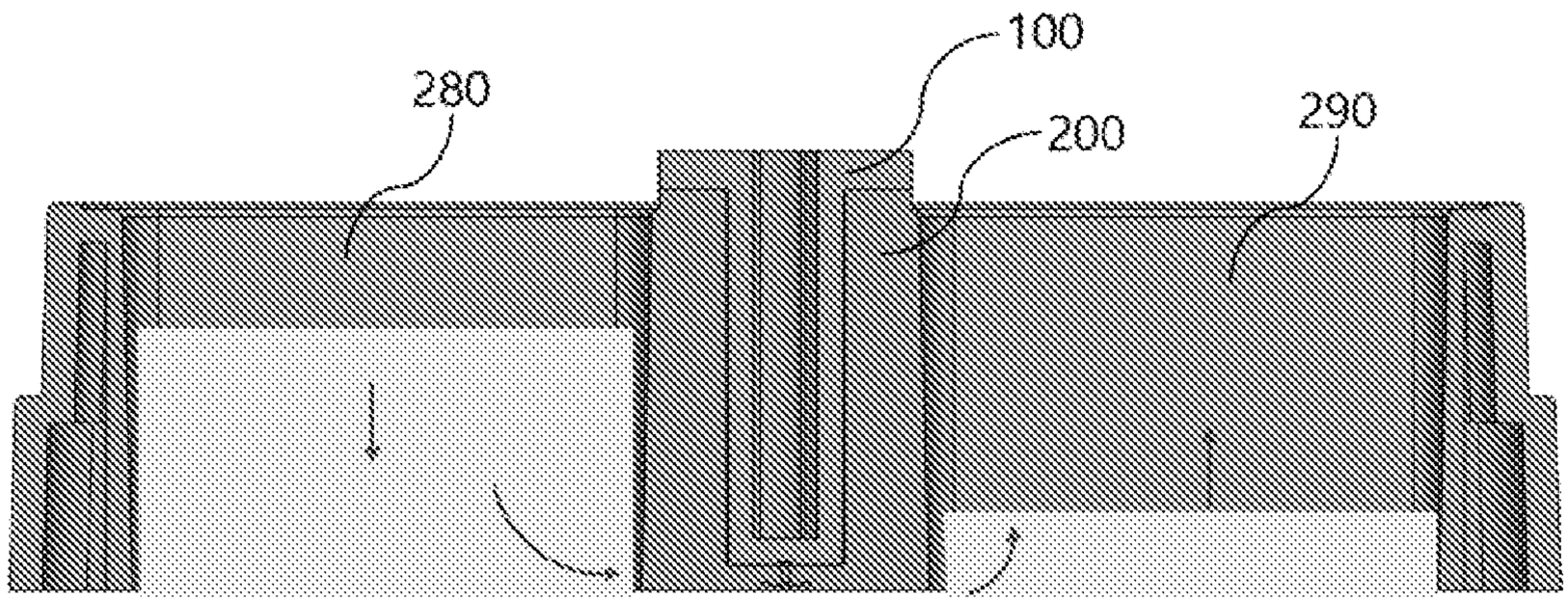


Fig. 26

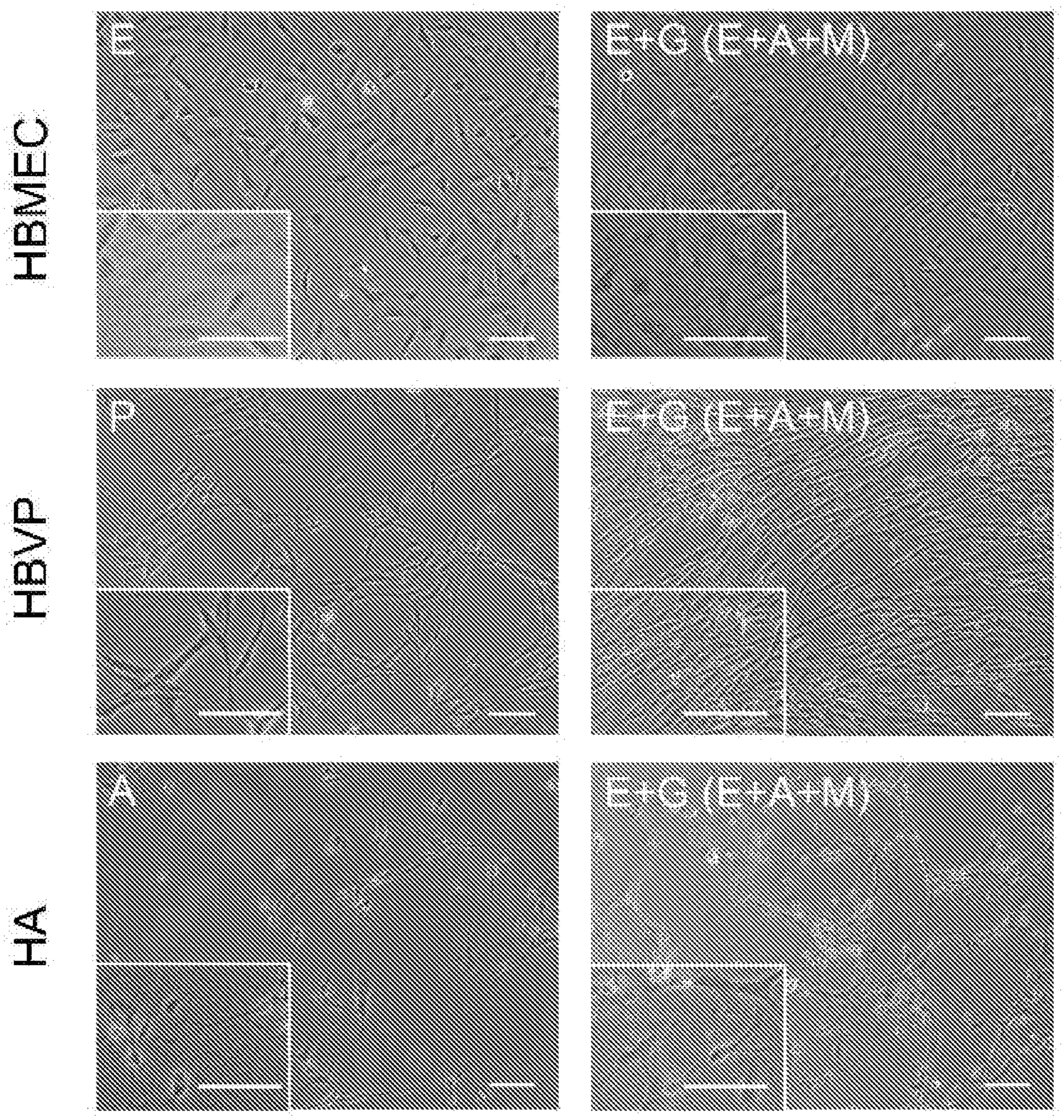


Fig. 27

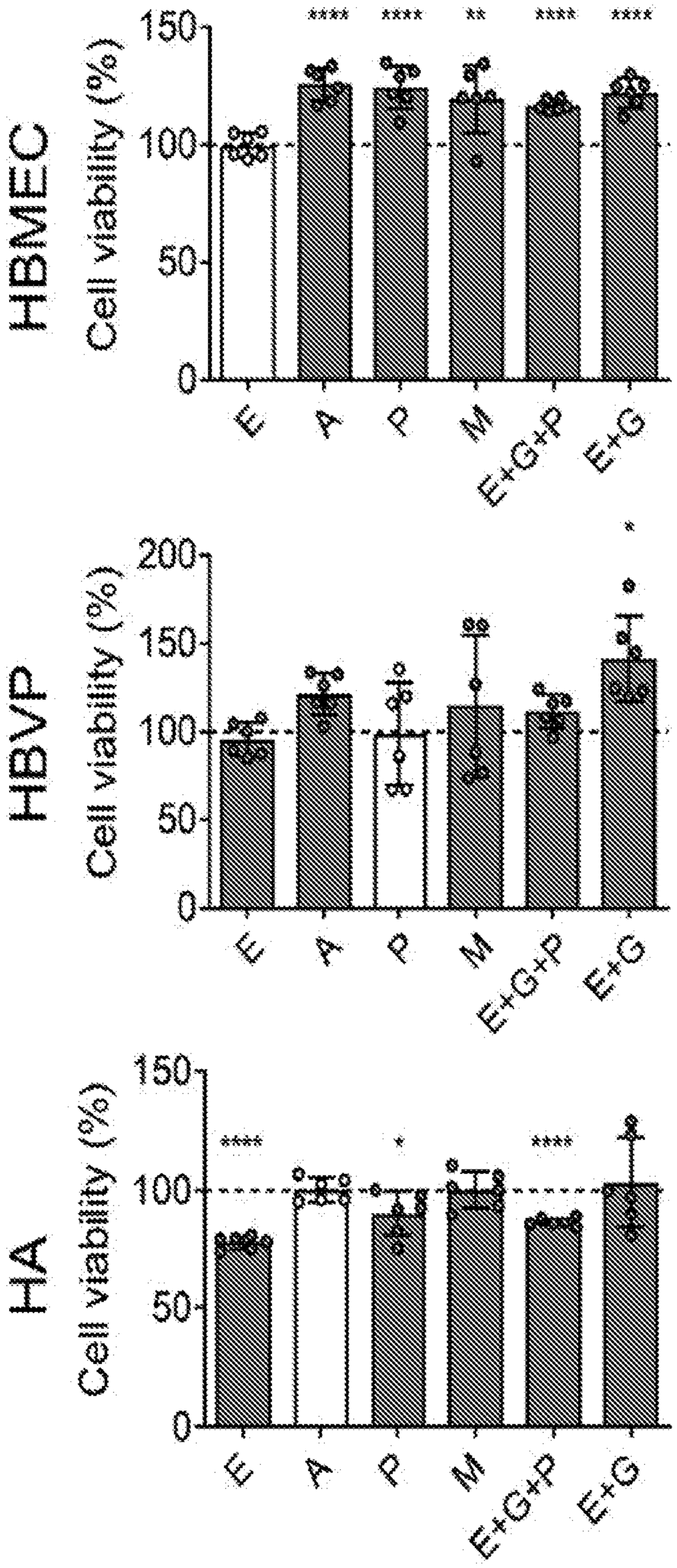

HBMEC
Cell viability (%)
150
100
50
0
****
****
**
****
****
E
A
P
M
E+G+P
E+G
HBVP
Cell viability (%)
200
150
100
50
0
E
A
P
M
E+G+P
E+G
HA
Cell viability (%)
150
100
50
0
****
*
****
E
A
P
M
E+G+P
E+G

Fig. 28

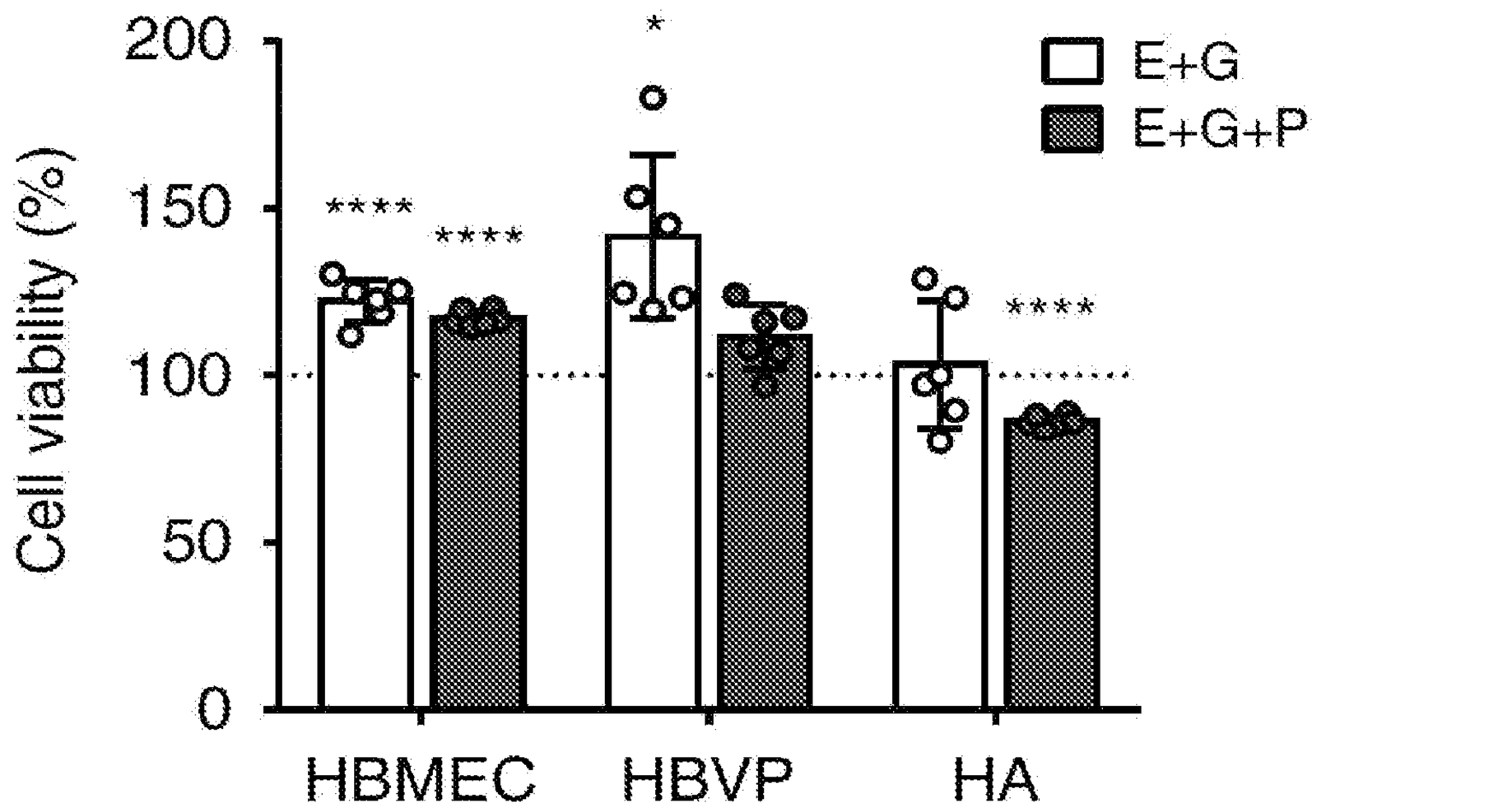


Fig. 29

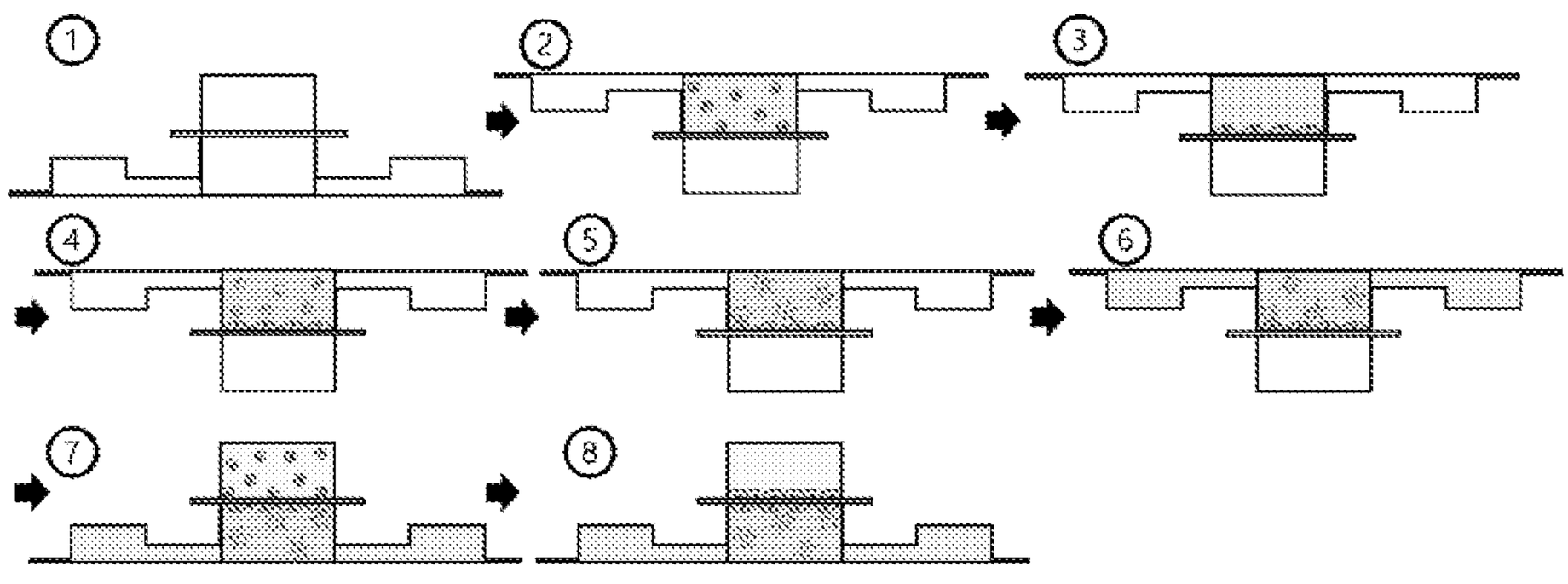


Fig. 30

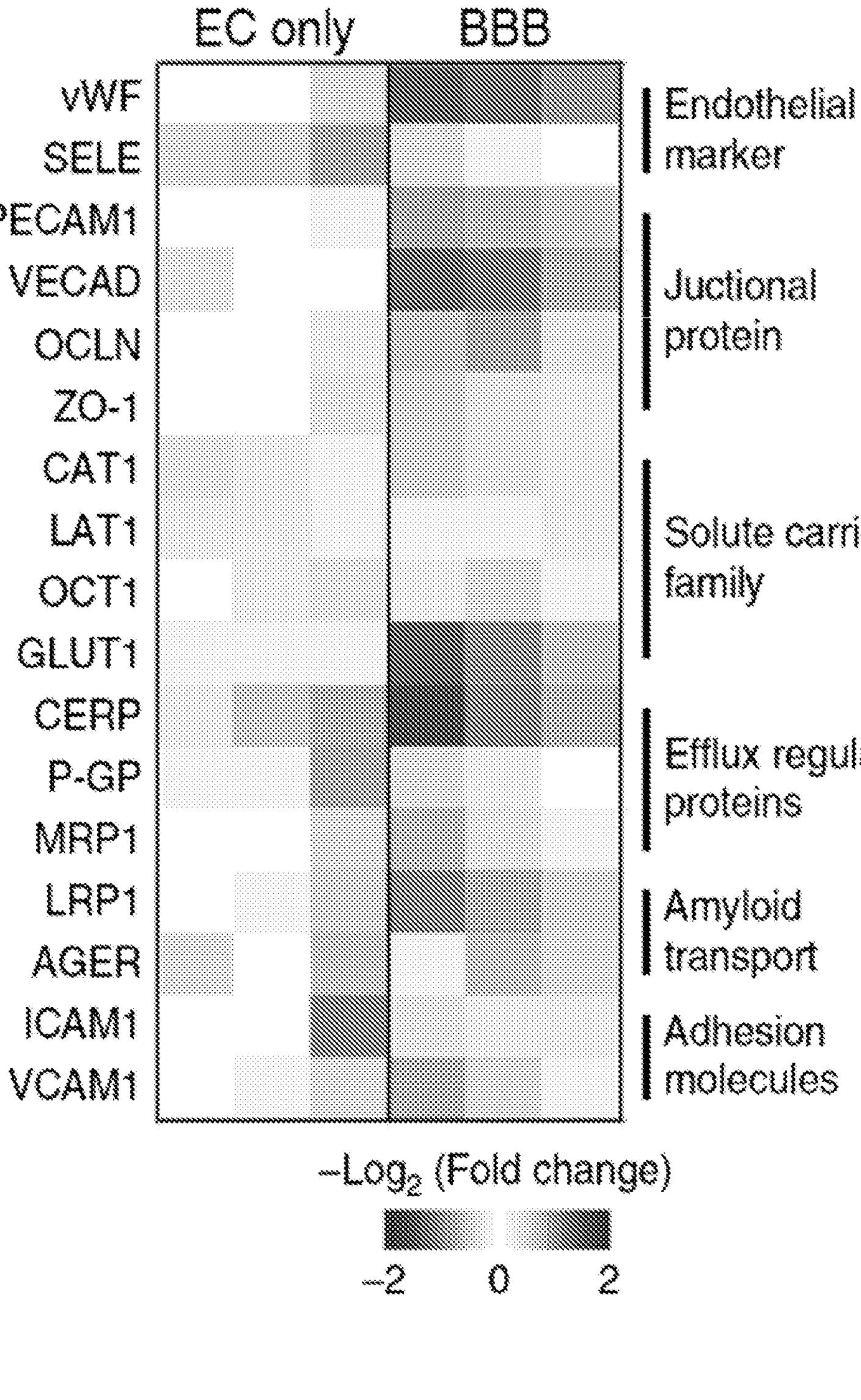

EC only
BBB
vWF
SELE
PECAM1
VECAD
OCLN
ZO-1
CAT1
LAT1
OCT1
GLUT1
CERP
P-GP
MRP1
LRP1
AGER
ICAM1
VCAM1
Endothelial marker
Juctional protein
Solute carrier family
Efflux regulatory proteins
Amyloid transport
Adhesion molecules
–Log2 (Fold change)
–2
0
2

Fig. 31

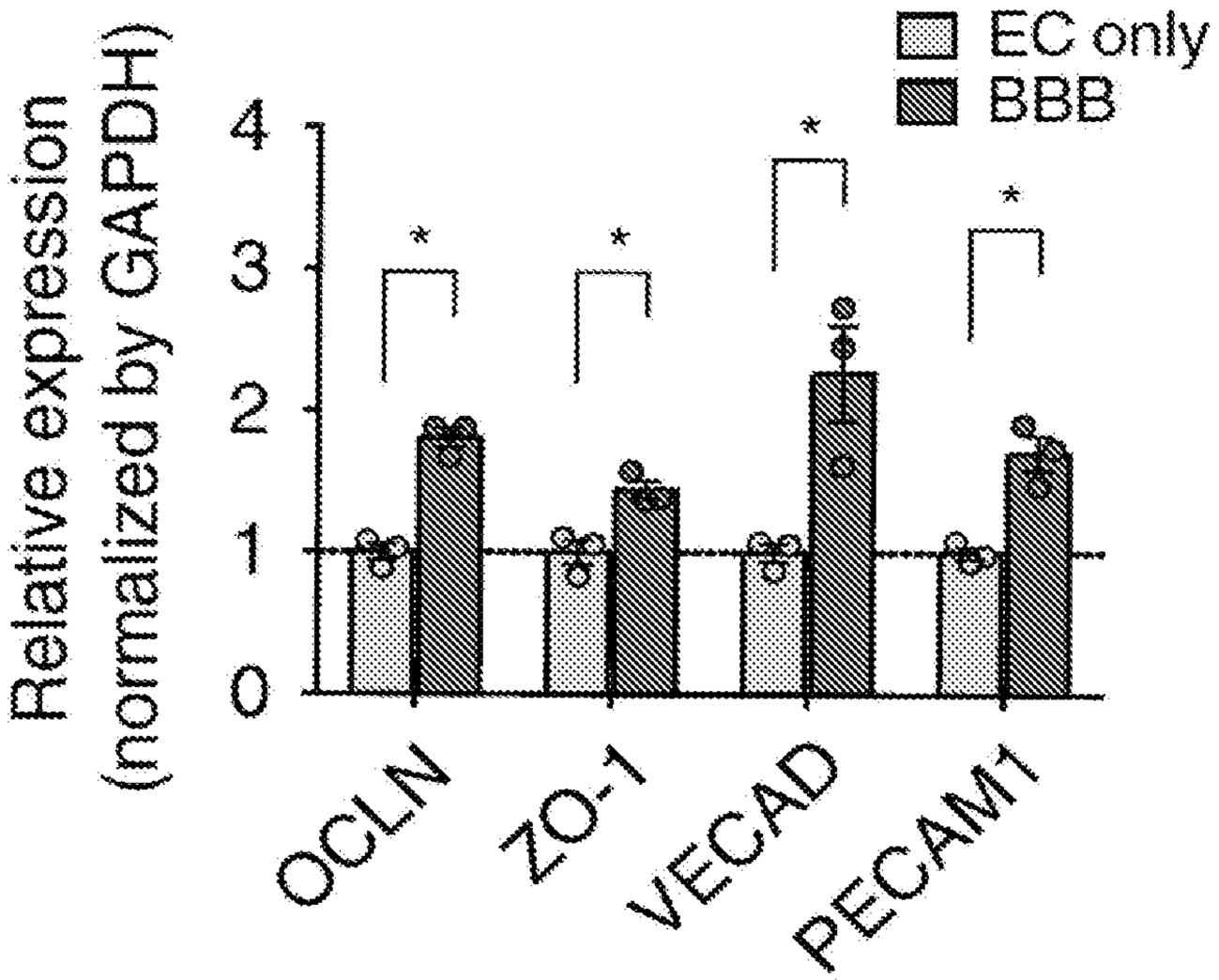

EC only
BBB
Relative expression
(normalized by GAPDH)
0
1
2
3
4
*
OCLN
ZO-1
VECAD
PECAM1

Fig. 32

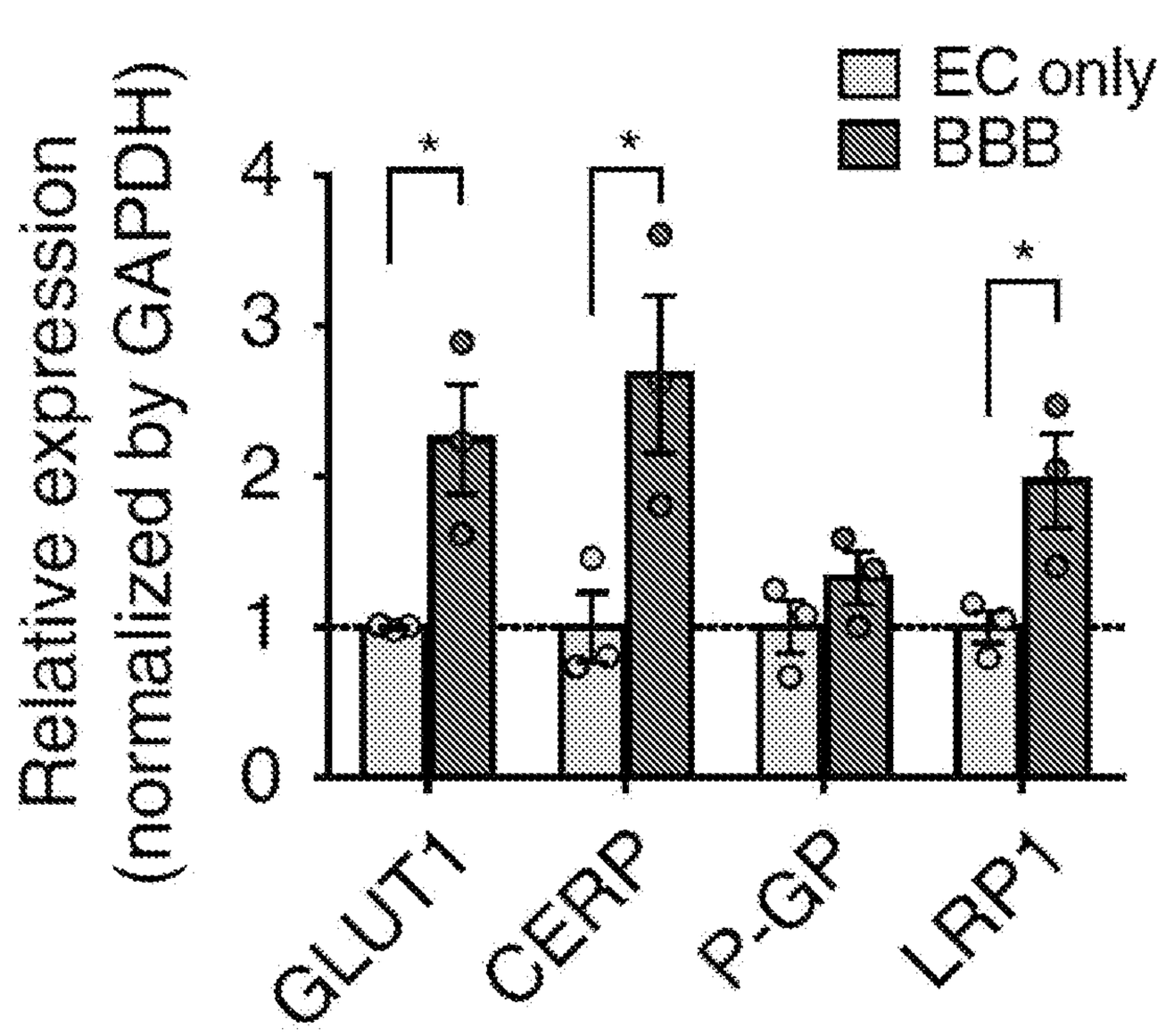

EC only
BBB
Relative expression
(normalized by GAPDH)
0
1
2
3
4
*
GLUT1
CERP
P-GP
LRP1

Fig. 33

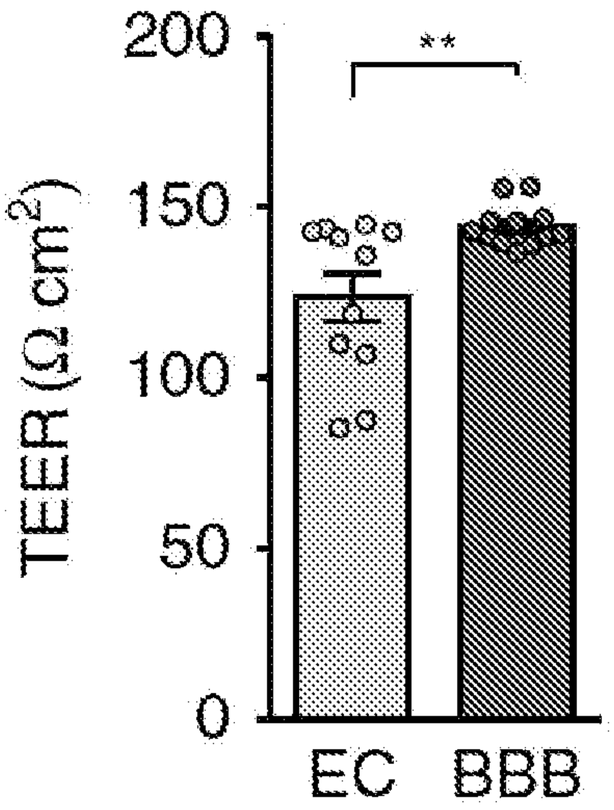

200
150
100
50
0
TEER (Ω cm²)
**
EC
BBB

Fig. 34

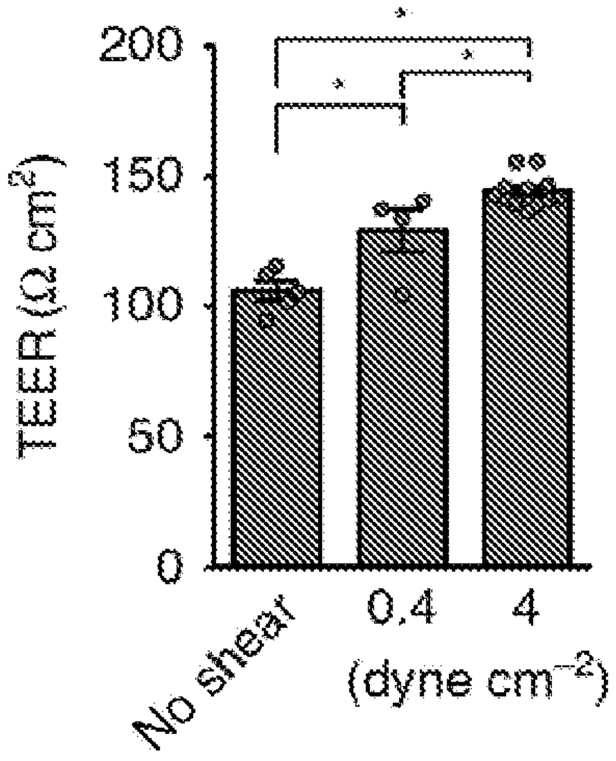

200
150
100
50
0
TEER (Ω cm²)
*
*
*
No shear
0.4
4
(dyne cm⁻²)

Fig. 35

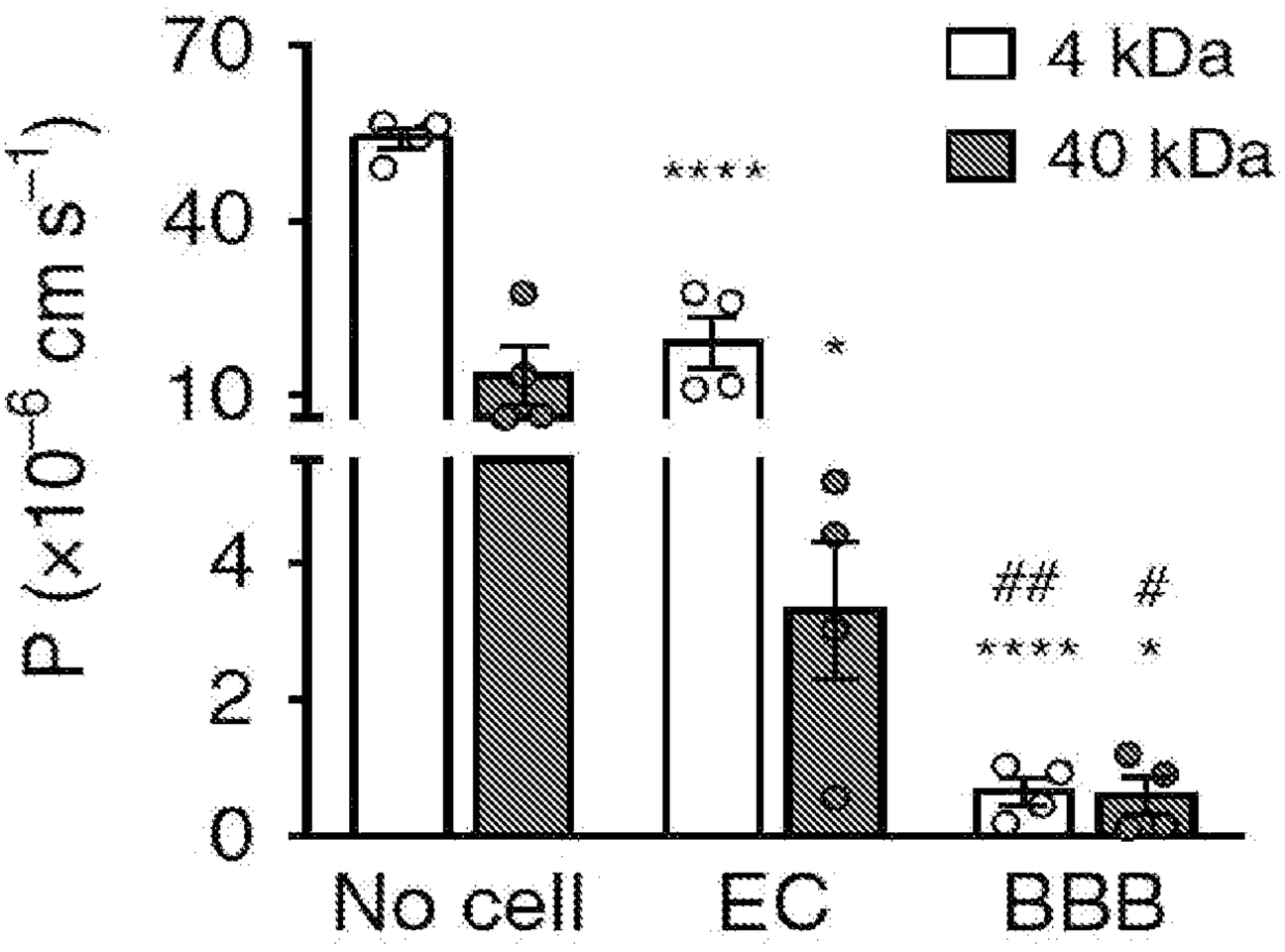


Fig. 36

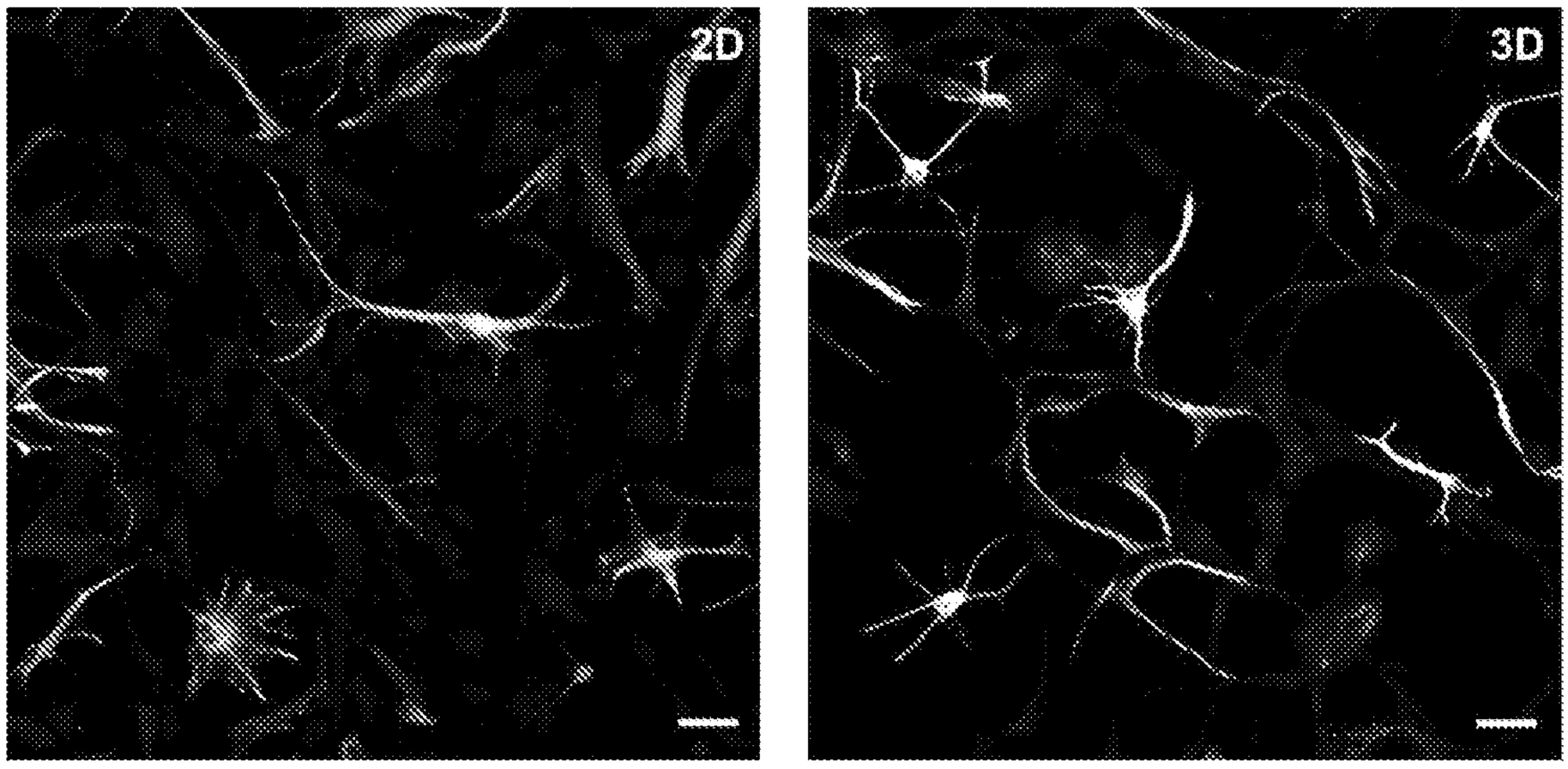


Fig. 37

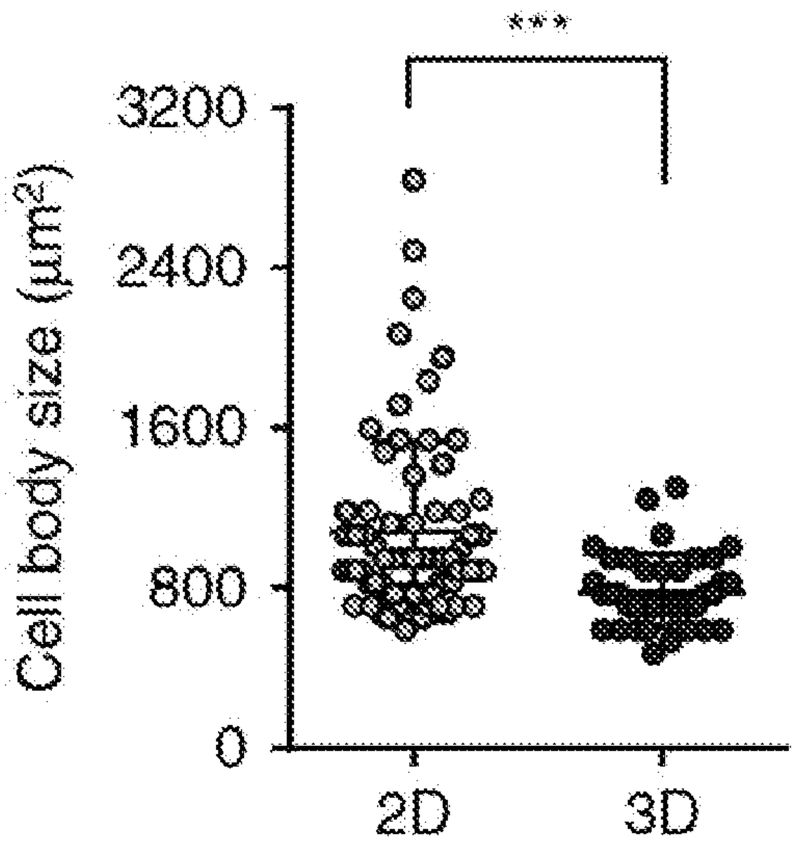

***
3200
2400
1600
800
0
Cell body size (μm²)
2D
3D

Fig. 38

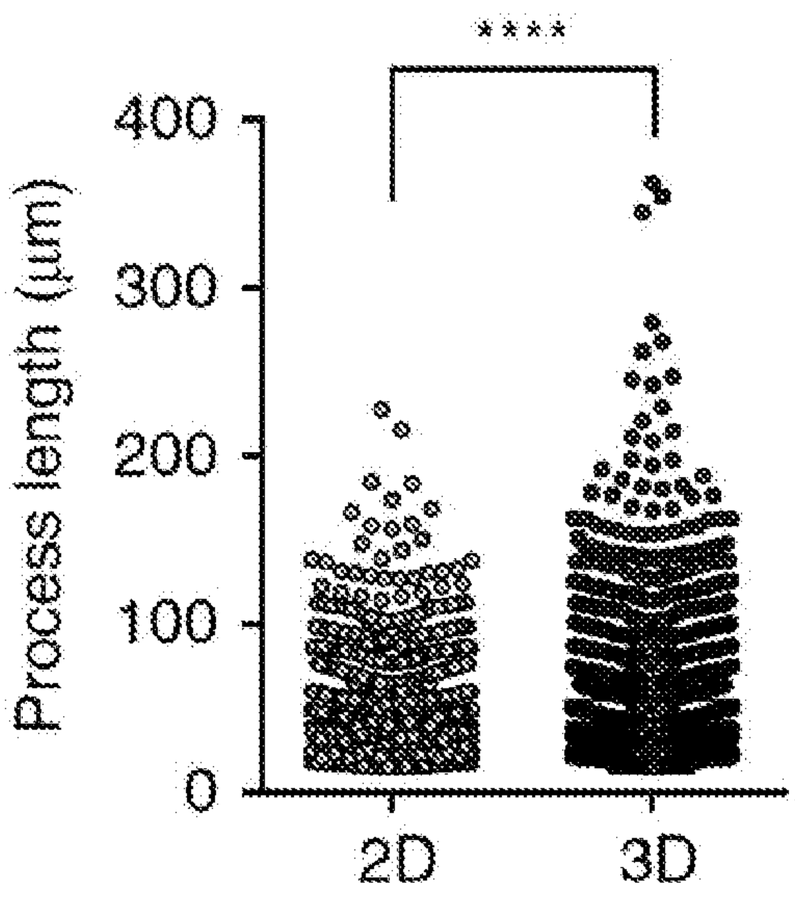

****
400
300
200
100
0
Process length (μm)
2D
3D

Fig. 39

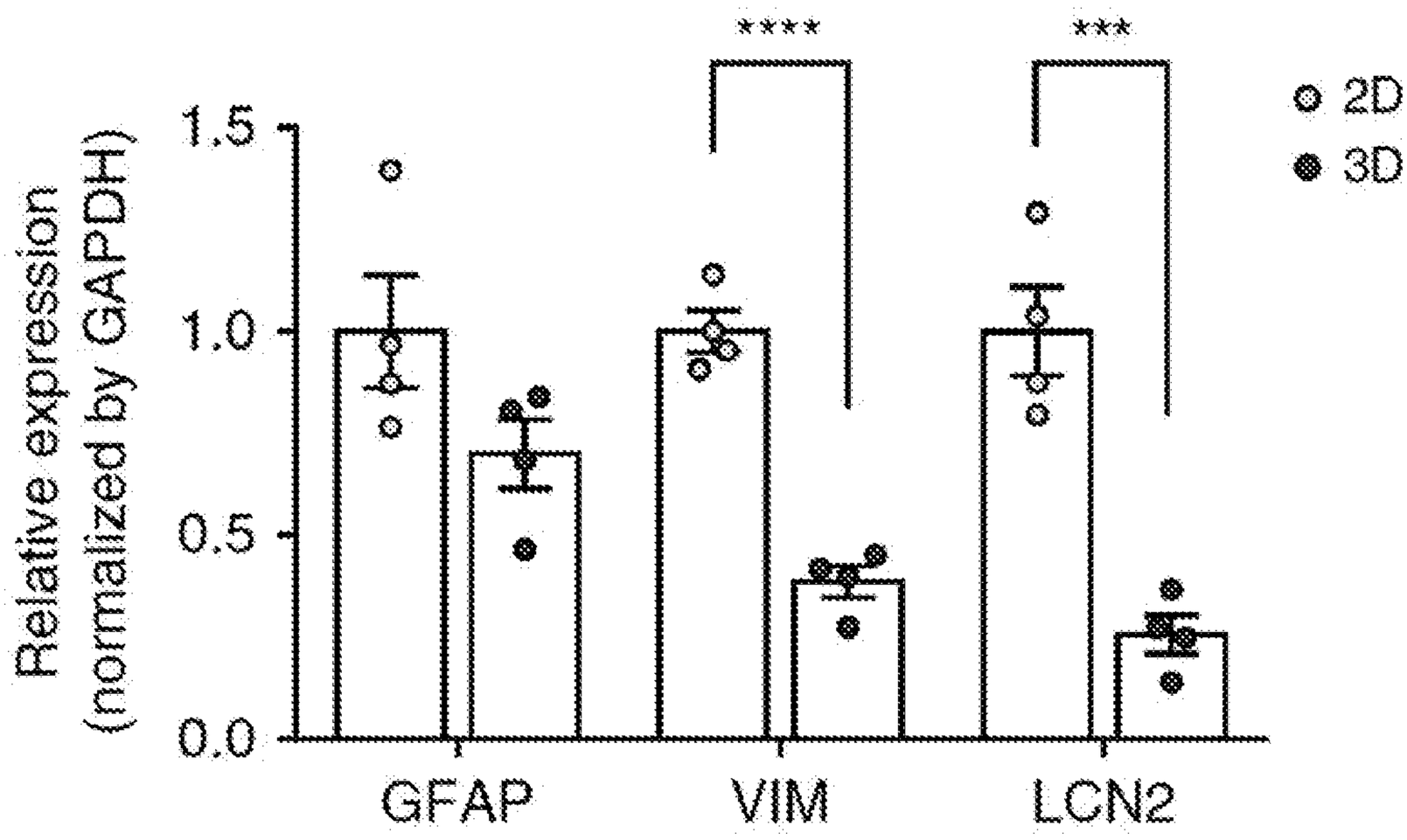

****
***
2D
3D
Relative expression
(normalized by GAPDH)
1.5
1.0
0.5
0.0
GFAP
VIM
LCN2

Fig. 40

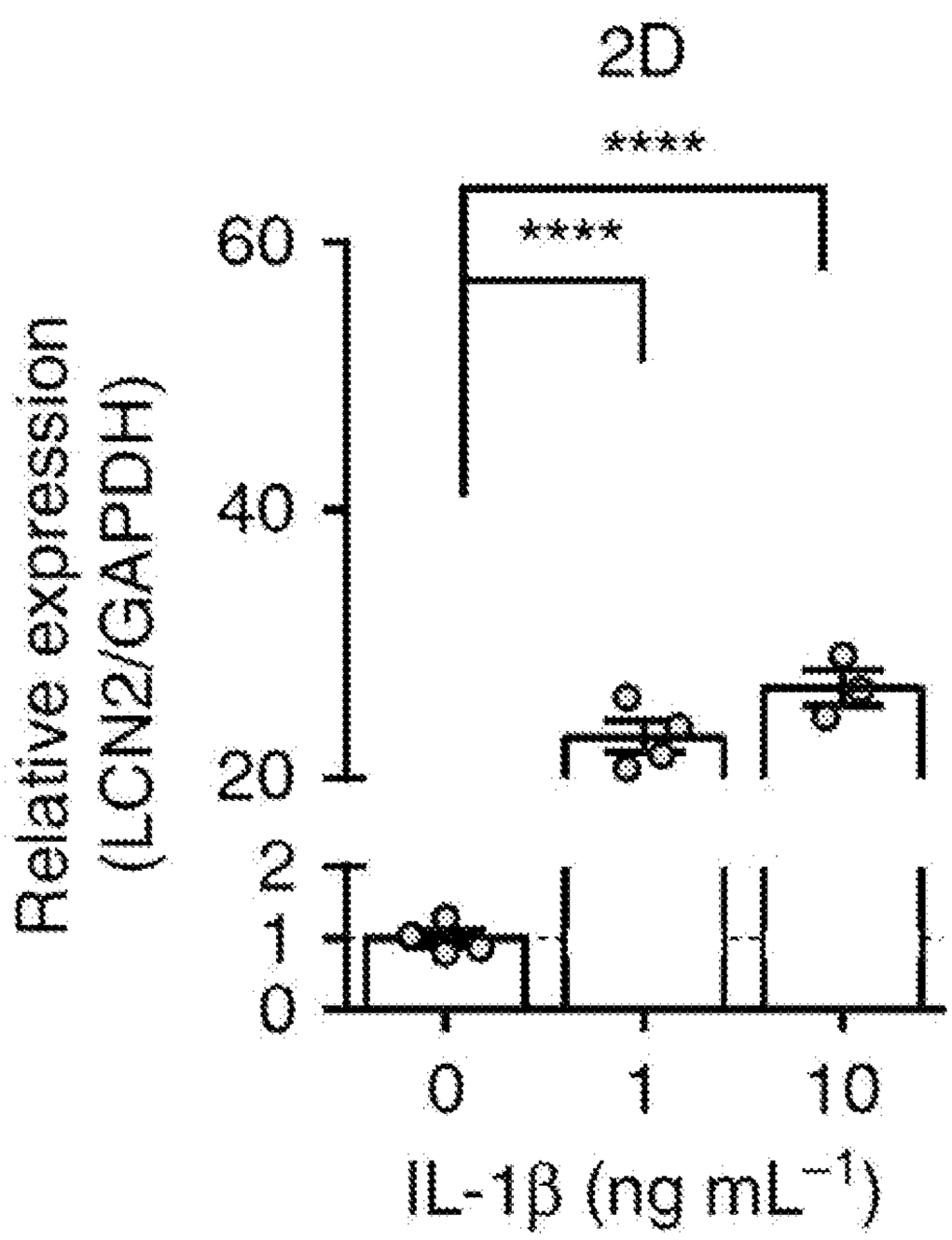

2D
****
****
Relative expression
(LCN2/GAPDH)
60
40
20
2
1
0
0
1
10
IL-1β (ng mL^{-1})

Fig. 41

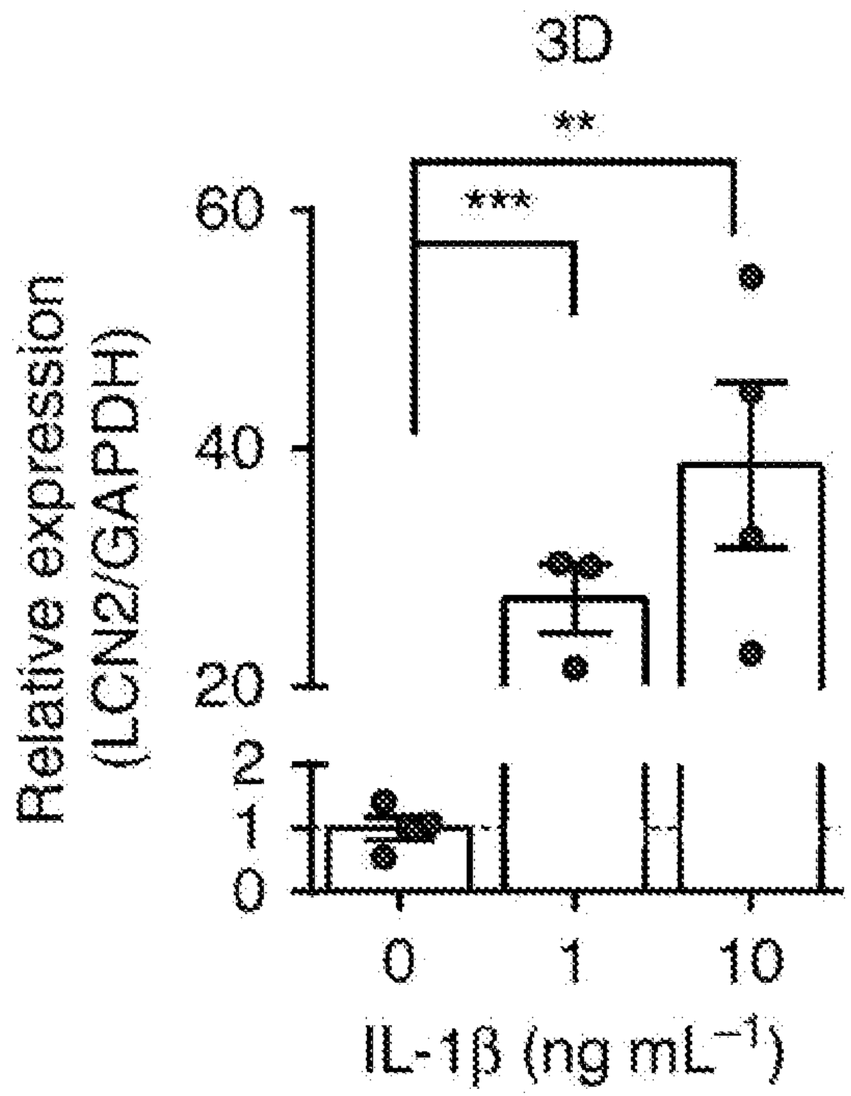


Fig. 42

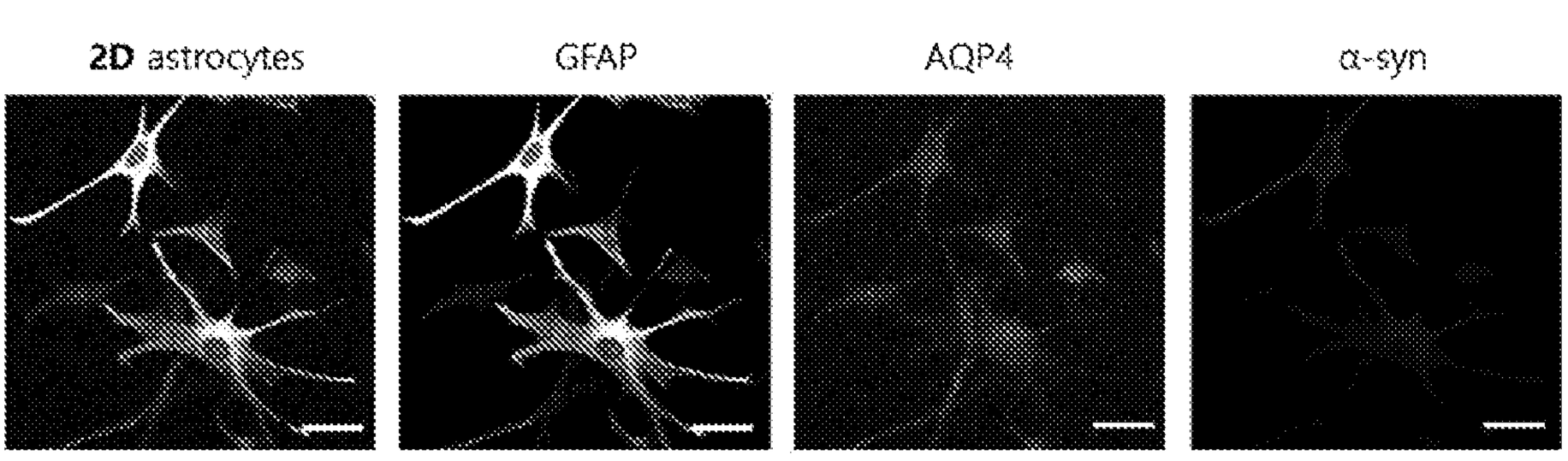


Fig. 43

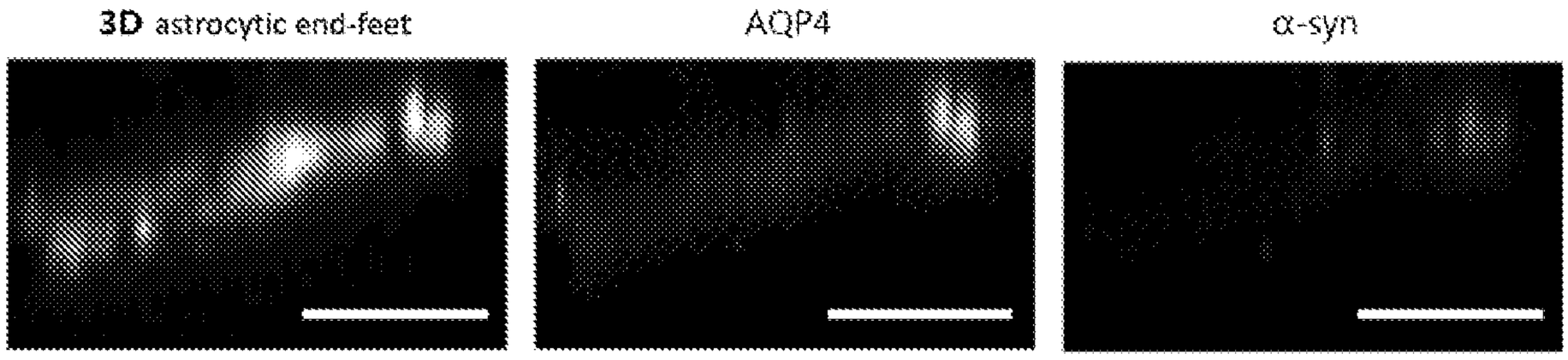


Fig. 44

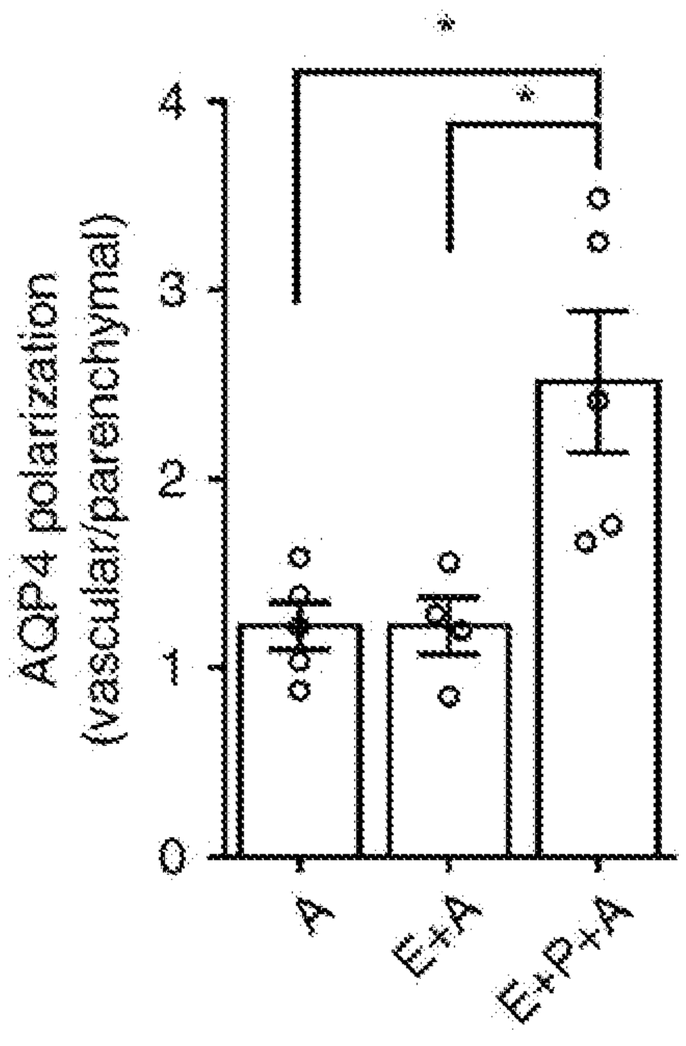

AQP4 polarization
(vascular/parenchymal)
0
1
2
3
4
A
E+A
E+P+A
*
*

Fig. 45

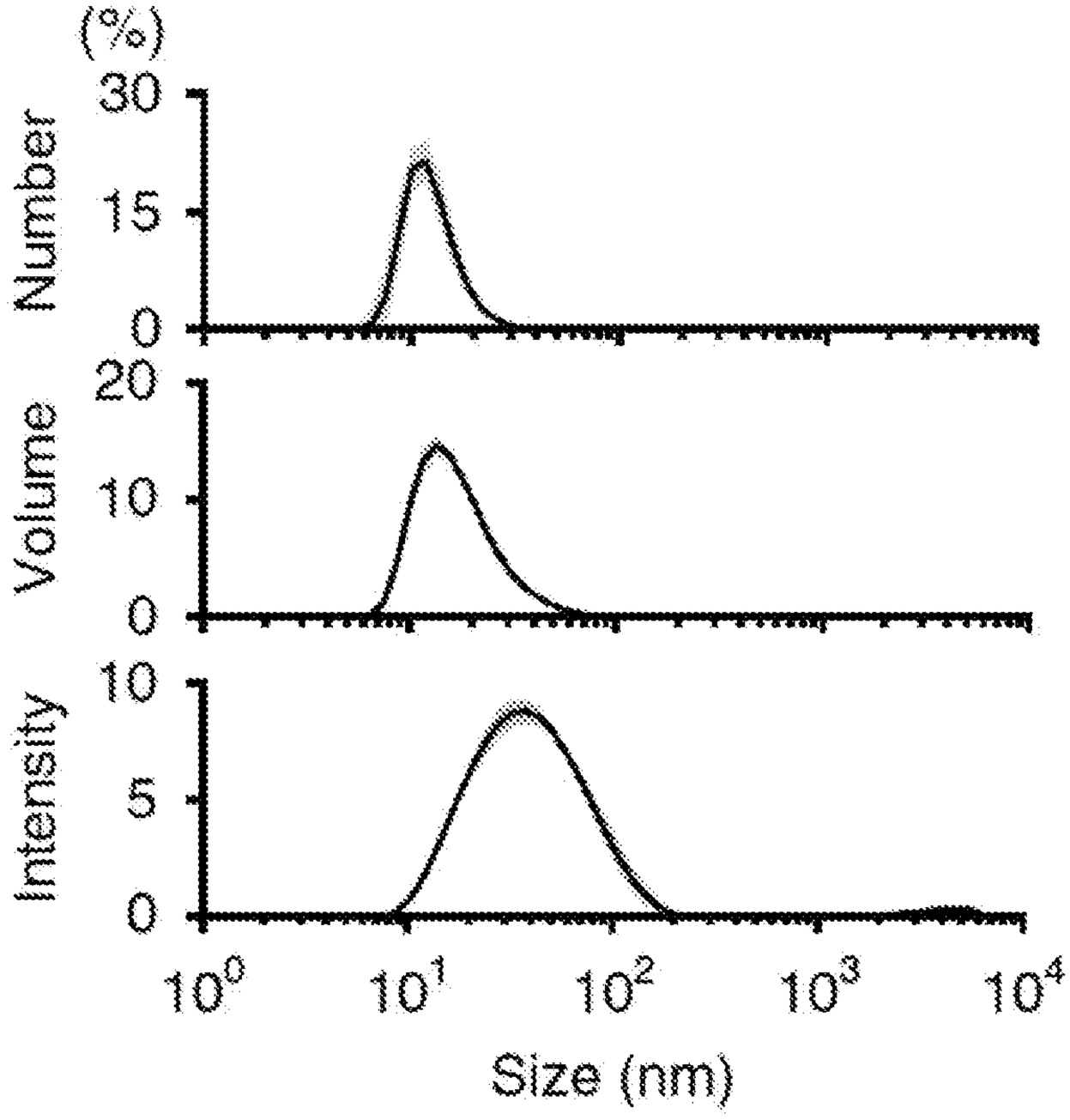

(%)
Number
0
15
30
Volume
0
10
20
Intensity
0
5
10
10^0
10^1
10^2
10^3
10^4
Size (nm)

Fig. 46

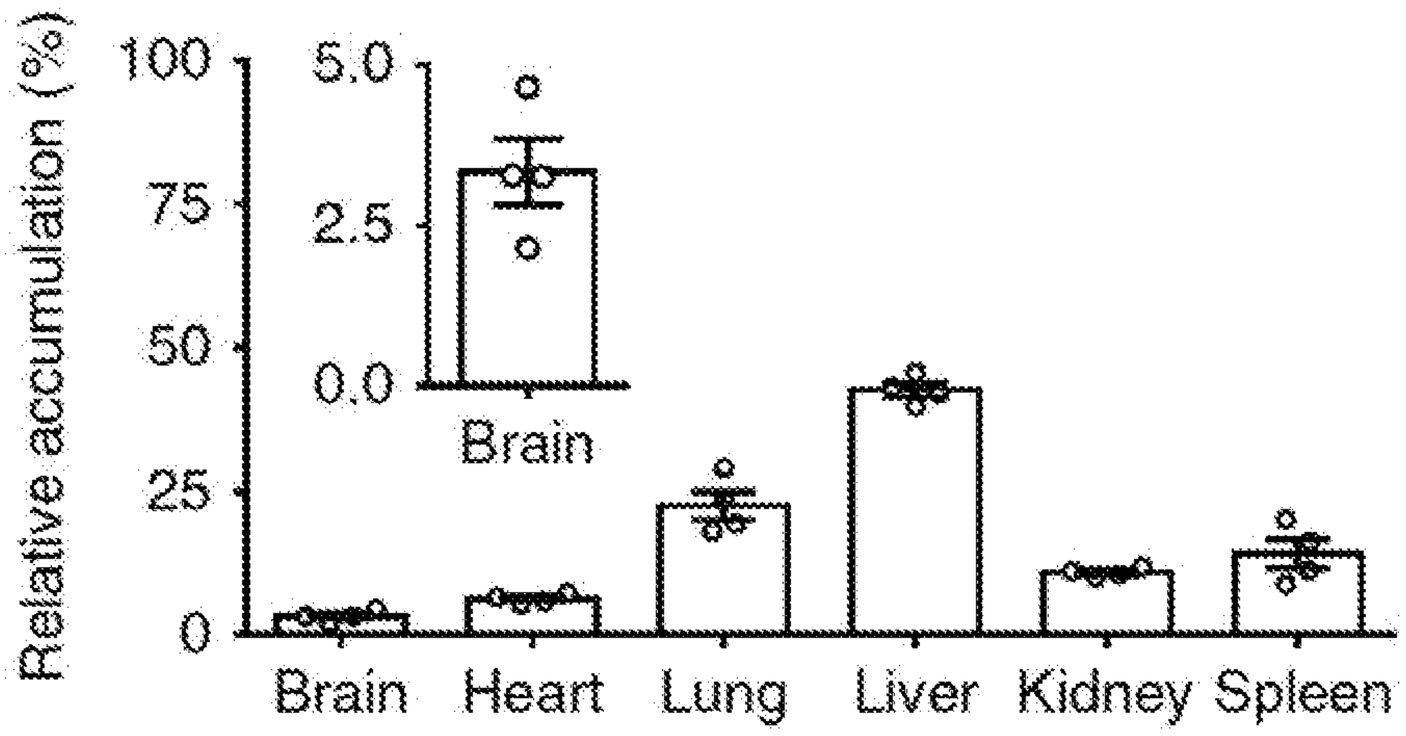

Relative accumulation (%)
100
75
50
25
0
5.0
2.5
0.0
Brain
Brain
Heart
Lung
Liver
Kidney
Spleen

Fig. 47

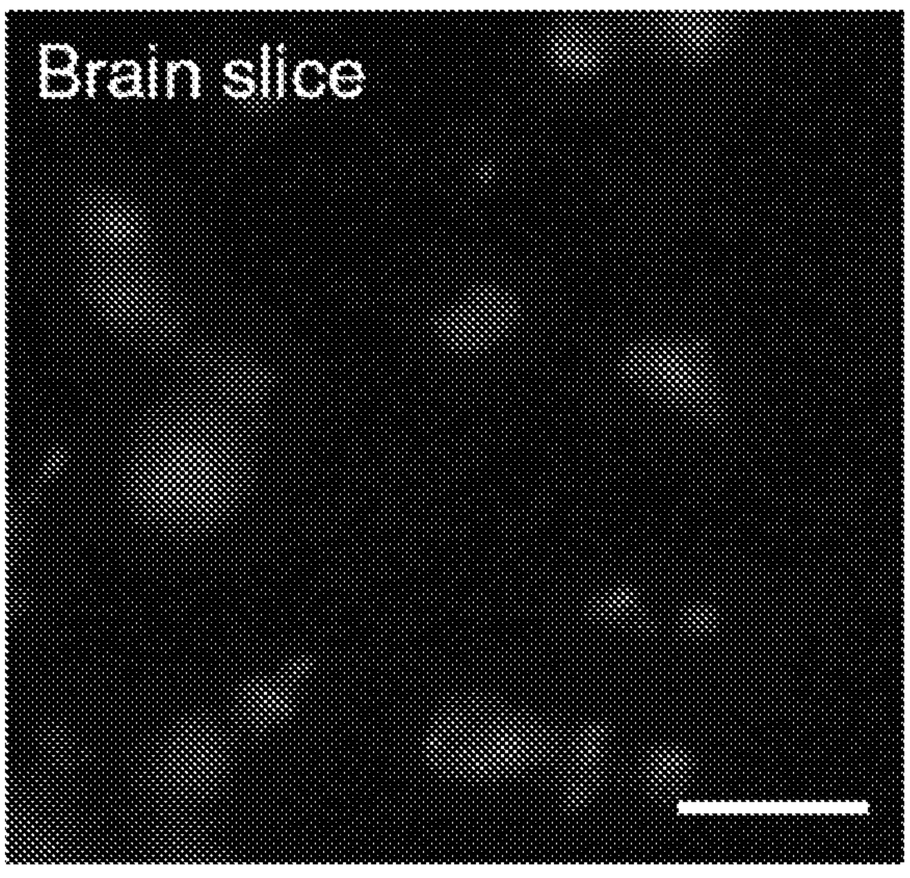

Brain slice

Fig. 48

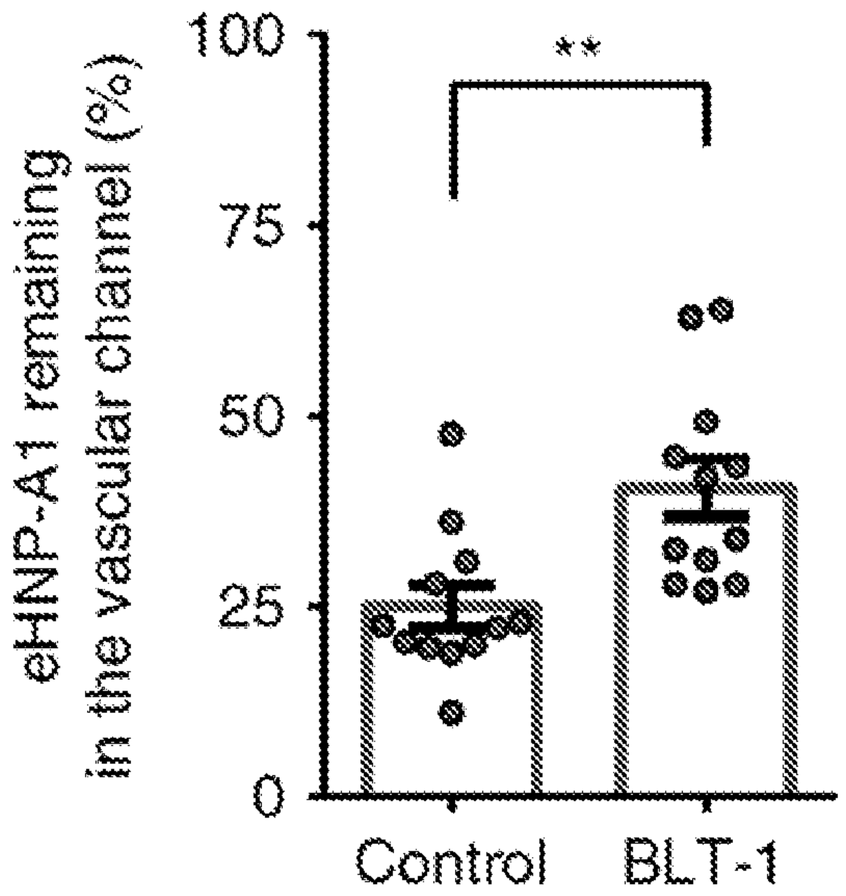

eHNP-A1 remaining in the vascular channel (%)
100
75
50
25
0
**
Control
BLT-1

Fig. 49

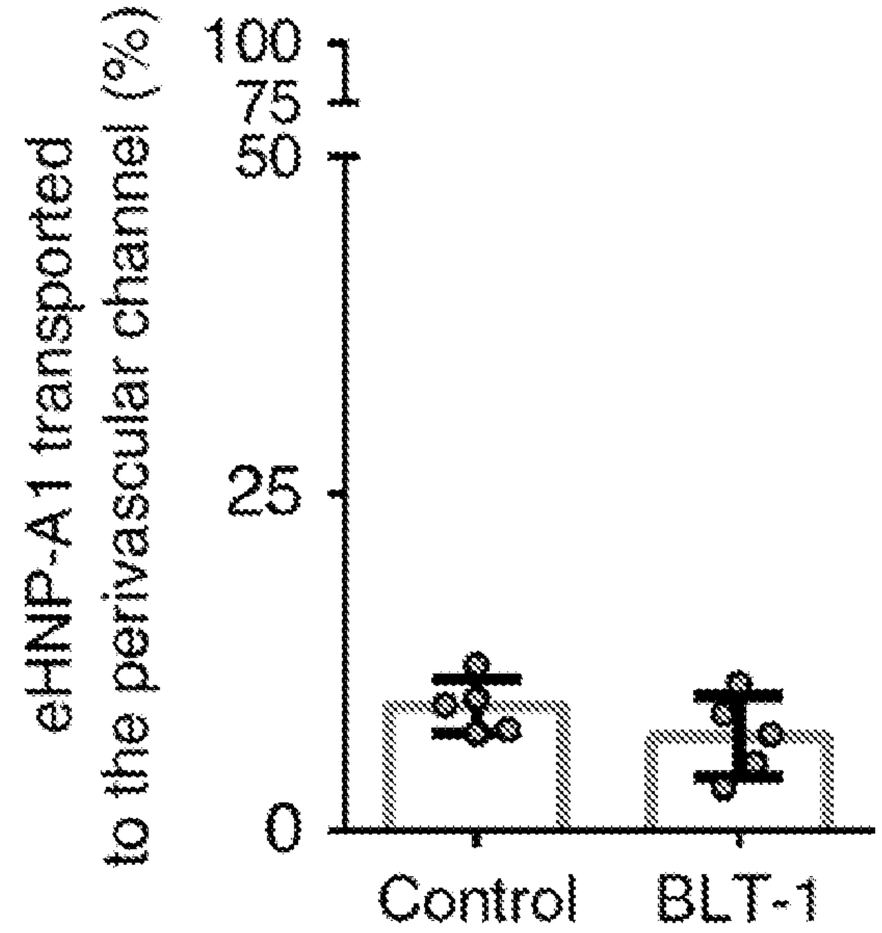

eHNP-A1 transported to the perivascular channel (%)
100
75
50
25
0
Control
BLT-1

Fig. 50

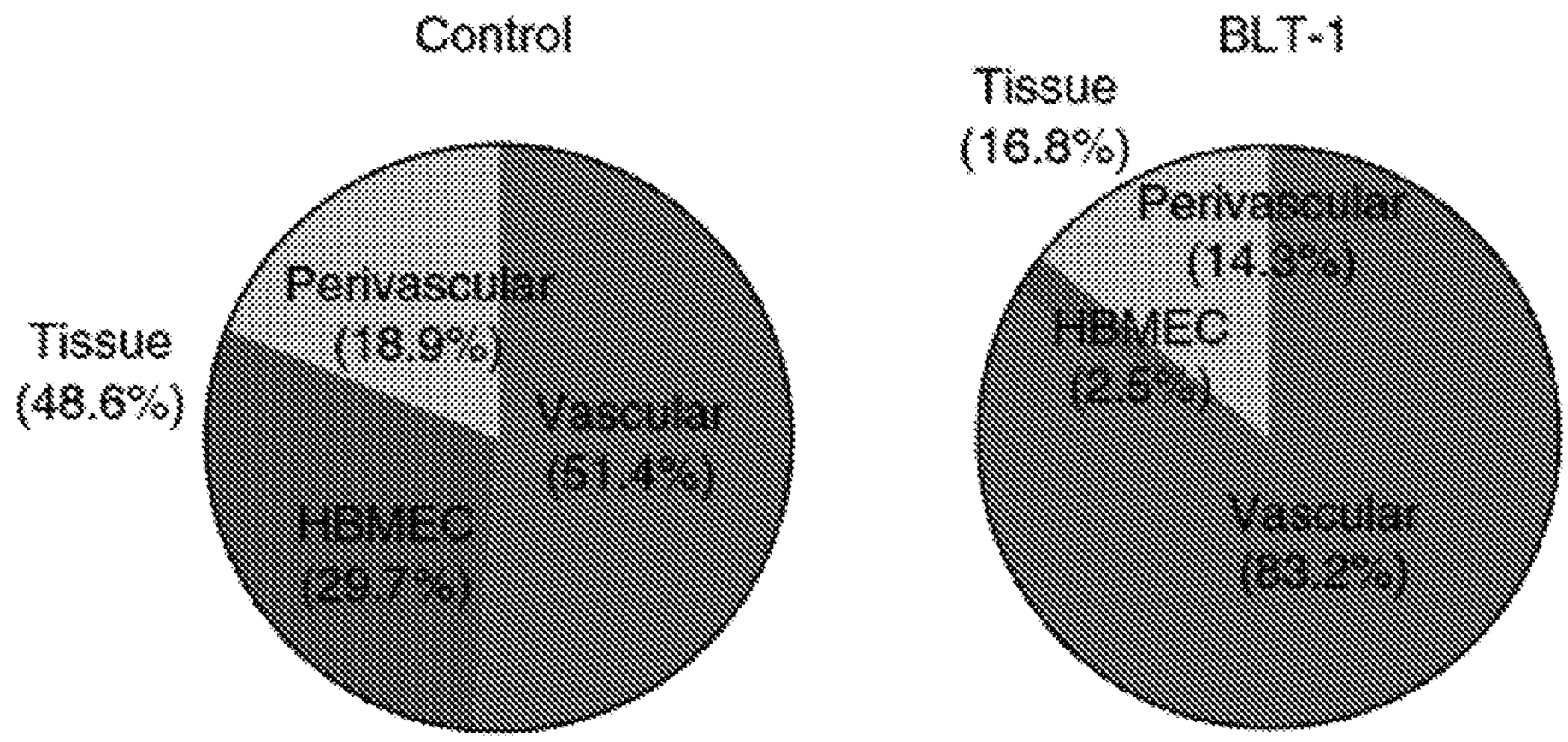

Control
Tissue
(48.6%)
Perivascular
(18.9%)
Vascular
(51.4%)
HBMEC
(29.7%)
BLT-1
Tissue
(16.8%)
Perivascular
(14.3%)
HBMEC
(2.5%)
Vascular
(83.2%)

Fig. 51

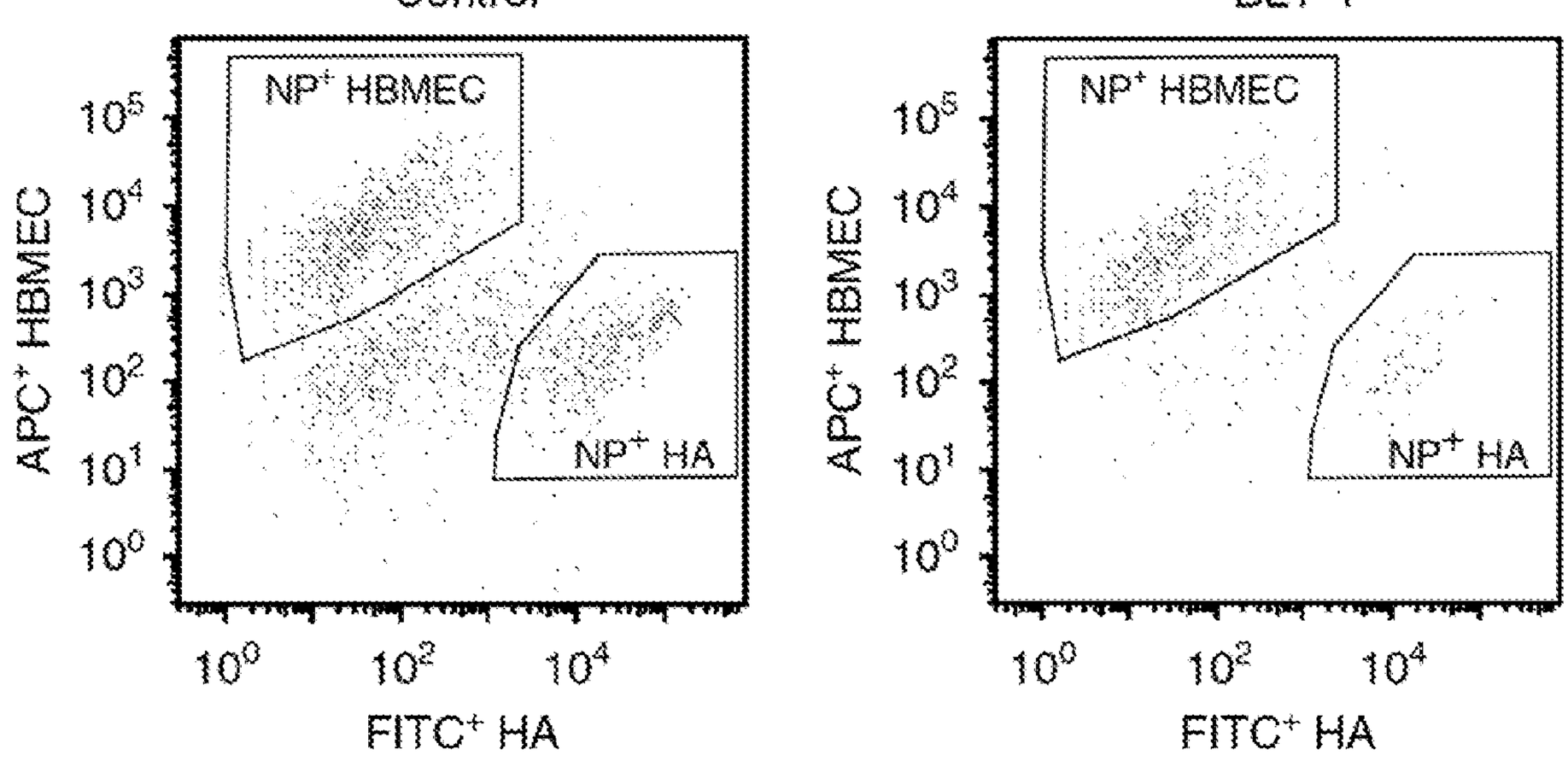
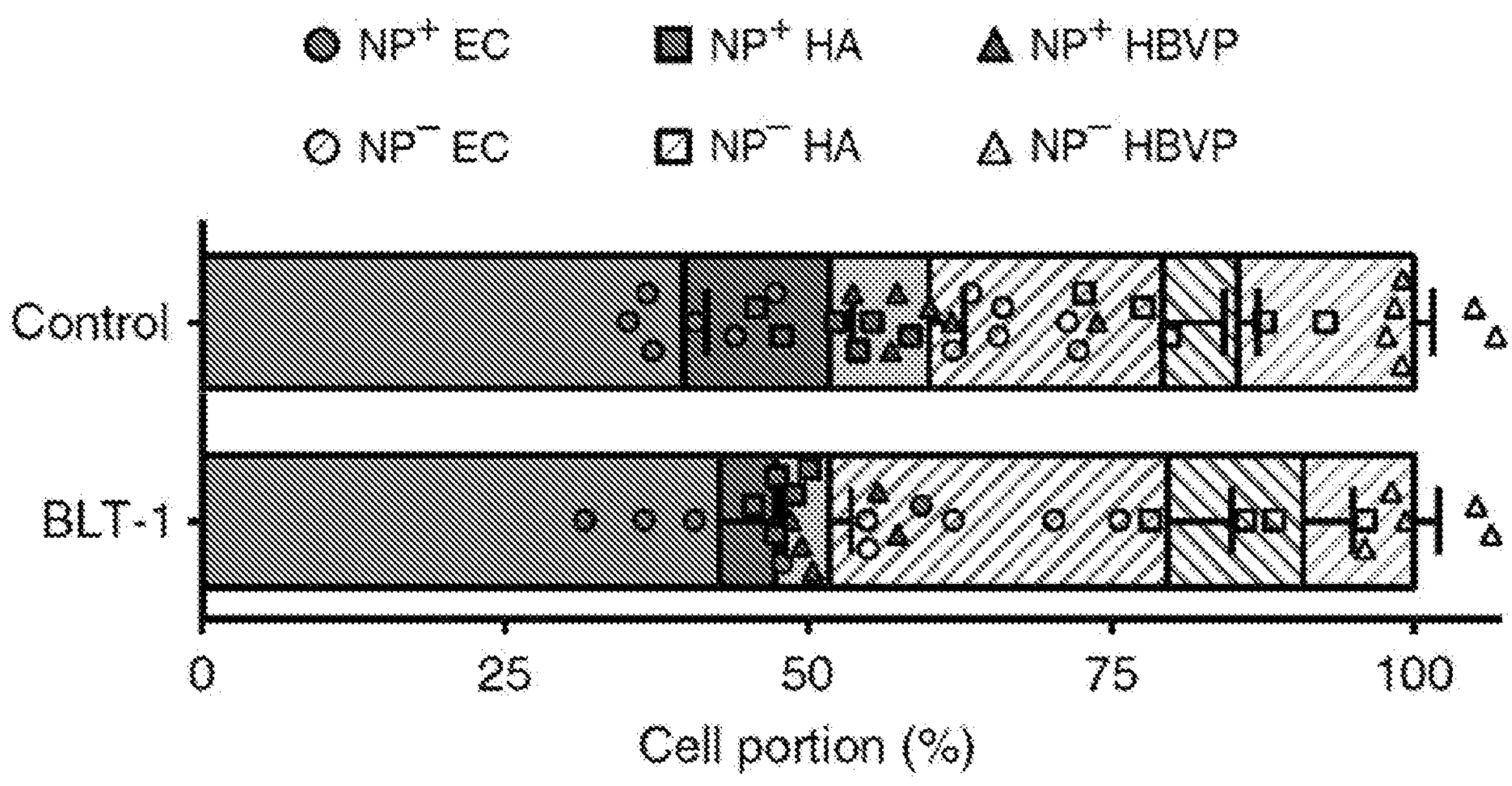

Control
BLT-1
NP+ HBMEC
NP+ HA
APC+ HBMEC
FITC+ HA
10^0
10^1
10^2
10^3
10^4
10^5

Fig. 52


NP+ EC
NP+ HA
NP+ HBVP
NP− EC
NP− HA
NP− HBVP
Control
BLT-1
0
25
50
75
100
Cell portion (%)

INTERNATIONAL SEARCH REPORT

International application No.
PCT/US2020/063636

A. CLASSIFICATION OF SUBJECT MATTER
IPC (20210101) C12M 3/00, C12N 5/00, C12M 3/06, C12M 1/12, C12M 1/34, B01L 3/00
CPC (20130101) C12M 21/08, C12N 5/0062, C12M 23/16, C12M 25/02, C12M 41/46, B01L 3/5027
According to International Patent Classification (IPC) or to both national classification and IPC

B. FIELDS SEARCHED

Minimum documentation searched (classification system followed by classification symbols)
IPC (20210101) C12M 3/00, C12N 5/00, C12M 3/06, C12M 1/12, C12M 1/34, B01L 3/00
CPC (20130101) C12M 21/08, C12N 5/0062, C12M 23/16, C12M 25/02, C12M 41/46, B01L 3/5027

Documentation searched other than minimum documentation to the extent that such documents are included in the fields searched

Electronic data base consulted during the international search (name of data base and, where practicable, search terms used)
Databases consulted: Esp@cenet, Google Patents, Orbit
Search terms used: microfluidic, organ on a chip, organomimetic, membrane, organ, channel, detach, attach, separate, fasten, connect, remove, culture

C. DOCUMENTS CONSIDERED TO BE RELEVANT

Category*	Citation of document, with indication, where appropriate, of the relevant passages	Relevant to claim No.
X	WO 2015138034 A2 HARVARD COLLEGE 17 Sep 2015 (2015/09/17) The whole document	1-27
A	US 20190032021 A1 HARVARD COLLEGE 31 Jan 2019 (2019/01/31) The whole document	1-27

☐ Further documents are listed in the continuation of Box C.

☒ See patent family annex.

* Special categories of cited documents:
"A" document defining the general state of the art which is not considered to be of particular relevance
"D" document cited by the applicant in the international application
"E" earlier application or patent but published on or after the international filing date
"L" document which may throw doubts on priority claim(s) or which is cited to establish the publication date of another citation or other special reason (as specified)
"O" document referring to an oral disclosure, use, exhibition or other means
"P" document published prior to the international filing date but later than the priority date claimed
"T" later document published after the international filing date or priority date and not in conflict with the application but cited to understand the principle or theory underlying the invention
"X" document of particular relevance; the claimed invention cannot be considered novel or cannot be considered to involve an inventive step when the document is taken alone
"Y" document of particular relevance; the claimed invention cannot be considered to involve an inventive step when the document is combined with one or more other such documents, such combination being obvious to a person skilled in the art
"&" document member of the same patent family

Date of the actual completion of the international search	Date of mailing of the international search report
05 Apr 2021	05 Apr 2021

Name and mailing address of the ISA:
Israel Patent Office
Technology Park, Bldg.5, Malcha, Jerusalem, 9695101, Israel
Email address: pctoffice@justice.gov.il

Authorized officer
ITIN Yulia
YuliaI@justice.gov.il
Telephone No. 972-2-5651680

INTERNATIONAL SEARCH REPORT
Information on patent family members

International application No.
PCT/US2020/063636

Patent document cited search report	Publication date	Patent family member(s)	Publication Date
WO 2015138034 A2	17 Sep 2015	WO 2015138034 A2	17 Sep 2015
		WO 2015138034 A3	10 Dec 2015
		AU 2014386209 A1	21 Jul 2016
		AU 2014386209 A2	29 Sep 2016
		AU 2014386209 B2	11 Mar 2021
		CA 2934662 A1	17 Sep 2015
		CN 106459898 A	22 Feb 2017
		EP 3083940 A2	26 Oct 2016
		EP 3083940 A4	23 Aug 2017
		GB 201612578 D0	31 Aug 2016
		GB 2538012 A	02 Nov 2016
		JP 2017504320 A	09 Feb 2017
		JP 2020058358 A	16 Apr 2020
		US 2016313306 A1	27 Oct 2016
		US 2021003561 A1	07 Jan 2021
US 20190032021 A1	31 Jan 2019	NONE	